SOCIAL ANXIETY DISORDER: FUNCTIONAL NEUROIMAGING AND SOCIAL COGNITIVE FEATURES

by
Alexander Govert George Doruyter

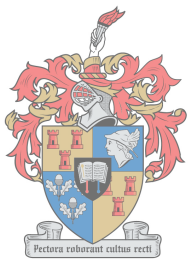

Dissertation approved for the degree of Doctor of Philosophy in the Faculty of Medicine and Health Sciences at Stellenbosch University

Supervisor: Prof James Matthew Warwick
Co-supervisor: Prof Christine Lochner

March 2018

Declaration

By submitting this dissertation electronically, I declare that the entirety of the work contained therein is my own, original work, that I am the sole author thereof (save to the extent explicitly otherwise stated), that reproduction and publication thereof by Stellenbosch University will not infringe any third party rights and that I have not previously in its entirety or in part submitted it for obtaining any qualification.

This dissertation includes **three** original papers published in peer-reviewed journals and **three** unpublished publications. The development and writing of the papers (published and unpublished) were the principal responsibility of myself and, for each of the cases where this is not the case, a declaration is included in the dissertation indicating the nature and extent of the contributions of co-authors.

(Declaration with signature in possession of candidate and supervisor.)
Signature

Alexander Govert George Doruyter
Name in full

March 2018
Date

Abstract

Neuroimaging has enabled important progress in understanding the neurobiology of social anxiety disorder (SAD). Functional neuroimaging experiments in SAD have mostly focused on regional neural activity in response to anxiety provocation or processing of emotional faces, and have found hyper-activations in limbic and paralimbic circuitry. Relatively little however, is known about resting-state conditions in SAD and how these are affected by pharmacotherapy. What is known is almost entirely based on functional magnetic resonance imaging (fMRI) techniques which, while powerful, have some important limitations. Similarly, there has been only limited work investigating the resting neural correlates of social cognitive biases in SAD; how reward processing is disrupted in the condition; and how these respective features are affected by therapy.

This thesis presents the first work on SAD investigating resting functional connectivity (RFC) based on nuclear neuroimaging methods. In an experiment that analysed RFC based on single photon emission computed tomography with technetium-99m hexamethyl propylene amine oxime, it was found that RFC differences in SAD were largely consistent with a contemporary network model based on fMRI, as well as implicating disrupted connectivity of the cerebellum. Another novel finding was how pharmacotherapy in SAD increased RFC of the anterior cingulate cortex.

Using graph theory and resting-state fMRI, the first evidence of reduced global efficiency and increased clustering coefficients within the theory-of-mind network in SAD as well as independent evidence of social attribution bias in the same sample were reported.

In an experiment that investigated regional resting metabolism in the disorder, there was evidence of abnormality in SAD compared to controls, as well as evidence of pharmacotherapy effects, in several biologically relevant regions. These results merit further investigation.

Finally, in an fMRI-based experiment on reward processing in SAD, initial results identified no evidence of disrupted processing on a monetary reward task.

The findings here support a neurobiological model of SAD in which alterations in resting regional metabolism may underlie disruptions in resting brain networks that have been implicated as being important in social cognitive processing. The results also suggest that pharmacotherapy may affect resting-state conditions through compensatory effects. Finally, the provisional findings are consistent with the theory that reward deficits in SAD may be limited to the processing of social reward, and may not extend to the processing of other reward types. Future SAD research should focus on collaborative work, using pooled datasets, and place greater emphasis on molecular disruptions in neurotransmitter systems involved in the disorder.

Opsomming

Breinbeelding het belangrike vooruitgang in ons begrip van die neurobiologiese onderbou van sosiale angssteuring (SAS) moontlik gemaak. Funksionele breinbeeldingseksperimente in SAS het tot dusver meestal gefokus op aktiwiteit in spesifieke areas in reaksie op die ontlokking van angs of tydens die verwerking van emosionele gesigsuitdrukkings, en resultate het op hiperaktiwiteit in limbiese en paralimbiese kringe gedui. Relatief min is egter bekend oor rustende breintoestande in SAS en hoe dit deur farmakoterapie geraak word. Wat wel bekend is, berus grootliks op tegnieke van funksionele magnetiese resonansie beelding (fMRB). Hierdie tegnieke, hoewel kragtig, het enkele belangrike beperkings. Daar is ook min bekend oor die veranderlikes in die brein wat verband hou met die disfunksionele kognitiewe sosiale vooroordele tipies van SAS, oor die verwerking van beloning in SAS, en hoe hierdie eienskappe deur terapie geaffekteer kan word.

Hierdie proefskrif sluit die eerste SAS-data oor rustende funksionele konnektiwiteit (RFK) in die brein – wat gebaseer is op kerngeneeskundige breinbeeldingsmetodes – in. Hierdie bevindinge oor RFK (wat gebaseer is op enkelfoton-emissie-rekenaartomografie wat technesium-99m heksametielpropileenamienoksiem gebruik), stem grootliks ooreen met 'n kontemporêre netwerkmodel wat op fMRB gebaseer is, en dat die RFK van die serebellum in SAS ontwrig is. Nog ’n nuwe bevinding is dat farmakoterapie in SAS RFK van die anterior singulaat korteks verhoog.

Deur gebruik te maak van grafiese teorie en fMRB in die rustende toestand, word die eerste bewyse van verminderde globale doeltreffendheid en verhoogde trosvormingskoëffisiënte binne die “theory-of-mind” breinnetwerk in SAS, sowel as onafhanklike bewyse van sosiale attribusie vooroordele (“social attribution bias”) in die steuring gelewer.

Na aanleiding van ’n ondersoek oor rustende metabolisme in sekere brein-areas in SAS, word abnormaliteite in SAS in vergelyking met gesonde kontrolepersone gerapporteer, sowel as bewyse van die effek van farmakoterapie op verskeie biologies-relevante areas gelewer. Hierdie resultate regverdig verdere navorsing.

Ten slotte, in 'n fMRB-gebaseerde eksperiment oor die verwerking van beloning in SAS was daar geen bewyse van ontwrigte verwerking in monetêre beloning nie.

Hierdie bevindinge ondersteun 'n neurobiologiese model van SAS waarin veranderinge in rustende metabolisme in sekere brein-areas onderliggend is aan die ontwrigting van rustende brein-netwerke wat belangrik is tydens sosiale kognitiewe prosessering. Die bevindinge dui ook daarop dat farmakoterapie RFK in SAS beïnvloed, moontlik via die aktivering van kompenseringsmeganismes. Ten slotte, die voorlopige resultate stem ooreen met die teorie dat tekorte ten opsigte van die verwerking van beloning in SAS moontlik beperk is tot die prosessering van sosiale beloning, en dat dit nie veralgemeen kan word na die verwerking van ander beloningstipes nie. Toekomstige SAS-navorsing behoort op samewerking met ander navorsingsgroepe te fokus, sodat gesamentlike groter datastelle gebruik kan word. Bykomend hiertoe behoort daar groter klem te wees op ondersoeke na die ontwrigting op molekulêre vlak in die neuro-oordragstelsels van individue met SAS.

Acknowledgements

I would like to express sincere thanks to several people without whom this thesis would have been impossible.

Prof James Warwick, my supervisor, was always at hand to provide guidance and assistance, no matter how heavy his clinical and research workload. He has provided sterling mentorship and friendship for which I am immensely grateful.

Prof Christine Lochner made more valuable contributions than can be listed here. She kept things light when the going got tough, and provided sage advice throughout. I keenly appreciate how lucky I was to have her as a co-supervisor.

Prof Patrick Dupont made multiple trips to South Africa to teach me neuroimaging analysis and fine-tuned our work over many teleconferences and email conversations. Thanks to his patience and his clear and logical approach I learned a huge amount on various aspects of brain analysis.

Thank you also to all my co-investigators for the time and effort they have put into collecting data and reviewing manuscripts. Their ideas and suggestions enriched this work tremendously. I would also like to extend my gratitude to the radiographers from the Western Cape Academic PET/CT centre and the Cape Universities Body Imaging Centre, for their professional and friendly assistance in scanning research participants.

I would like to thank my funders who generously supported various components of my research: the South African Medical Research Council, the Nuclear Technologies in Medicine and Biosciences Initiative (NTeMBI), and the Harry Crossley Foundation.

Finally, I would like to acknowledge my wife and family for their love and continual support over the past few years.

Dedication

This thesis is dedicated to the memory of my father, Jacobus Doruyter (1946-2013).

Table of Contents

List of Abbreviations

Most abbreviations have been defined in the text when used for the first time. A full list of all abbreviations used in this thesis appears below.

^{1}H	Proton
3T	3-tesla
3-D	3-dimensional
5-HT$_{1A/1B/2A/4/6}$	Serotonin receptor type 1A/1B/2A/4/6
5-HTP	5-hydroxytryptophan
5-I-A-85380	5-iodo-3-[2 (S)-2-azetidinylmethoxy] pyridine
7T	7-tesla
β-CIT	methyl 3β-(4-iodophenyl) tropane-2b-carboxylate
Δ%LSAS	Percentage change in score on Liebowitz Social Anxiety Scale
λ	Mean characteristic path length
λ_i	Nodal characteristic path length
μ_l	Linear attenuation coefficient
A$_{1/2A}$	Adenosine receptor type 1/2A
AADC	Aromatic L-amino acid decarboxylase
AAL	Automated anatomical labelling (atlas)
ACC	Anterior cingulate cortex
AChE	Acetylcholine esterase
adACC	Anterior-dorsal anterior cingulate cortex
AI	Anterior insula
ANOVA	Analysis of variance
Ala	Alanine
ANSIR	Advanced NeuroScience Imaging Research
Asc	Ascorbate
ASD	Autism spectrum disorder
ASL	Arterial spin labelling
ATL	Anterior temporal lobe
AZ10419369	5-methyl-8-(4-methylpiperazin-1-yl)-N-(4-morpholin-4-ylphenyl)-4-oxochromene-2-carboxamide

BA	Brodmann Area
BC	Mean betweenness centrality
BC_i	Nodal betweenness centrality
BDI-II	Beck Depression Inventory, version 2
BOLD	Blood oxygen level dependent
bvFTD	Behavioural variant of frontotemporal dementia
C	Mean clustering coefficient
C-11	Carbon-11
CB_1	Cannabinoid receptor type 1
CGI-I/S	Clinical global impressions scale – improvement/severity
C_i	Nodal clustering coefficient
cm	centimetre
CM	Centromedial amygdala
Cr	Creatine
CSF	Cerebrospinal fluid
CT	(x-ray) Computed tomography
D1/2	Dopamine receptor type 1/2
DASB	3-amino-4-(2-dimethylaminomethylphenylsulfanyl)-benzonitrile
DAT	Dopamine transporter
DICOM	Digital communications in medicine
dlPFC	Dorsolateral prefrontal cortex
DM1	Myotonic dystrophy type-1
DMN	Default mode network
dmPFC	Dorsomedial prefrontal cortex
DPN	Diprenorphine
DSM-IV, DSM-V	Diagnostic statistical manual of mental disorders, versions 4 and 5
DTBZ	Dihydrotetrabenazine
DTPA	Diethylenetriaminepentaacetic acid
E	Mean global efficiency
EB	Externalizing bias
ECD	Ethyl cysteinate dimer
E_{loci}	Nodal local efficiency
ENIGMA	Enhancing Neuro Imaging Genetics by Meta-Analysis

EPI	Echo-planar imaging
EVC	Early visual cortex
F-18	Fluorine-18
fALFF	Fractional amplitude of low-frequency fluctuations
FC	Functional connectivity
FCS	Functional connectivity strength
FDG	2-deoxy-2-(Fluorine-18)fluoro-D-glucose
FDOPA	Fluorodeoxyphenylalanine
FDR	False-discovery rate
FFA	Fusiform face area
FFG	Fusiform gyrus
FLAIR	Fluid-attenuated inversion recovery
FLB457	(S)-(-)-5-bromo-N-((1-ethyl-2pyrrolidinyl)methyl)-2,3-dimethoxybenzamide
FMeNER-D2	(S,S)-2-(a-(2-fluoro[2H2]methoxyphenoxy)benzyl)morpholine
FMPEP-D2	(3R,5R)-5-[3-[dideuterio(fluoranyl)methoxy]phenyl]-3-[[(1R)-1-phenylethyl]amino]-1-[4-(trifluoromethyl)phenyl]pyrrolidin-2-one
fMRI	Functional magnetic resonance imaging
fMRS	Functional magnetic resonance spectroscopy
FMZ	Flumazenil
FOV	Field of view
fPOC	Frontopolar cortex
FWE	Family-wise error
FWHM	Full width at half maximum
GABA	Gamma-aminobutyric acid
$GABA_A$	benzodiazepine receptor type A
GE	General Electric
Glu	Glutamine
Gly	Glycine
GR205171	(2S,3S)-N-[[2-[11C]methoxy-5-[5-(trifluoromethyl)tetrazol-1-yl]phenyl]methyl]-2-phenyl-piperidin-3-amine
GPC	Glycerophosphocholine
GSH	Glutathione

GSK215083	3-(3-fluorophenyl)sulfonyl-8-(4-methylpiperazin-1-yl)quinoline
H_1	Histamine receptor type 1
HC	Healthy control
Hz	hertz
HMPAO	Hexamethyl propylene amine oxime
I-123	Iodine-123
IBASPM	Individual brain atlases using statistical parametric mapping
IBZM	Iodobenzamide
ICA	Independent component analysis
ICH/GCP	International Conference on Harmonisation/Good Clinical Practice
IFG	Inferior frontal gyrus
IOM	Iomazenil
iPAT	Integrated parallel acquisition technique (Siemens)
IPSAQ	Internal, personal and situational attributions questionnaire
KU	Katholieke Universiteit (Leuven)
kVP	Peak kilovoltage
L	Left
Lac	Lactate
LOR	Line of response
LSAS	Liebowitz social anxiety scale
mAChR	Muscarinic acetylcholine receptor
MACM	Meta-analytic connectivity modelling
MADAM	N,N-dimethyl-2-(2-amino-4-methylphenylthio)benzylamine
MADRS	Montgomery- Åsberg depression rating scale
MAO-A/B	Monoamine oxidase A/B
MAOI	Monoamine oxidase inhibitor
mAs	milliampere-second
MBq	megabecquerel
McN5652	(6R,10bS)-6-(4-methylsulfanylphenyl)-1,2,3,5,6,10b-hexahydropyrrolo[2,1-a]isoquinoline
MDD	Major depressive disorder
ME-MPRAGE	Multi-echo magnetization prepared rapid gradient echo (imaging)
MFG	Middle frontal gyrus

MFGOrb	Middle frontal gyrus, orbital part
MID	Monetary incentive delay (task)
MM	Macromolecules
mm	millimetre
MNI	Montreal Neurological Institute
mOFC	Medial orbitofrontal cortex
MOG	Middle occipital gyrus
MOR/KOR/DOR	μ-/κ-/δ-opioid receptor
MPDX	8-(dicyclopropylmethyl)-1-methyl-3-propyl-7H-purine-2,6-dione
mPFC	Medial prefrontal cortex
MR(I)	Magnetic resonance (imaging)
MRC	(South African) Medical Research Council
MRS	Magnetic resonance spectroscopy
ms	millisecond
mSFG	Medial superior frontal gyrus
MTG	Middle temporal gyrus
MTV	Middle temporal visual area
myo-Ins	Myo-inositol
NAA	N-acetylaspartate
NAAG	N-acetylaspartylglutamate
nAChR	Nicotinic acetylcholine receptor
Necsa	South African Nuclear Energy Corporation
NET	Noradrenaline (norepinephrine) transporter
NIfTI	Neuroimaging Informatics Technology Initiative
NIMH	National Institute of Mental Health
NK_1	Neurokinin receptor 1
NMPB	N-methyl-4-piperidylbenzilate
NTeMBI	Nuclear Technologies in Medicine and the Biosciences Initiative
O-15	Oxygen-15
OCD	Obsessive-compulsive disorder
OFA	Occipital face area
OSEM	Ordered subset expectation maximization
PBn/p	Personalizing bias for negative/positive events

PC	Phosphocholine
PCC	Posterior cingulate cortex
PCr	Phosphocreatine
PE	Phosphoethanolamine
PET	Positron emission tomography
PET/CT	Positron emission tomography/(x-ray) computed tomography
PET/MR(I)	Positron emission tomography/magnetic resonance (imaging)
PIB	Pittsburgh compound B
PK11195	1-(2-Chlorophenyl)-N-methyl-N-(1-methylpropyl)-3-isoquinolinecarboxamide
PO	per os
Precun	Precuneus
pSTS	Posterior superior temporal sulcus
PTSD	Post-traumatic stress disorder
R	Right
rCBF	Regional cerebral blood flow
RDoC	Research Domain Criteria (initiative)
ReHo	Regional homogeneity (analysis)
RFC	Resting functional connectivity
ROI	Region of interest
rs-fMRI	Resting-state functional magnetic resonance imaging
SAD	Social anxiety disorder
SAMRC	South African Medical Research Council
SB207145	(4-{[(8-amino-7-chloro-2,3-dihydro-1,4-benzodioxin-5-yl)carbonyloxy]methyl}piperidin-1-yl)methylidyne
SCH 23390	8-chloro-3-methyl-5-phenyl-1,2,4,5-tetrahydro-3-benzazepin-7-ol
SCID	Structured clinical interview for DSM
scyllo-Ins	Scyllo-inositol
SD	Standard deviation
SDS	Sheehan disability scale
SERT	Serotonin transporter
SFG	Superior frontal gyrus
sgACC	Subgenual anterior cingulate cortex

SPECT	single photon emission tomography
SPM	Statistical parametric mapping
SSRI	Selective serotonin reuptake inhibitor
STAI-S	State-trait anxiety inventory - state version
STEAM	Stimulated echo acquisition mode
Tau	Taurine
STG	Superior temporal gyrus
Tc-99m	Technetium-99m
TE	Echo time
TEI	Trait emotional intelligence
TF, TOF	Time of flight
TMSX	7-methyl-(E)-8-(3,4,5-Trimethoxystyryl)-1,3,7-trimethylxanthine; 1,3,7-tri(methyl)-8-[(E)-2-(3,4,5-trimethoxyphenyl)ethenyl]purine-2,6-dione
ToM	Theory of mind
TPH2	Tryptophan hydroxylase-2
TPJ	Temporoparietal junction
TPO	Temporal pole
TR	Repetition time
TRODAT-1	2-[2-[[(1S,3S,4R,5R)-3-(4-chlorophenyl)-8-methyl-8-azabicyclo[3.2.1]octan-4-yl]methyl-(2-sulfanylethyl)amino]ethylamino]ethanethiol
TSPO	18-kDa translocator protein
UCL	University College London
UK	United Kingdom
USA	United States of America
UT	University of Texas
$VMAT_2$	Vesicular monoamine oxidase A transporter type 2
vmPFC	Ventromedial prefrontal cortex
VOI	Volume of interest
WAY-100635	N-[2-[4-(2-methoxyphenyl)piperazin-1-yl]ethyl]-N-pyridin-2-ylcyclohexanecarboxamide
WFU	Wakefield Forest University

List of Tables

List of Figures

Contributions

Declaration by the candidate:

With regard to the following chapters/articles, the nature and scope of my contribution were as follows:

	Nature of contribution	**Extent of contribution (%)**
Nuclear neuroimaging in social anxiety disorder: a review **(p1 - 29)**	Literature review and manuscript	80
Resting functional connectivity in social anxiety disorder and the effect of pharmacotherapy **(p30 - 54)**	Literature review, data collation, processing and analysis, manuscript	65
Resting-state fMRI and social cognition: an opportunity to connect **(p55 - 68)**	Literature review and manuscript	65
Social attribution and resting graph metrics within the theory of mind network in social anxiety disorder **(p69 - 96)**	Literature review, data collection, processing and analysis, manuscript	60
Regional brain metabolism in social anxiety disorder and the effect of moclobemide therapy **(p97 - 118)**	Literature review, data collection, processing and analysis, manuscript	65
Reward processing in social anxiety disorder: An fMRI investigation **(p119 - 136)**	Literature review, data collection, processing and analysis, manuscript	55

The following co-authors have contributed to chapters/articles as detailed below:

Nuclear neuroimaging in social anxiety disorder: a review **(p1 - 29)**	**e-mail address**	**Nature of contribution**	**Extent of contribution (%)**
P. Dupont	patrick.dupont@kuleuven.be	Manuscript review	5
DJ. Stein	dan.stein@uct.ac.za	Manuscript review	5
C. Lochner	cl2@sun.ac.za	Manuscript review	5
JM. Warwick	jw@sun.ac.za	Manuscript review	5
Resting functional connectivity in social anxiety disorder and the effect of pharmacotherapy **(p30 - 54)**	**e-mail address**	**Nature of contribution**	**Extent of contribution (%)**
C. Lochner	cl2@sun.ac.za	Manuscript review	5
GP. Jordaan	gpj2@sun.ac.za	Data collection, manuscript review	5
DJ. Stein	dan.stein@uct.ac.za	Manuscript review	5

P. Dupont	patrick.dupont@kuleuven.be	Processing and analysis, manuscript review	15
JM. Warwick	jw@sun.ac.za	Data collection, manuscript review	5
Resting-state fMRI and social cognition: an opportunity to connect **(p55 - 68)**	**e-mail address**	**Nature of contribution**	**Extent of contribution (%)**
NA. Groenewold	nynke.groenewold@uct.ac.za	Manuscript review	20
P. Dupont	patrick.dupont@kuleuven.be	Manuscript review	5
DJ. Stein	dan.stein@uct.ac.za	Manuscript review	5
JM. Warwick	jw@sun.ac.za	Manuscript review	5
Social attribution and resting graph metrics within the theory of mind network in social anxiety disorder **(p69 - 96)**	**e-mail address**	**Nature of contribution**	**Extent of contribution (%)**
P. Dupont	patrick.dupont@kuleuven.be	Processing and analysis, manuscript review	15
L. Taljaard	liant@sun.ac.za	Screening, data collection, manuscript review	5
DJ. Stein	dan.stein@uct.ac.za	Manuscript review	5
C. Lochner	cl2@sun.ac.za	Screening, data collection, manuscript review	10
JM. Warwick	jw@sun.ac.za	Manuscript review	5
Regional brain metabolism in social anxiety disorder and the effect of moclobemide therapy **(p97 - 118)**	**e-mail address**	**Nature of contribution**	**Extent of contribution (%)**
P. Dupont	patrick.dupont@kuleuven.be	Processing and analysis, manuscript review	5
L. Taljaard	liant@sun.ac.za	Screening, data collection, manuscript review	10
DJ. Stein	dan.stein@uct.ac.za	Manuscript review	5
C. Lochner	cl2@sun.ac.za	Screening, data collection, manuscript review	10
JM. Warwick	jw@sun.ac.za	Manuscript review	5

Reward processing in social anxiety disorder: An fMRI investigation **(p119 - 136)**	**e-mail address**	**Nature of contribution**	**Extent of contribution (%)**
P. Dupont	patrick.dupont@kuleuven.be	Processing and analysis, manuscript review	15
L. Taljaard	liant@sun.ac.za	Screening, data collection, manuscript review	10
DJ. Stein	dan.stein@uct.ac.za	Manuscript review	5
C. Lochner	cl2@sun.ac.za	Screening, data collection, manuscript review	10
JM. Warwick	jw@sun.ac.za	Manuscript review	5

Signature of candidate: *(Declaration with signature in possession of candidate and supervisor.)*

Date: ……3 January 2018…..

Declaration by co-authors:

The undersigned hereby confirm that

1. the declaration above accurately reflects the nature and extent of the contributions of the candidate and the co-authors in the specified chapters/articles.

2. no other authors contributed to the specified chapters/articles besides those specified above, and

3. potential conflicts of interest have been revealed to all interested parties and that the necessary arrangements have been made to use the material in the specified chapters/articles of this dissertation.

Signature	**Institutional affiliation**	**Date**
Prof Gerhard P. Jordaan	Stellenbosch University Faculty of Medicine and Health Sciences, Department of Psychiatry.	
Dr Nynke Groenewold	University of Cape Town Faculty of Health Sciences, Department of Psychiatry.	
Mr. Lian Taljaard	MRC Unit on Risk and Resilience in Mental Disorders, Stellenbosch University Faculty of Medicine and Health Sciences, Department of Psychiatry.	
Prof Patrick Dupont	KU Leuven, Department of Neurosciences, Laboratory of Cognitive Neurology.	
Prof Dan J. Stein	MRC Unit on Risk and Resilience in Mental Disorders, University of Cape Town Faculty of Health Sciences, Department of Psychiatry.	
Prof Christine Lochner	MRC Unit on Risk and Resilience in Mental Disorders, Stellenbosch University Faculty of Medicine and Health Sciences, Department of Psychiatry.	
Prof James M. Warwick	Stellenbosch University Faculty of Medicine and Health Sciences, Division of Nuclear Medicine.	

(Declaration with signatures in possession of candidate and supervisor.)

Introduction

Background Information

People with social anxiety disorder (SAD) experience excessive anxiety during, or while anticipating, social interactions. Sufferers exhibit excessive fear that they will be embarrassed or humiliated by their actions or words, and dread that evidence of their distress (such as sweating, tremor, blushing, stammering) will be noticed by others. As a result, social situations are either avoided, or endured with intense discomfort (American Psychiatric Association and DSM-5 Task Force 2013). When one considers that humans are an inherently social species, that we have a need to feel accepted and liked by others, and that we derive much of our joy from the reward of interpersonal relationships, it becomes clear that a condition that impairs one's ability to experience and enjoy social interaction is particularly cruel. SAD sufferers have been shown to experience a lower quality of life, and have higher rates of unemployment and absenteeism, greater risk of suicide, and higher risk of comorbid substance abuse and depression (Wittchen and Beloch 1996; Lecrubier et al. 2000).

SAD typically starts in childhood or adolescence (between 10 and 16.6 years of age), is more common in women than men (3:2), and has a higher lifetime prevalence in developed (6-12%) than in developing (2.1%) countries (Wittchen and Fehm 2003; Kessler RC et al. 2005; Stein et al. 2010, 2017). While there are several treatment options for SAD, including cognitive behaviour therapy and pharmacotherapy (e.g. with selective serotonin reuptake inhibitors or monoamine oxidase inhibitors), a significant proportion of patients do not respond to interventions (National Collaborating Centre for Mental Health (UK) 2013). Despite its prevalence and its morbidity, SAD has remained relatively understudied (Liebowitz et al. 1985; Nagata et al. 2015).

Early research in SAD was mostly limited to investigating the behavioural features of the condition. These studies were predominantly focused on developing instruments to assist in diagnostic evaluation of anxiety patients, but some also explored the cognitive processing that characterized the disorder, and to a more limited extent, its underlying biology (Liebowitz et al. 1985). Such work for example, suggested differences in how patients with

SAD processed social information such as when attributing causes to socially-relevant outcomes (Heimberg et al. 1989), and confirmed physiological arousal (on monitoring of heart rate, breathing and skin conductance) in performance contexts (Johansson and Öst 1982). This work was important, but could only progress knowledge of the disorder so far. The real breakthrough that would fundamentally change neuropsychiatric research came in the mid-1980s. This period marked the adoption and rapid growth in availability of scanners capable of imaging brain anatomy and function in three dimensions. Since then, functional neuroimaging techniques such as single photon emission tomography (SPECT), positron emission tomography (PET), and functional magnetic resonance imaging (fMRI) have been used to great effect in furthering our understanding of psychiatric conditions, including SAD.

The great value of neuroimaging in psychiatric research is that it provides a non-invasive means to study the structure and function of the living brain (Fallgatter 2009; Linden 2012). The technical sophistication of neuroimaging techniques has grown dramatically over the past three decades. It is now possible to image the brain with high anatomical resolution, to image regional neural activity both at rest and while performing tasks, to study the brain's chemical composition, as well as image neurotransmitter systems with great accuracy. In parallel with these developments, has been the evolution of techniques to quantify and analyse neuroimaging data, in combination with the use of ever more-powerful computing resources. In this thesis, work using several of these state of the art techniques applied to the study of SAD is presented.

Purpose of Study, Research Objectives

In defining research objectives, it is useful to consider the broader objectives of neuroimaging research in psychiatric conditions in general. Firstly, we want to understand the pathophysiology ("neurobiology") of the disorder: in terms of features that predispose to the condition, in terms of features that are present (and may eventually be diagnostic) once the disorder is manifest, and the change in these features during the disease's natural progression. Secondly, we want to understand the influence of genetics (including epigenetics) and environmental factors on the brain (its neurochemistry, neural systems, and anatomy), and how these effects result in witnessed behaviours (phenotype). This levels-based approach to brain research has been termed the *endophenotype* concept (Gottesman and Gould 2003).

Finally, neuroimaging research may be extremely valuable to study therapy: in terms of identifying therapeutic targets, in terms of investigating the mechanisms of action of various interventions, and perhaps in the future, identifying features that predict response to treatment options (Linden 2006, 2012; Fallgatter 2009).

Placed in this context, very little is actually known about SAD. Researchers have however, taken several crucial steps in investigating some of the important basic neural features of the disorder and have gone some way to identify several candidate endophenotypes (Bas-Hoogendam et al. 2016). Fundamentally, functional neuroimaging studies in SAD (including both magnetic resonance and nuclear imaging experiments) have contributed in two ways. Firstly, they have compared neural activity in the disorder with that of healthy controls, both in terms of regional differences, and in terms of how functional relationships between different regions (functional connectivity) are altered. Such studies have found SAD-related differences within multiple regions (and in interregional relationships), including within (and between) limbic and paralimbic structures, various frontal cortical regions, insula, fusiform gyrus, precuneus and striatum (Etkin and Wager 2007; Freitas-Ferrari et al. 2010; Brühl et al. 2014a). The second principal contribution of functional neuroimaging techniques has been to elucidate, to a limited degree, disruptions in brain chemistry and neurotransmitter function in SAD. These studies have for example, found evidence for differences in regional glutamate and N-acetyl-aspartate concentration (Howells et al. 2015) as well as evidence that implicates the serotonergic and dopaminergic neurotransmitter systems in the condition (Doruyter et al. 2017a). Limited evidence suggests that therapy (principally pharmacotherapy) affects some of these neural features of SAD in various ways (Brühl et al. 2014a; Doruyter et al. 2017a).

There is still much work to be done before a comprehensive neurobiological model of SAD is established and therapy effects are properly understood. In this thesis, several key knowledge gaps that merited further research were identified. On reviewing the academic literature in SAD, one observation is the paucity of nuclear neuroimaging studies performed in recent years. This is mostly due to a shift from nuclear techniques to magnetic resonance imaging (MRI) techniques. There are several advantages to MRI that explain this technique's appeal but several important limitations too, that make nuclear methods either more appropriate or complementary for the provision of some information (Doruyter et al. 2017a). Findings on nuclear imaging studies that support results of MRI-based experiments strengthen the existing evidence. However where results differ, questions must be raised regarding the

relationship between each measurement and the normally more fundamental biological process for which they serve as a surrogate, as well as the reliability of each measurement.

Prior to work presented herein, no resting functional connectivity experiments had been performed with nuclear imaging techniques in SAD, and only a single study had investigated resting regional metabolism in the disorder.

Two studies using fMRI are presented. With the exception of one study linking resting functional connectivity to the processing of facial emotion, no previous fMRI experiments had attempted to correlate resting functional connectivity measures in SAD with a social cognition measure. In addition, this work includes one of the few SAD experiments utilizing graph theory (functional connectivity at the network level) and is the first to correlate resting graph metrics with a measure of social attributional style. This sort of work is valuable in that it seeks to identify the behavioural significance of neuroimaging findings in the condition. The other fMRI study adds to the limited body of work on reward processing in SAD by performing task-based fMRI with a modified version of the monetary incentive delay task. Further research in this direction is important, given indirect evidence that reward processing may be affected in the condition. Finally, an additional feature common to all the experiments in this thesis, was the inclusion of a therapy component in which the effect of a course of pharmacotherapy on neuroimaging measures in SAD participants was tested. Neuroimaging research on the effects of treatment in SAD is sparse, and yet vitally important given the unpredictability of treatment response and incomplete knowledge of how medications exert their effects.

The studies presented in this thesis thus had several objectives:

- To identify, using nuclear imaging techniques, differences in resting functional connectivity and resting regional neural activity between SAD participants and healthy controls (HCs).
- To test whether graph metrics based on resting-state fMRI were different between SAD and HC groups and whether these could be correlated with a neurocognitive measure of social cognition.
- To detect whether there were any differences in reward processing, measured on task-based fMRI, between SAD and HC groups.

- To investigate whether a course of an approved medication for the treatment of SAD, had any effect on the above measures.

Thesis, delineation, research questions

This thesis has been compiled in one of the accepted alternative formats, namely a number of published and unpublished articles. One of these articles describes a retrospective experiment, three describe prospective experiments, and one represents a narrative review. The study population for all experiments was comprised of SAD participants in the Cape Town region (South Africa). All studies were conducted with the approval of the Stellenbosch University Health Research Ethics Committee.

Experiments were designed around the following research questions:

- Is there evidence, using nuclear imaging methods, of disrupted resting functional connectivity in SAD? How does resting regional neural activity change in SAD after a course of moclobemide or citalopram?
- Is there evidence, using nuclear imaging methods, of disrupted resting regional neural activity in SAD? How does resting regional neural activity change in SAD after a course of pharmacotherapy?
- Are there differences in graph metrics, based on resting-state fMRI, within the theory of mind network in SAD? Are there deficits in social attributional style in SAD? Can these graph metrics be correlated with social attributional style measures? How does a course of moclobemide in SAD affect these measures?
- Are there any differences in how participants with SAD process monetary reward during a monetary incentive delay task on fMRI? How does a course of moclobemide affect monetary reward processing in SAD?

Assumptions and limitations

The principal assumption in all experiments was that there are intrinsic and generally consistent differences in neurobiology and/or neurocircuitry between people with SAD and people without psychiatric morbidity which can be detected using currently available neuroimaging and analysis techniques. It was also assumed that the samples would be

sufficiently representative of the SAD population, that findings would be generalizable to the condition, and that any group differences or effects of therapy would be sufficiently large to detect using the methods available.

Brief Paper overviews

Paper 1 (pg. 1) represents an overview of nuclear neuroimaging and how it compares to MRI techniques, reviews the contribution of nuclear neuroimaging in SAD research to date, and discusses possible future directions for SAD research in general. This manuscript has not yet been submitted for publication.

Paper 2 (pg. 34) presents a retrospective experiment using perfusion SPECT data in which resting functional connectivity between SAD and HC groups was compared, and the effect of pharmacotherapy with either moclobemide or citalopram investigated in the SAD group. This work has been published in *Psychiatric Research: Neuroimaging* (Doruyter et al. 2016).

Paper 3 (pg. 61) is written in the format of a short communication. It builds the argument for performing resting-state fMRI in social cognition research and presents a summary of literature in which resting-state fMRI measures were correlated with social cognition measures. This work has been published in *Human Psychopharmacology: Clinical and Experimental* (Doruyter et al. 2017d).

Paper 4 (pg. 76) presents a prospective experiment in which resting graph metrics (based on resting-state fMRI) within the theory of mind network in SAD and HC participants were compared, group differences in social attributional style were tested for, and correlations between graph metrics and a social cognition measure investigated. The effects of moclobemide therapy on these measures in the SAD group were also investigated. This work is being prepared for journal submission.

Paper 5 (pg. 104) presents another prospective experiment in which resting regional neural activity on PET between SAD and HC groups was compared, and the effect of moclobemide in the SAD group investigated. This work was awaiting decision by the journal at the time of

dissertation submission and has subsequently been published in *Metabolic Brain Disease* (Doruyter et al. 2017b).

Paper 6 (pg. 128) presents a prospective experiment in which the processing of monetary reward between SAD and HC groups was compared (using fMRI) and the effects of moclobemide on reward processing in the SAD group investigated. Data collection on this experiment has been extended and there is a plan to submit this work for publication when the group sizes are larger.

Nuclear neuroimaging in social anxiety disorder: a review

Authors: Alexander Doruyter[1], Patrick Dupont[2], Dan J Stein[3], Christine Lochner[4], James M Warwick[1]

[1]Stellenbosch University Faculty of Medicine and Health Sciences, Division of Nuclear Medicine, Cape Town, South Africa.
[2]KU Leuven, Department of Neurosciences, Laboratory of Cognitive Neurology, Leuven, Belgium.
[3]MRC Unit on Risk and Resilience in Mental Disorders, University of Cape Town Department of Psychiatry, Cape Town, South Africa.
[4]MRC Unit on Risk and Resilience in Mental Disorders, Stellenbosch University Department of Psychiatry, Cape Town, South Africa.

Publication status: Unpublished manuscript; being prepared for journal submission.

Abstract

In psychiatric research, nuclear imaging methods are complementary to those of magnetic resonance imaging (MRI). Nuclear methods can be used to study regional neural activity, and offer quantitative means of studying neurochemistry in-vivo. While recent neuroimaging reviews in social anxiety disorder (SAD) have predominantly focused on studies using MRI, the purpose of this paper was to review the contribution of nuclear imaging methods in SAD research to date. We discuss developments in, and future directions of nuclear imaging research in this field.

Keywords: social anxiety disorder, positron emission tomography, single photon emission computed tomography; functional neuroimaging; molecular imaging

Introduction

Social anxiety disorder (SAD) is characterized by excessive anxiety in social or performance situations, a marked fear of negative evaluation, embarrassment and humiliation, leading to

clinically significant distress and functional impairment (American Psychiatric Association and DSM-5 Task Force 2013). Epidemiological data demonstrate that the condition is common, with a 6–12 % lifetime prevalence in developed countries (Kessler RC et al. 2005; Stein et al. 2010, 2017). Why developing countries seem to have lower prevalence rates of SAD (e.g. 2.8% in South Africa) (Stein et al. 2008) is uncertain, but may relate to both genetic and environmental factors, as well as underreporting to lay interviewers. Functional impairment and morbidity due to SAD is frequently severe. Sufferers experience lower quality of life, higher rates of unemployment and longer absences from work, together with greater risk of suicide and increased comorbidity of depression and substance abuse (Wittchen and Beloch 1996; Lecrubier et al. 2000; Katzelnick et al. 2001). There is evidence that both genetic and environmental factors play a role in the pathogenesis of SAD (Mathew et al. 2001; Miskovic and Schmidt 2012; Fox and Kalin 2014) but research into how the disorder develops, which neurobiological processes are involved, and why only some patients respond favourably to therapy is still a long way from complete.

Current clinical guidelines on the management of SAD advocate cognitive behavioural therapy or pharmacotherapy as first line options. While many patients experience improvements in symptoms from these therapies, the proportion of patients that fully remit is uncertain (National Collaborating Centre for Mental Health (UK) 2013). Certainly, a significant proportion of patients experience minimal or no relief from therapy while responders frequently experience a recurrence of the disorder (Bruce et al. 2005). Greater understanding of how various treatments exert their effects in SAD and whether neuroimaging biomarkers can predict therapy response may represent a key focus of future research efforts.

Neuroimaging modalities represent valuable tools to investigate brain function in psychiatric disorders, including in SAD. Several excellent reviews and meta-analyses of functional neuroimaging in SAD have consistently highlighted hyperactivity in limbic and paralimbic structures (Etkin and Wager 2007; Freitas-Ferrari et al. 2010) and have led to a network model of the disorder (Brühl et al. 2014a). Of these reviews, only those by Freitas-Ferrari et al. and Etkin and Wager included nuclear neuroimaging studies, while Brühl et al. focused exclusively on magnetic resonance imaging (MRI-) based work. Several additional nuclear imaging experiments have been conducted since the publication of these reviews. The aim of this narrative review is to summarize the contribution of nuclear neuroimaging to the SAD literature to date, and thereby complement recent reviews that have omitted molecular imaging

experiments. In the next section of this paper we will provide a brief introduction to nuclear imaging techniques and compare them to more familiar magnetic resonance methods.

Methods

Relevant literature was identified using the search terms ("social phobia" OR "social anxiety") AND ("SPECT" OR "SPET" OR "single photon" OR "positron" OR "PET") in PubMed (https://www.ncbi.nlm.nih.gov/pubmed).

Nuclear imaging techniques

Nuclear emission imaging (nuclear imaging) techniques rely on the principle that certain radionuclides emit gamma photons as a consequence of nuclear decay. These gamma photons pass through human tissue and can be detected and localized in three-dimensional space with specialized scanners. After injecting molecules of interest, labelled with such radionuclides (radiotracers), it is possible to image the brain at a specific time (static imaging) or, with certain radiotracers, over extended periods (dynamic imaging). Depending on the properties of the radiotracer and the limitations of the imaging system, various study designs allow researchers to investigate a variety of neurophysiological processes at rest, as well as during or after intervention.

Imaging of radioactive emissions can be broadly separated into two main technologies, defined by the characteristics of the radioactive decay they image. Radionuclides that emit a *single* gamma photon per radioactive decay event are imaged using single photon emission computed tomography (SPECT). SPECT cameras are typically designed with one or more rectangular detectors that rotate around a patient. These detectors rely on collimation to register only photons travelling perpendicular to the detector plane, thereby limiting the emission location to somewhere in line with the relevant collimator hole. In this way, SPECT systems are able to record a series of two-dimensional projections from different angles and reconstruct these into a single three-dimensional volume, in which the regional distribution of radiotracer is relatively accurately represented.

Some radionuclides decay by emission of a positron (the antiparticle of an electron). The positron and a nearby electron will annihilate which results in the simultaneous emission of *two* photons travelling in opposite directions, per decay event. These photons are imaged using positron emission tomography (PET). Unlike SPECT cameras, modern PET cameras typically have hundreds of detector elements arranged in multiple ring arrays. These ring arrays completely encircle the subject and are stationary. Due to the fact that the photons of positron decay are emitted simultaneously and in opposite directions (180°), these systems are able to localize the location of a decay event (and thus the position of a radiotracer molecule) as somewhere between two detectors that have registered a simultaneous detection (coincidence) event. Coincidence logic results in more precise "lines of response" than those obtained with collimation in SPECT, with resultant improvements in spatial resolution and quantitative accuracy. With advancements in electronics, it has become possible to measure tiny discrepancies in the arrival time (at the detector) of each photon pair produced by positron decay, which allows systems to estimate a likely origin zone along individual lines of response, thereby improving spatial resolution still further. Our group has demonstrated previously how such time of flight (TOF) techniques are of benefit in brain imaging (Moalosi 2016). The simultaneous coverage of most projection angles as well as the superior localization capability of PET systems, make it better suited than SPECT to perform quantitative imaging and to image dynamic processes in vivo. The superior temporal and spatial resolution of PET is especially valuable in tracer kinetic modelling (Nelissen et al. 2012). Both PET and SPECT systems make corrections for the amount of attenuation photons undergo while traveling through tissues, typically by using serially-acquired low-dose x-ray computed tomography (CT). The principles of SPECT and PET imaging are illustrated in **Fig 1.1**, while examples of SPECT and PET images of the brain are illustrated in **Fig 1.2**. Examples of the (patho-) physiological processes that can be imaged with nuclear techniques, and the relevant radiotracers are summarized in **Table 1.1**. Much of the growth in the development of these tracers is driven by the fact that with carbon-11, a positron emitter, it is theoretically possible to manufacture the radiotracer equivalent of any molecule of interest, provided it contains carbon. In practice, the utility of such tracers is constrained by laboratory capability in producing the radiolabelled molecules of interest as well as the physical half-life of the relevant radionuclides which inherently limits the duration they can be imaged. It should also be pointed out that imaging of C-11 based tracers necessitates an on-site cyclotron, due to this isotope's short half-life (20 min). There has however also been quite some work on tracers labelled with

fluorine-18 which due to its longer half-life (110 min) hold greater promise for commercial applications.

Comparison with magnetic resonance imaging

Like nuclear methods, MRI can be considered a functional neuroimaging modality. MRI relies on the application of a powerful magnetic field to modify the orientation of the spin of endogenous hydrogen atoms. The radiofrequency excitation induced in the brain by this magnetic field, can be detected using specialized coils.

The targets of functional neuroimaging (both nuclear and MR-based) can be divided into two main categories: *neuronal activity*, and *neurochemistry*.

While neuronal activity cannot be imaged directly, the tight coupling between neuronal firing and blood flow (neurovascular coupling), as well as neuronal firing and metabolism (neurometabolic coupling) offers several indirect means of imaging neural activity in vivo (Bélanger et al. 2011). In the case of functional magnetic resonance imaging (fMRI) this is performed by blood oxygen level dependent (BOLD) or arterial spin labelling (ASL) imaging which rely on the magnetic properties of either deoxyhaemoglobin or intra-arterial water respectively, to perform rapid, sequential imaging. In the case of nuclear imaging, measures of regional neuronal activity are obtained through dynamic imaging of regional cerebral blood flow with O-15 water PET, or by using static techniques such as F-18 fluorodeoxyglucose (FDG) PET and Tc-99m hexamethyl propylene amine oxime (HMPAO) SPECT which typically image integrated activity over a standardized uptake period. Nuclear and magnetic resonance techniques offer complementary information in this regard. Major advantages of fMRI techniques relate to their good temporal resolution and lack of ionizing radiation. Major advantages of nuclear methods relate to their relative resistance to artefact; homogeneity of signal-to-noise ratio; and the close correlation between the signal detected and target physiological processes. With both fMRI and nuclear methods, it is possible to analyse interregional correlations in neuronal activity (functional brain networks). Depending on the neuroimaging method, such brain networks can either be analysed using interregional temporal correlations or interregional cross-subject correlations, or both. A summary comparison of

fMRI and common nuclear techniques for the measurement of regional neural activation is presented in **Table 1.2**.

The other main research area in functional neuroimaging is brain chemistry. The ability to perform in-vivo imaging of biologically active compounds in the brain has the potential to provide great insight into neurobiology and broaden our understanding of therapy effects. Again, both magnetic resonance and nuclear techniques play complementary roles in this regard. Magnetic resonance spectroscopy (MRS) is a technique that records a spectrum of atomic nuclear (typically proton – ^{1}H) resonances across a range of magnetic gradients for different regions of brain tissue, typically on a voxel level (McRobbie 2006). On the basis that different brain metabolites exhibit different frequencies of resonance, it is theoretically possible to measure in vivo concentrations of these molecules by isolating individual peaks in the imaged spectra (**Fig 1.3**). It is also possible to perform dynamic MRS (fMRS) to study real-time changes in brain chemistry (Apšvalka et al. 2015). There are currently two main factors that limit the application of MRS in imaging of brain function however. The first relates to the technical difficulties in separating peaks in the MR spectra. Peaks (of different chemicals) overlap, making accurate determination of individual chemical concentrations challenging, especially at the low (and frequently heterogeneous) signal to noise ratios experienced in 3-tesla (3T) scanners (McKay and Tkáč 2016). The second limitation of MRS relates to the range of molecules that can currently be imaged. While with proton (^{1}H) imaging, it is theoretically possible to quantify regional concentrations of about 20 chemicals (**Fig. 1.3**), and by imaging other nuclei (e.g. ^{13}C, ^{19}F) it is possible to image administered tracers labelled with these isotopes (including organic molecules such as glucose) (McRobbie 2006), the accurate quantification of these chemicals typically requires very high magnetic field strengths (7T) and techniques to make quantification reliable are still in development. Currently with 3T MRI cameras it is possible to quantify regional concentrations of only four molecules, namely lactate, creatine, choline and N-acetylaspartate (McKay and Tkáč 2016). On the other hand, techniques for investigating neurochemistry with PET and SPECT are highly sensitive and less constrained by technical challenges; are already well-validated and are more widely available. A large number of radiotracers that can be used to accurately and quantitatively probe neurochemical processes already exists and continues to grow (for examples see **Table 1.1**).

In the next section of this review we will focus on the contribution nuclear neuroimaging methods have made to SAD research.

Nuclear imaging in SAD: blood flow

Rest

Research into regional cerebral blood flow (rCBF) during resting conditions in SAD is limited to two studies that used HMPAO SPECT. Confining their analysis to 9 a priori regions of interest (ROIs), Stein and Leslie reported no differences in rCBF between their SAD and healthy control (HC) groups (Stein and Leslie 1996). In contrast, Warwick et al. performed a whole brain, voxel-based analysis and reported increased rCBF in several frontal regions and in cerebellum, as well as rCBF reductions in pons, cerebellum and precuneus (Warwick et al. 2008). Disease severity in that study correlated positively with a frontal cluster and negatively with clusters in the fusiform and lingual gyri. Data from the same study were later used to perform a whole-brain analysis of resting functional connectivity (RFC) of 14 a priori seed regions, with interregional correlations performed on a cross-subject basis (Doruyter et al. 2016). That study found that in the SAD group there was reduced connectivity between amygdala and a frontal cluster; as well as between a posterior cingulate cortex/precuneus seed and a cerebellar cluster; and increased connectivity between thalamus and a frontal cluster.

Several studies have investigated the effect of therapy on resting rCBF in SAD. A single dose of cannabidiol has been shown to reduce resting rCBF measured with Tc-99m ECD SPECT in parahippocampal gyrus, hippocampus, and inferior temporal gyrus and increase rCBF in posterior cingulate (Crippa et al. 2011). Van der Linden et al. reported that after a course of a selective serotonin reuptake inhibitor (SSRI; citalopram), SAD participants exhibited reductions in resting rCBF measured with Tc-99m HMPAO SPECT in anterior and lateral temporal cortex, multiple mid-frontal cortical regions and the left cingulum, and that baseline rCBF in several temporal and frontal regions was higher in responders than in non-responders (van der Linden et al. 2000). Combining this dataset with a similar group of SAD participants treated with moclobemide (a MAO-A inhibitor), Warwick et al. performed a whole-brain analysis and reported reductions (in the combined groups) in bilateral insula post-therapy (Warwick et al. 2006). They also found that when comparing subgroups, participants treated with citalopram demonstrated a greater reduction in superior cingulate rCBF than those treated with moclobemide. A later analysis of this data by the same group reported that

pharmacotherapy resulted in increased RFC of dorsal anterior cingulate cortex (ACC) with precuneus and middle occipital gyrus (Doruyter et al. 2016). In a combined group consisting of participants with SAD; OCD; or PTSD, Carey et al. reported reductions in resting rCBF (on HMPAO SPECT) to superior cingulate, right thalamus, ACC, and left hippocampus after a course of citalopram (Carey et al. 2004).

Provocation

Most nuclear rCBF studies in SAD have been performed using provocation paradigms (all using O-15 water PET). These studies typically imaged participants during the performance of a task designed to elicit disorder-specific anxiety (e.g. a public speech), sometimes combined with the use of a control condition (e.g. a private speech). This work has added to knowledge on the neurological correlates of social anxiety in SAD. For example, in studies performed on SAD samples only, such stressors induced reductions in rCBF in temporal pole and cerebellum (Tillfors et al. 2002) and lingual gyrus and medial frontal gyrus (van Ameringen et al. 2004); and increases in rCBF in dorsolateral prefrontal cortex, inferior temporal cortex and the amygdalo-hippocampal region (Tillfors et al. 2002). Several of these studies also found correlations between anxiety levels during such provocation experiments and rCBF to distributed brain regions (Tillfors et al. 2001; Laukka et al. 2011). Only two provocation studies have compared SAD and HC groups: Tillfors et al. reported provocation-induced rCBF reductions in SAD and increases in HC in orbitofrontal, insular, and temporal pole regions and also reported a less marked increase in rCBF to parietal and secondary visual cortices and absent responses in rCBF to perirhinal and retrosplenial cortices in the SAD group (Tillfors et al. 2001). Kilts et al. reported provocation-induced rCBF differences between HC and SAD groups in fusiform, lingual, and middle temporal gyri; lateral orbitofrontal cortex; temporal pole; and hippocampus (Kilts et al. 2006). Although not demonstrably specific to the disorder, several studies have also found some interesting physiological correlates to rCBF changes on provocation in SAD samples. Correlations between rCBF and stress-induced cortisol levels (Åhs et al. 2006), high-frequency heart rate variability (Åhs et al. 2009), and functional polymorphisms in the human serotonin transporter gene (Furmark et al. 2004) have been reported in SAD.

In line with the National Institute of Mental Health Research Domain Criteria (RDoC) initiative (Cuthbert and Insel 2013), the neural mechanisms of conditioned fear extinction in SAD have

been studied by Åhs et al. who reported reductions in amygdalar (but not in ventromedial prefrontal cortex or hypothalamic) rCBF upon repeat provocation (Åhs et al. 2017). Provocation work by Fredrikson and Furmark found evidence to suggest functional lateralization of the amygdalae. Work from their laboratory suggests that rCBF in the right but not left amygdala during provocation is positively correlated with anxiety provocation in SAD, specific phobia, post-traumatic stress disorder, and fear conditioning in healthy volunteers (Fredrikson and Furmark 2003).

Studies investigating how therapy affected rCBF changes during provocation of social anxiety using O-15 water PET have reported some interesting results. Furmark et al. found that placebo-induced reductions in amygdalar rCBF during provocation were demonstrable only in patients with certain serotonergic polymorphisms (Furmark et al. 2008), providing important information on the possible mechanisms of the placebo effect. Compared to placebo, there is evidence that SSRIs, cognitive behavioural therapy and the experimental NK-1 antagonist vofopitant (GR205171) all result in reductions in rCBF to rhinal cortex, amygdala, hippocampal and parahippocampal regions, and that these reductions are greater in responders than non-responders (Furmark et al. 2002, 2005). Similar results were reported by Faria et al. who found that responders to SSRI therapy (citalopram or paroxetine) and placebo demonstrated greater reductions in amygdalar rCBF during provocation (Faria et al. 2012) and that the changes in provocation-related functional connectivity of the amygdala were different between responders and non-responders (Faria et al. 2014). Interestingly however, that group reported no difference in rCBF changes between patients that responded to SSRI and those that responded to placebo (Faria et al. 2012). Frick et al. reported that citalopram (SSRI), vofopitant (NK-1 receptor antagonist GR205171) and placebo all resulted in reductions in provocation-induced amygdalar rCBF and that this was paralleled by reductions in amygdalar serotonin synthesis rates measured on C-11 5-hydroxtryptophan PET (Frick et al. 2016). Work by Kilts et al. found that a course of nefazodone (a phenylpiperazine serotonin reuptake inhibitor and 5-HT2 receptor antagonist) led to reductions in rCBF during provocation in precentral gyrus, insula, midbrain/hypothalamus, and middle frontal and dorsal anterior cingulate cortices; and increases in middle occipital and bilateral lingual gyri, postcentral gyrus, gyrus rectus and hippocampus (Kilts et al. 2006).

Emotional processing

A single study has investigated affective processing in the disorder. Using O-15 water PET that study reported that in both SAD and HC groups, there were increases in amygdalar rCBF during the processing of angry faces. While no difference in this amygdalar response was detected between the two groups, the researchers did report a correlation between amygdalar reactivity and serotonergic polymorphisms (Furmark et al. 2009).

Nuclear imaging in SAD: metabolism

Only one study investigating regional glucose metabolism has to date been published in SAD (Evans et al. 2009). In that study, researchers used F-18 FDG PET to scan a group of SAD participants as well HCs at rest before and after a course of therapy with tiagibine, a γ-aminobutyric acid (GABA) reuptake inhibitor. Compared to controls, the SAD group demonstrated reduced metabolism in anterior cingulate cortex and ventromedial prefrontal cortex (vmPFC). After therapy, SAD participants exhibited increased metabolism in the vmPFC, the degree of response also being inversely correlated with baseline metabolism in this region – results which suggest a possible mechanism of treatment effect with this drug.

An illustration summarizing neural activity findings in SAD reported in nuclear imaging experiments is found in **Fig 1.4**.

Nuclear imaging in SAD: receptor-based research

Serotonin

Genetic modification of serotonergic targets in mice has implicated the serotonergic system in anxiety and depression phenotypes (Albert et al. 2014). The importance of the serotonergic system in SAD is further underscored by the relative efficacy of SSRIs in treating the disorder (Ipser et al. 2008). In-vivo, nuclear imaging of the serotonin system, targeting both presynaptic and post-synaptic neurons, has made important contributions to knowledge of serotonin's role in SAD. The rate of influx of C-11 5-hydroxytryptophan (C-11 5-HTP), a serotonin precursor, can be used to measure the rate of serotonin synthesis in presynaptic neurons. Studies using

this tracer suggest that in SAD there are higher rates of serotonin synthesis in hippocampus, basal ganglia, amygdala and anterior cingulate (Frick et al. 2015a; Furmark et al. 2016) and that serotonin synthesis decreases in amygdala after therapy, paralleled by reductions in amygdalar rCBF on O-15 water PET (Frick et al. 2016). Furmark et al. have linked high serotonin synthesis rates in amygdala and anterior cingulate with a specific genetic polymorphism (tryptophan-2 G-703T) in SAD (Furmark et al. 2016). Another means of probing presynaptic serotonergic function is by imaging the serotonin transporter (SERT). This was first performed in SAD by Kent et al, who performed PET with C-11 McN5652, which binds to SERT. In SAD participants at baseline and several months into a course of paroxetine they demonstrated increased occupancy of SERT during therapy (Kent et al. 2002). Using another PET ligand (C-11 DASB), Frick et al. have demonstrated that SAD participants have increased SERT binding potential (reflecting higher SERT availability) than HCs in the raphe nuclei region, caudate nucleus, putamen, thalamus, and insular cortex (Frick et al. 2015a). Only one study investigating post-synaptic serotonergic function has been performed in SAD. In that study, Lanzenberger et al. performed C-11 WAY-100635 PET to measure binding of the serotonin 1A (5-HT_{1A}) receptor in SAD and HC participants. That group reported significantly lower binding potentials in several limbic and paralimbic regions, including amygdala, anterior cingulate, insula and dorsal raphe nucleus in the patient group. Binding potential in the hippocampus was not affected (Lanzenberger et al. 2007). In a later analysis of the same data, the researchers also reported a negative correlation between serum cortisol levels and 5-HT_{1A} binding in amygdala, hippocampus and retrosplenial cortex across all subjects with stronger correlations in the amygdala and hippocampus in the SAD group (Lanzenberger et al. 2010). Given the discrete functional roles of different serotonergic targets in rodent models of anxiety (Albert et al. 2014), and the limited in-vivo imaging studies in humans with SAD, more research using these tracers is warranted.

Dopamine

The dopaminergic system has an established role in reward processing (Wise and Rompré 1989). Social interaction activates the reward system in similar ways to non-social rewards such a money, food or addictive substances (Richey et al. 2017). The rewards achieved through personal interactions are thought to drive social affiliation. Consequently, the observation that SAD sufferers typically shun social interaction has led some researchers to propose that the biology of SAD may have a dopaminergic component. Further evidence of dopamine's

possible role is that patients with idiopathic Parkinson's disease, a condition characterized by dopaminergic degeneration, have much higher rates of SAD that the general population or those with chronic medical conditions (Richard 2005). Several studies have investigated the dopaminergic system in SAD, both in striatum and in frontal and extrastriatal limbic regions. Similar to serotonergic targets, dopaminergic nuclear imaging can investigate both presynaptic neurons (using radiolabelled dopamine precursors, or tracers that target the dopamine transporter – DAT) and postsynaptic neurons (with ligands that bind to D1 and D2 receptors). All studies on presynaptic dopaminergic function in SAD have used SPECT tracers that target DAT, such as I-123 ioflupane, I-123 β-CIT, and Tc-99m TRODAT-1. Evidence from those studies has to date been inconclusive of abnormality in striatal DAT binding in SAD participants compared to healthy controls, with work suggesting decreases (Tiihonen et al. 1997), no difference (Schneier et al. 2009), or increases (van der Wee et al. 2008a) in the disorder. Postsynaptic dopaminergic research in SAD has focused on D2 receptors and has been similarly inconclusive of abnormality in the disorder. The earliest study by Schneier et al. used I-123 IBMZ to image D2 receptor binding and reported reduced striatal D2 binding potential in SAD compared to controls but found no significant correlation with disease severity (Schneier et al. 2000). Later studies by the same group (Schneier et al. 2009) found no difference in striatal D2 binding between SAD and HC groups using C-11 raclopride PET (an arguably more reliable technique). Plavén-Sigray et al. performed PET with another D2 receptor ligand, C-11 FLB457 and confined their analysis to extrastriatal regions. They reported increased D2 binding in SAD in orbitofrontal cortex and dorsolateral prefrontal cortex (Plavén-Sigray et al. 2017).

The effects of therapy on nuclear dopaminergic measures has also been investigated in SAD. The effect of escitalopram therapy on DAT binding was studied by Warwick et al. who reported a therapy-related increase in striatal DAT binding measured on I-123 ioflupane SPECT though no correlation between symptom improvement and binding was found (Warwick et al. 2012). Post-therapy increases in caudate DAT binding in that study was also seen in a subgroup of patients that were homozygous for A10 DAT genotype. Cervenka et al. investigated the effect of cognitive behavioural therapy (CBT) on the interaction between disease severity and extrastriatal D2 binding in SAD by performing C-11 FLB 457 PET(Cervenka et al. 2012). They reported a relationship between symptom reduction after CBT and D2 binding in dorsolateral prefrontal cortex, medial prefrontal cortex and hippocampus. This study was also noteworthy in that it reinforced the understanding of psychotherapy as a *biological* intervention, in many

respects comparable to pharmacotherapy (Linden 2006). Studies that used nuclear techniques to investigate dopaminergic function in SAD patients with comorbid Parkinson's disease (Moriyama et al. 2011) and obsessive-compulsive disorder (Schneier et al. 2008) have also been conducted.

Conflicting results from these few available nuclear imaging studies suggest that further research is necessary to establish the role (if any) of dopamine in the disorder. Continued interest in dopamine is supported by several recent fMRI studies of the reward system in SAD, which reported differences in how SAD participants process both monetary and social reward (Manning 2015; Cremers et al. 2015; Richey et al. 2017), and research in healthy volunteers linking D1 binding in fusiform gyrus with performance on a facial recognition task (Rypma et al. 2015).

Substance P

High concentrations of the neurokinin-1 receptor (NK-1) are expressed in several limbic structures (Ribeiro-da-Silva and Hökfelt 2000) and it has been suggested that substance P, which binds to this receptor, may play an important role in anxiety disorders (Ebner et al. 2008). A single study that used the PET radiotracer C-11 GR205171 to image NK-1 binding in SAD demonstrated that compared to HCs, NK-1 binding in the amygdala was higher in the disorder (Frick et al. 2015b).

An illustration summarizing the findings of nuclear imaging experiments that targeted neurotransmitter systems in SAD is found in **Fig 1.5**.

Discussion and future directions

Much is already known about the neuroanatomy relevant in social anxiety (Miskovic and Schmidt 2012). Neuroimaging research using both fMRI and nuclear techniques further support functional models of SAD with increased neuronal activity in limbic and paralimbic regions during anxiety provocation in which reductions in anxiety lead to attenuation of this hyper-reactivity. Research using nuclear techniques has been complementary to fMRI research in this regard. Although resting-state fMRI has provided data on brain networks in the disorder,

PET and SPECT work has extended this work by focusing on regional resting neuronal activity and suggesting disrupted resting activity in key regions including medial frontal cortex, insula and fusiform gyrus as well as in regions that have to date received little consideration in SAD, such as cerebellum.

This knowledge, of regional neuronal activity in baseline conditions is important for two reasons. Firstly, it allows for the accurate interpretation of disruptions in resting-state functional connectivity, typically studied using resting-state fMRI. For example, a reduction in resting functional connectivity between two regions may be driven by increases or decreases in neuronal activity in either region or unequal increases or decreases in both. While it is relatively simple to identify interregional correlations at rest, teasing out the regional changes in neuronal activity that drive these correlations is more complex and is difficult to investigate with commonly used fMRI methods. Secondly, knowledge of both resting regional activity and resting functional connectivity is important in contextualizing the results of task-based experiments, since it shifts the focus from context-dependent changes (reactivity or functional connectivity on task) to intrinsic variations in the underlying functional network architecture (Tavor et al. 2016). Taken together then, nuclear techniques are useful in delineating the complex relationships between resting regional activity, resting connectivity and task-based reactivity.

Within regions involved in SAD, it is key to understand the relevant neurochemistry. A handful of nuclear imaging studies suggest roles for several neurotransmission systems, including serotonergic, dopaminergic and substance P, for which there is already evidence of disruption from other sources. Given their small number, additional studies of these neurotransmitter systems are justified. It is also worth noting that nuclear imaging of neurotransmitter targets in SAD has to date entirely focused on resting-state. Research using receptor-based PET imaging during task performance is also possible (Christian et al. 2006; Ceccarini et al. 2012) and will hopefully be conducted in SAD. Such research might prove key in our understanding of the behavioural correlates of functional neuroimaging findings. Beyond the systems presented in this review, the examples listed in **Table 1.1** show that there are multiple other molecular tracers (e.g. GABAergic, cholinergic, etc.) that present interesting research targets in SAD. In addition, progress is being made on the development of a PET tracer that is selective for the oxytocin receptor in the brain (Wenzel et al. 2016). This would raise the prospect of in-vivo imaging of central oxytocin action in SAD, which is of considerable interest given the putative

role of this peptide hormone in social anxiety and social cognition (Kirsch 2015). Research using new ligands has the potential to identify novel molecular targets for future drug development.

Nuclear studies of rCBF and metabolism have provided new insights into how anxiolytics change regional neuronal activity both at rest and during symptom provocation in SAD. More than this, imaging techniques that target specific brain receptors have identified differences in neurochemistry in the disorder. Such findings are relevant to our understanding of the neurobiology of SAD; and the mechanisms by which drugs exert their anxiolytic properties. This is relevant for drug discovery. While some early work suggests that certain nuclear imaging features can predict individual patients' response to a specific treatment, there is to date insufficient evidence that these predictors can be applied clinically. The prospect of personalized medicine based on molecular imaging results is tantalizing, and more research and the sharing of data will hopefully lead to progress in this regard.

Two further key developments have the potential to impact the role of nuclear imaging methods in SAD research in the near future. The first, and arguably most important of these, is the recent advent of hybrid PET/MR systems. The ability to simultaneously image BOLD or ASL signal and dynamically image a wide range of molecular targets, both during rest and during task, promises to transform functional neuroimaging research. The benefit of this synchronous measurement is that it allows for the direct temporal correlation between processes imaged by fMRI (such as neural activity) and those imaged by PET (such as neurotransmitter kinetics) – something impossible to do (due to the impossibility of perfectly matching scan conditions) with sequential imaging (Judenhofer et al. 2008; Wehrl et al. 2013). The second development relates to the establishment of shared data repositories, which provide open access to researchers. Initiatives such as the Human Connectome Project and UK Biobank (which currently include only MRI-based neuroimaging data) have enabled mega-analyses that vastly increase statistical power, and also allow researchers to use normative modelling as an alternative to the typical clustering used in case-control studies (Marquand et al. 2016). Similar benefits are seen from the trend towards large-scale, international collaborations such as the ENIGMA consortium (Thompson et al. 2017). The future inclusion of nuclear imaging data in such repositories and collaborations would potentially add great value to new research initiatives, especially when studied in combination with phenotyping and genotyping data.

Conclusion

Nuclear neuroimaging techniques represent powerful tools to investigate brain function in SAD and the neurobiological effects of therapy that are complementary to MRI-based techniques, and have extended upon results of studies utilizing MRI. While basic models of the fear response are now well-characterized, research into both regional activity and interregional relationships of diverse brain regions outside of the limbic and paralimbic circuits must still be conducted. Limited nuclear imaging evidence of disrupted neurochemistry in the disorder requires further study to draw definitive conclusions and to provide a foundation for potentially targeting treatments based on individuals' molecular signatures. The development of novel brain tracers, the advent of hybrid PET/MRI systems, and the growth of open access data repositories which will hopefully include nuclear imaging contributions, all lend promise to high quality future research in this condition.

Contributors

Manuscript: A Doruyter
Manuscript review: All authors
Supervisors: JM Warwick, C Lochner

Conflicts of interest

None.

Acknowledgments

The PhD from which this work emanated was funded by the South African Medical Research Council under the MRC Clinician Researcher Programme.
The authors would like to thank the Nuclear Technologies in Medicine and the Biosciences Initiative (NTeMBI), a national technology platform developed and managed by the South African Nuclear Energy Corporation (Necsa) and funded by the department of Science and Technology.

No funder played any role in study design; collection, analysis, or interpretation of data; in the writing of this article or in the decision to submit it for publication.

Tables and Figures

Table 1.1 Selected (patho-) physiological processes relevant to neuroscience that can be studied with nuclear imaging (Fumita and Innis 2002; Ross and Seibyl 2004; Heiss and Herholz 2006; Paterson et al. 2013; Venneti et al. 2013; Hommet et al. 2014; Fowler et al. 2015; Kassenbrock et al. 2016; Tronel et al. 2017).

(Patho-) physiological process	Molecular target	Example radiotracer(s)	Imaging modality	SAD
Proxies of regional neuronal activity				
Blood flow	N/A	O-15 water	PET	*
Regional perfusion (no temporal component)	Lipid cell membrane	Tc-99m HMPAO Tc-99m ECD	SPECT SPECT	* *
Glucose metabolism	Hexokinase	F-18 FDG	PET	*
Neurotransmitter systems				
Monoaminergic	$VMAT_2$	C-11 DTBZ	PET	
	MAO_A	C-11 clorgyline	PET	
	MAO_B	C-11 L-deprenyl-D2	PET	
Dopaminergic	AADC	F-18 FDOPA	PET	
	DAT	I-123 ioflupane I-123 β-CIT Tc-99m TRODAT C-11 cocaine	SPECT SPECT SPECT PET	* * *
	D1	C-11 SCH-23390	PET	

	D2-like	I-123 IBZM C-11 raclopride C-11 FLB457 F-18 fallypride	SPECT PET PET PET	* * *
Serotonergic	TPH2	C-11 HTP	PET	*
	$5\text{-}HT_{1A}$	C-11 WAY-100635	PET	*
	$5\text{-}HT_{1B}$	C-11 AZ10419369	PET	
	$5\text{-}HT_{2A}$	F-18 Altanserin	PET	
	$5\text{-}HT_{4}$	C-11 SB207145	PET	
	$5\text{-}HT_{6}$	C-11 GSK215083	PET	
	SERT	C-11 DASB C-11 McN5652	PET PET	* *
Noradrenergic	NET	F-18 FMeNER-D2	PET	
GABAergic	$GABA_A$	C-11 FMZ I-123 IOM	PET SPECT	
Endocannabinoid	CB_1	F-18 FMPEP-D2	PET	
Adenosine	A_1	C-11 MPDX	PET	
	A_{2A}	C-11 TMSX	PET	
Histaminic	H_1	C-11 pyrilamine	PET	
Cholinergic	AChE	C-11 donepezil	PET	
	mAChR	C-11 NMPB	PET	
	nAChR	I-123 5-I-A-85380	SPECT	
Opioid	MOR	C-11 carfentanyl	PET	
	MOR/KOR/DOR	C-11 DPN F-18 Cyclofoxy	PET PET	
Neuropeptide substance P	NK_1	C-11 GR205171	PET	*
Other				
Microglial/macrophage activity	TSPO	C-11 PK11195	PET	

Blood-brain barrier integrity	N/A	Tc-99m DTPA Ga-68 DTPA	SPECT PET	
Protein deposition	β-amyloid	C-11 PIB F-18 florbetaben F-18 florbetapir	PET PET PET	
	Tau	F-18 THK-5351 F-18 AV1451	PET PET	

Abbreviations: **5-HTP**:5-hydroxytryptophan**; 5-HT$_{1A/1B/2A/4/6}$**: serotonin receptor type 1A/1B/2A/4/6; **5-I-A-85380**: 5-iodo-3-[2 (S)-2-azetidinylmethoxy] pyridine; **A$_{1/2A}$**: adenosine receptor type 1/2A; **AADC**: aromatic L-amino acid decarboxylase; **AChE**: acetylcholine esterase; **AV1451**: 7-(6-fluoropyridin-3-yl)-5H-pyrido[4,3-b]indole; **AZ10419369**: 5-methyl-8-(4-methylpiperazin-1-yl)-N-(4-morpholin-4-ylphenyl)-4-oxochromene-2-carboxamide; **C-11**: carbon-11; **CB$_1$**: cannabinoid receptor type 1; **D$_{1/2}$**: dopamine receptor type 1/2; **DASB**:3-amino-4-(2-dimethylaminomethylphenylsulfanyl)-benzonitrile; **DAT**: dopamine transporter; **DPN**: diprenorphine ; **DTBZ**: dihydrotetrabenazine ; **DTPA**: diethylenetriaminepentaacetic acid; **ECD**: ethyl cysteinate dimer; **F-18**: fluorine-18; **FDG**: fluorodeoxyglucose; **FDOPA**: fluorodeoxyphenylalanine; **FMeNER-D2**: (S,S)-2-(a-(2-fluoro[2H2]methoxyphenoxy)benzyl)morpholine; **FMPEP-D2**: (3R,5R)-5-[3-[dideuterio(fluoranyl)methoxy]phenyl]-3-[[(1R)-1-phenylethyl]amino]-1-[4-(trifluoromethyl)phenyl]pyrrolidin-2-one; **FMZ**: flumazenil; **FLB457**: (S)-(-)-5-bromo-N-((1-ethyl-2pyrrolidinyl)methyl)-2,3-dimethoxybenzamide; **GABA**: gamma-aminobutyric acid; **GABA$_A$**: benzodiazepine receptor type A; **GR205171**: (2S,3S)-N-[[2-[11C]methoxy-5-[5-(trifluoromethyl)tetrazol-1-yl]phenyl]methyl]-2-phenyl-piperidin-3-amine; **GSK215083**: 3-(3-fluorophenyl)sulfonyl-8-(4-methylpiperazin-1-yl)quinoline; **H$_1$**: histamine receptor type 1; **HMPAO**: hexamethyl propylene amine oxime; **I-123**: iodine-123; **IBZM**: iodobenzamide ; **IOM**: iomazenil; **mAChR**: muscarinic acetylcholine receptor; **MAO$_{A/B}$**: monoamine oxidase A/B; **McN5652**:(6R,10bS)-6-(4-methylsulfanylphenyl)-1,2,3,5,6,10b-hexahydropyrrolo[2,1-a]isoquinoline; **MOR/KOR/DOR**: μ-/κ-/δ-opioid receptor; **MPDX**: 8-(dicyclopropylmethyl)-1-methyl-3-propyl-7H-purine-2,6-dione; **nAChR**: nicotinic acetylcholine receptor; **NET**:

noradrenaline (norepinephrine) transporter; **NMPB**: N-methyl-4-piperidylbenzilate ; **NK_1**: neurokinin receptor 1; **O-15**: oxygen-15; **PET**: positron emission tomography; **PIB**: Pittsburgh compound B; **PK11195**: 1-(2-Chlorophenyl)-N-methyl-N-(1-methylpropyl)-3-isoquinolinecarboxamide; **SB207145**: (4-{[(8-amino-7-chloro-2,3-dihydro-1,4-benzodioxin-5-yl)carbonyloxy]methyl}piperidin-1-yl)methylidyne; **SCH 23390**: 8-chloro-3-methyl-5-phenyl-1,2,4,5-tetrahydro-3-benzazepin-7-ol; **SPECT**: single photon emission tomography; **Tc-99m**: technetium-99m; **THK-5351**: (2S)-1-fluoro-3-[2-[6-(methylamino)pyridin-3-yl]quinolin-6-yl]oxypropan-2-ol; **TMSX**: 7-methyl-(E)-8-(3,4,5-Trimethoxystyryl)-1,3,7-trimethylxanthine; 1,3,7-tri(methyl)-8-[(E)-2-(3,4,5-trimethoxyphenyl)ethenyl]purine-2,6-dione; **TPH2**: tryptophan hydroxylase-2; **TRODAT-1**: 2-[2-[[(1S,3S,4R,5R)-3-(4-chlorophenyl)-8-methyl-8-azabicyclo[3.2.1]octan-4-yl]methyl-(2-sulfanylethyl)amino]ethylamino]ethanethiol; **TSPO**: 18-kDa translocator protein; **$VMAT_2$**: vesicular monoamine oxidase A transporter type 2; **WAY-100635**: N-[2-[4-(2-ethoxyphenyl)piperazin-1-yl]ethyl]-N-pyridin-2-ylcyclohexanecarboxamide; **β-CIT**: methyl 3β-(4-iodophenyl) tropane-2b-carboxylate.

Tracers marked with a (*) have previously been used in SAD research.

Table 1.2 Comparison of MR and nuclear techniques to investigate regional neuronal activity (Arthurs and Boniface 2002; Detre and Wang 2002; Hertz and Dienel 2002; Zang et al. 2004, 2007; Zou et al. 2008; Kameyama et al. 2016)

	fMRI		**Nuclear**		
	BOLD	**ASL**	**O-15 water PET**	**Tc-99m HMPAO SPECT**	**F-18 FDG PET**
Physiological target	Blood flow; blood volume; oxygen consumption	Blood flow	Blood flow	Blood flow	Glucose metabolism
Tracer	Difference in magnetization between oxyhaemoglobin and deoxyhaemoglobin	Magnetically-labelled arterial water	Radioactive water	Radioactive, highly-lipophilic molecule	Radioactive glucose-analogue
Biological components of final signal	Neuronal and glial cell activity; neurometabolic coupling; neurovascular coupling; blood flow; blood oxygenation; blood volume; haematocrit	Neuronal and glial cell activity; neurovascular coupling; blood flow	Neuronal and glial cell activity; neurovascular coupling; blood flow	Integrated neuronal and glial cell activity; neurovascular coupling; blood flow	Integrated neuronal and glial cell activity; neurometabolic coupling; neurovascular coupling; blood flow; endogenous glucose and insulin concentration

Signal proportional to regional neuronal activity	No	Yes	Yes	Yes	Yes
Ability to quantify regional neuronal reactivity to stimulus	Excellent	Excellent	Good	Limited	Limited
Network characterization	Interregional **temporal** correlations	Interregional **temporal** correlations	Interregional **temporal** correlations	Interregional **cross-subject** correlations	Interregional **cross-subject** correlations
Spatial resolution	Excellent	Excellent	Fair	Fair	Good
Temporal resolution	Excellent	Good	Fair	N/A	N/A
Sensitivity	Fair	Fair	High	High	High
Effective radiation dose (mSv)	Nil	Nil	~ 1.5 †	~ 5.5 ††	~ 2.5 ‡
Artefact concerns	Susceptibility; motion; baseline drift; heterogeneity in magnetic field; noise (physiological; 1/f) (Detre and Wang 2002; Borogovac and Asllani 2012)	Vascular artefact; motion (less than BOLD); baseline drift (less than BOLD); low SNR; (Borogovac and Asllani 2012)	CT-based attenuation correction: artefact due to misregistration between CT and PET	CT-based attenuation correction: artefact due to misregistration between CT and SPECT	CT-based attenuation correction: artefact due to misregistration between CT and PET

Invasive	No	No	No, but intravenous access	No, but intravenous access	No, but intravenous access

Abbreviations: **ASL** – arterial spin labelling; **BOLD** – blood oxygen level dependent; **CT** – (x-ray) computed tomography; **EPI** – echo-planar imaging; **F-18 FDG** – Fluorine-18 fluorodeoxyglucose; **fMRI** – functional magnetic resonance imaging; **O-15** – oxygen-15; **PET** – positron emission tomography; **SPECT** – single photon emission tomography; **Tc-99m HMPAO** – Technetium-99m hexamethyl propylene amine oxime; **TE** – echo time; **TR** – repetition time;

† Based on administered dose of 1500 MBq (Andersson 2015)

†† Based on administration of 555 MBq (Andersson 2015)

‡ Based on administered dose of 150 MBq (Andersson 2015)

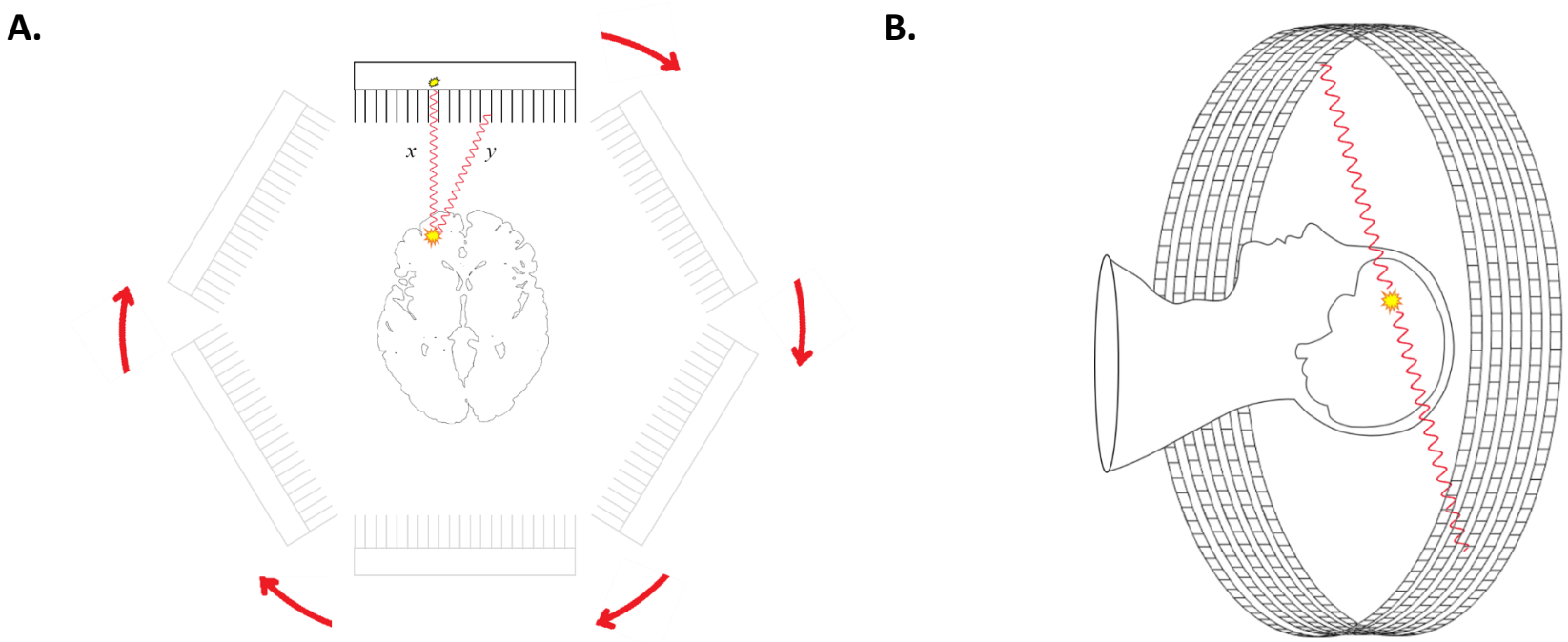

Figure 1.1 Basic principles of nuclear imaging. **A.** In single photon emission tomography (SPECT), one or more detectors rotate around the subject, which due to absorptive collimation, register only photons traveling perpendicular to the detector plane (*x*) and exclude photons that travel at oblique angles (*y*). SPECT imaging results in multiple 2-D projection images from different angles which are then reconstructed into a single 3-D image. **B.** In positron emission tomography (PET), individual decay events result in two gamma photons, traveling in opposite directions which are then detected near simultaneously (coincidence event). A line connecting these to the detectors registering these coincident events is known as a line of response (LOR). A typical PET scan will image millions of such LORs and this information is reconstructed into a 3-D image to accurately localize regional radiotracer concentrations.

A.

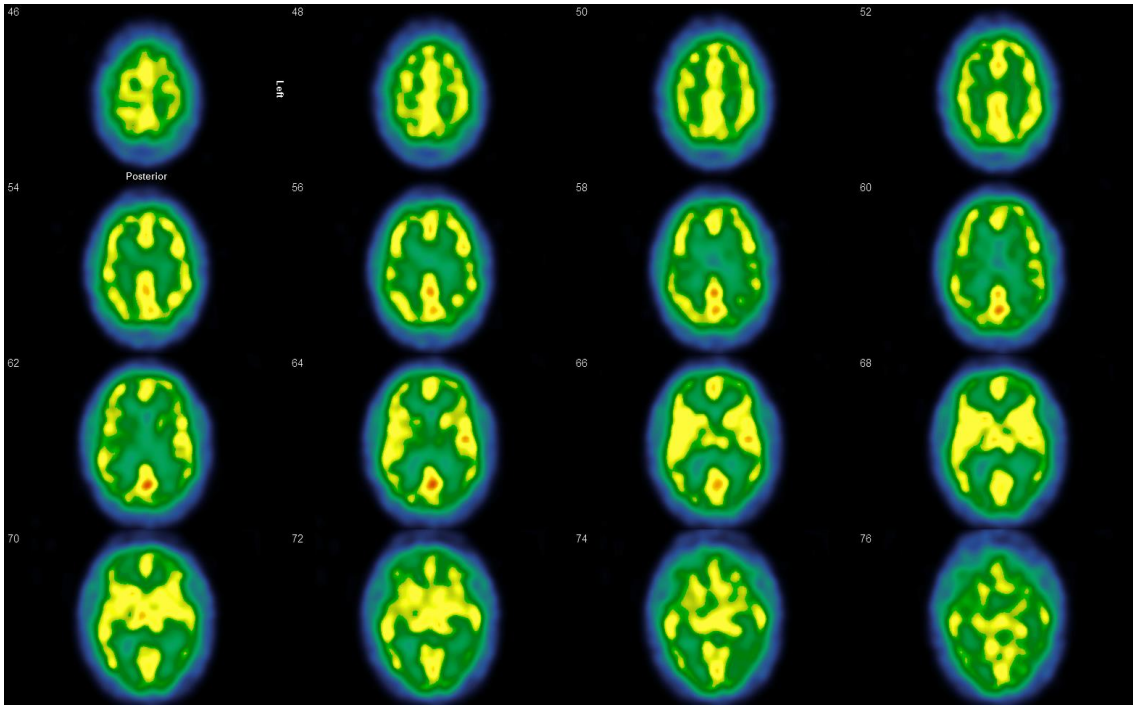

B.

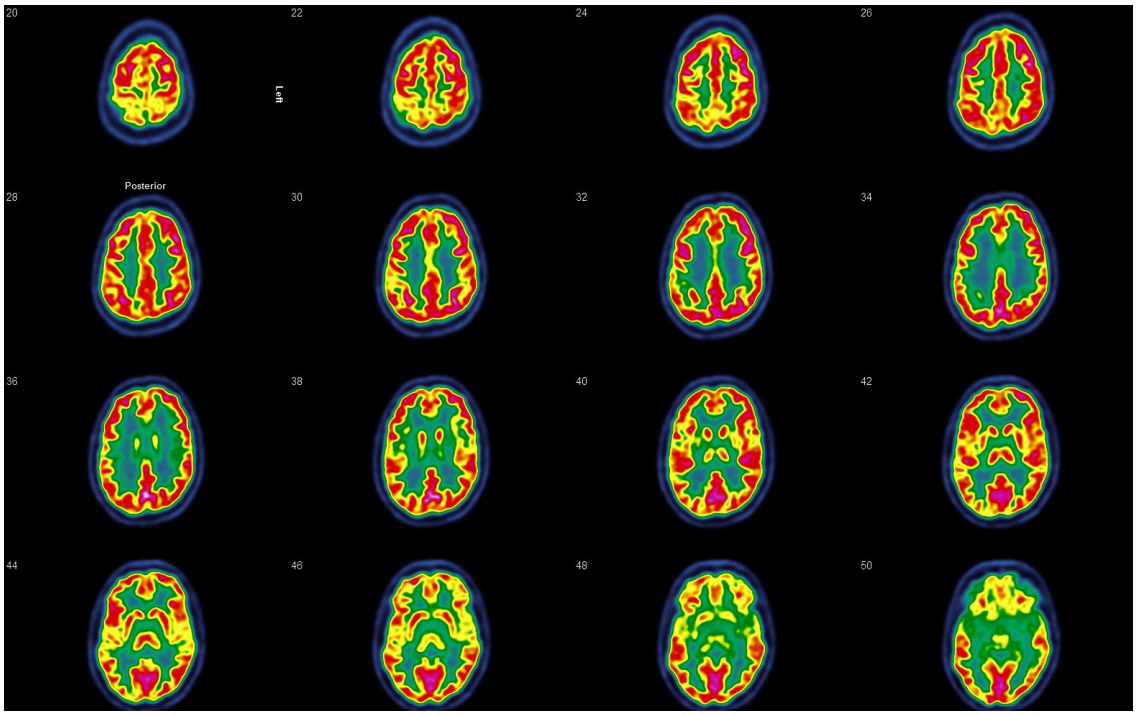

Figure 1.2 Examples of nuclear imaging techniques. **A:** Cerebral perfusion study performed with Tc-99m HMPAO SPECT (transverse slices). **B:** Cerebral metabolism study performed with F-18 FDG PET. Note the higher resolution of the PET images.

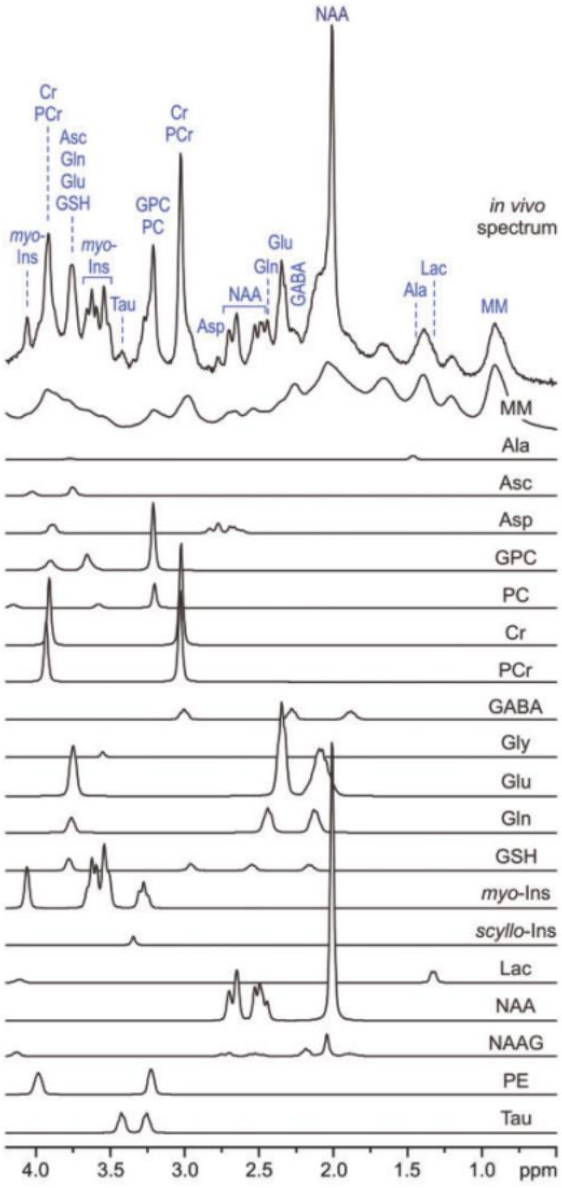

Figure 1.3 LCModel analysis of an in vivo 1H MR spectrum acquired from the human brain at 7T (STEAM, TE = 6 ms, TR = 5 s, NT = 160, grey-matter-rich occipital cortex). In vivo spectrum can be modelled as a linear combination of brain metabolite spectra from the LCModel basis set: macromolecules (**MM**), alanine (**Ala**), ascorbate (**Asc**), glycerophosphocholine (**GPC**), phosphocholine (**PC**), creatine (**Cr**), phosphocreatine (**PCr**), c-aminobutyric acid (**GABA**), glycine (**Gly**), glutamate (**Glu**), glutamine (**Gln**), glutathione (**GSH**), myo-inositol (**myo-Ins**), scyllo-inositol (**scyllo-Ins**), lactate (**Lac**), N-acetylaspartate (**NAA**), N-acetylaspartylglutamate (**NAAG**), phosphoethanolamine (**PE**), taurine (**Tau**). *Figure and legend from* (McKay and Tkáč 2016).

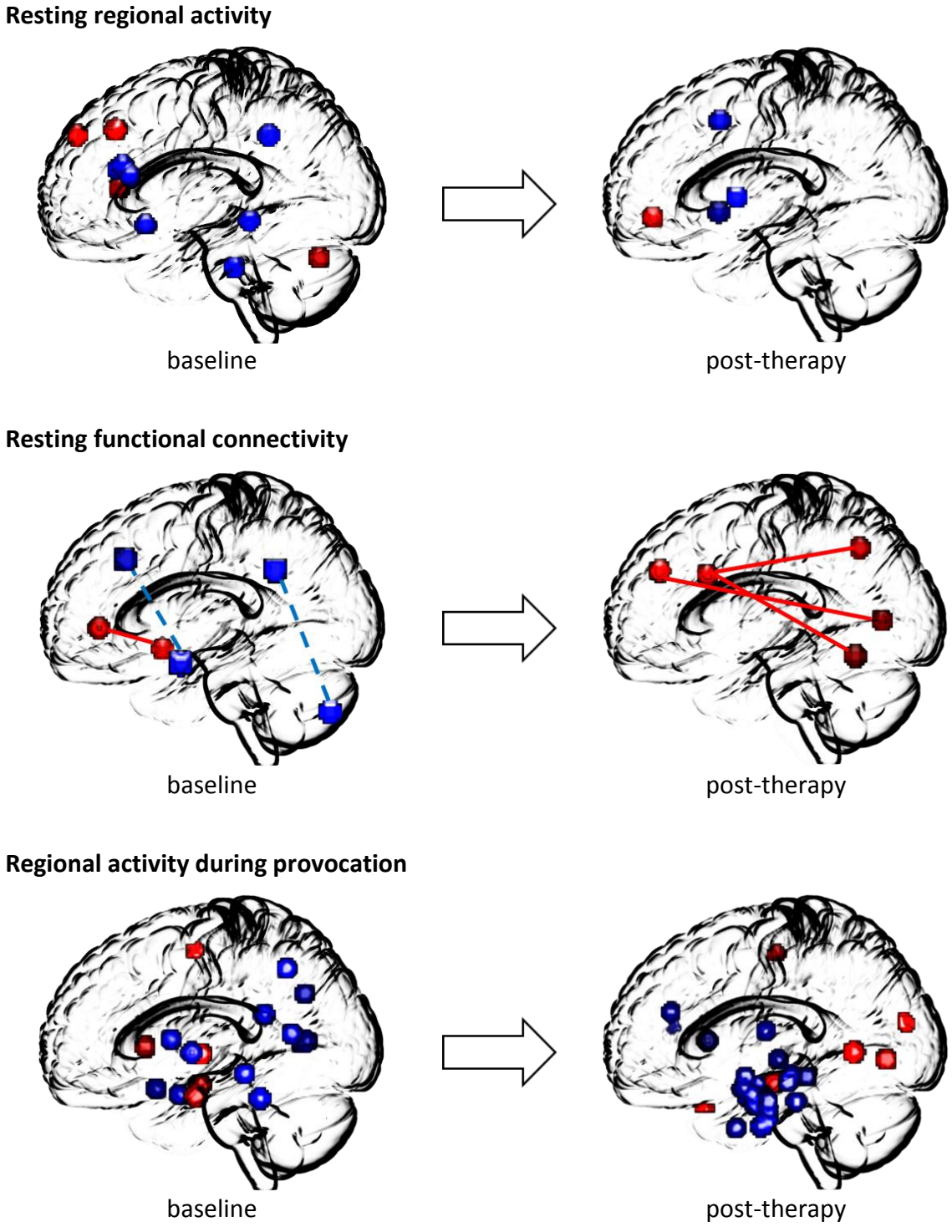

Figure 1.4 Summary of neural activity changes in SAD reported in nuclear imaging experiments. In SAD at baseline compared to healthy controls (left) and in SAD post-therapy (right). Spheres centred on reported cluster maxima. Red = increased; blue = decreased; red spheres with solid line = increased RFC; blue spheres with dashed line = decreased RFC. *Images generated in MRIcroGL (Chris Rorden, www.mricro.com).*

Serotonergic system

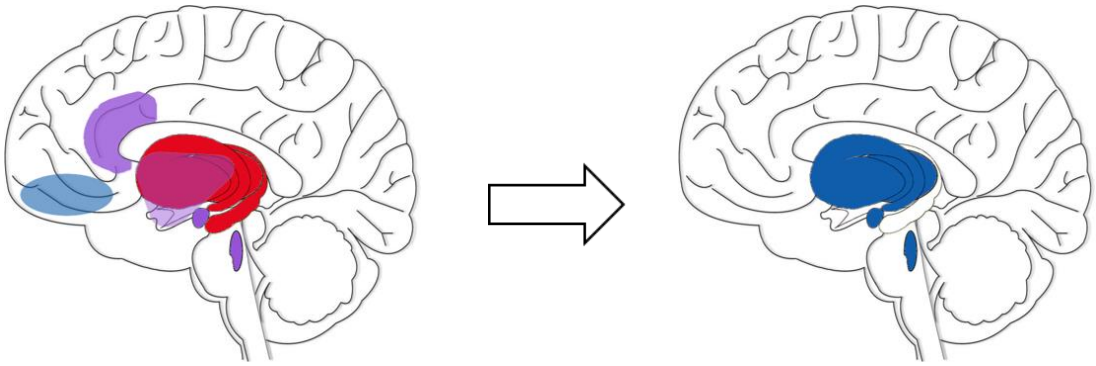

baseline post-therapy

Dopaminergic system

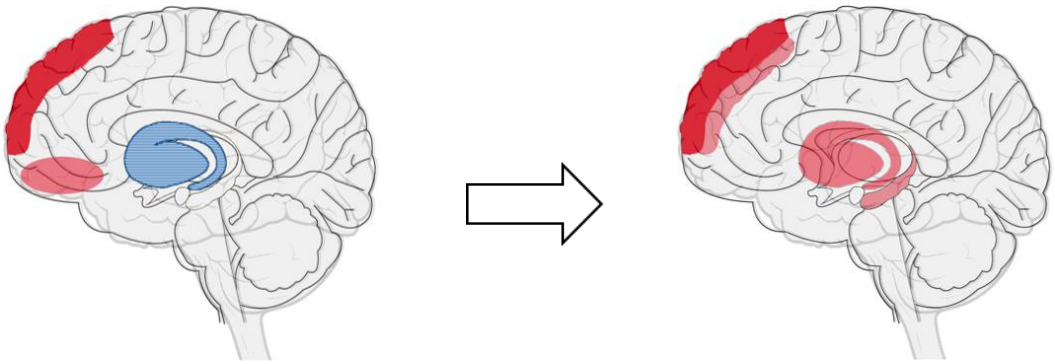

baseline post-therapy

Substance P

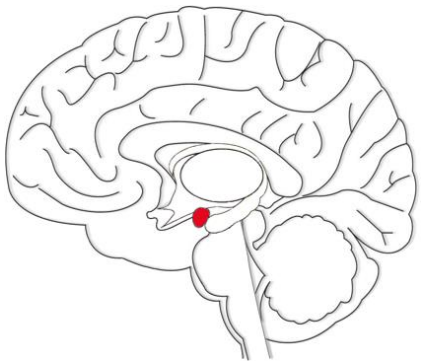

baseline

Figure 1.5 Summary of changes in neurotransmitter systems in SAD reported in nuclear imaging experiments. In SAD at baseline compared to healthy controls (left) and in SAD post-therapy (right). Implicated regions and structures are illustrated. Red = increased; blue = decreased; purple = both increased and decreased depending on molecular target. *Images generated using GNU Image Manipulation Program (GIMP) 2.8.14 (http://www.gimp.org/)*

Resting functional connectivity in social anxiety disorder and the effect of pharmacotherapy

Authors: Alexander Doruyter[1], Christine Lochner[2], Gerhard P. Jordaan[3], Dan J. Stein[4], Patrick Dupont[5], James M Warwick[1]

[1]Division of Nuclear Medicine, Faculty of Medicine and Health Sciences, Stellenbosch University, Cape Town, South Africa.
[2]MRC Unit on Risk and Resilience in Mental Disorders, Stellenbosch University Department of Psychiatry, Cape Town, South Africa.
[3]Stellenbosch University Department of Psychiatry, Cape Town, South Africa.
[4]MRC Unit on Risk and Resilience in Mental Disorders, University of Cape Town Department of Psychiatry, Cape Town, South Africa.
[5]KU Leuven, Department of Neurosciences, Laboratory of Cognitive Neurology, Leuven, Belgium.

Publication status: Published manuscript (Doruyter et al. 2016).

Abstract

Neuroimaging research has reported differences in resting-state functional connectivity (RFC) between social anxiety disorder (SAD) patients and healthy controls (HCs). Limited research has examined the effect of treatment on RFC in SAD. We performed a study to identify differences in RFC between SAD and HC groups, and to investigate the effect of pharmacotherapy on RFC in SAD. Seed-based RFC analysis was performed on technetium-99m hexamethylpropylene amine oxime (Tc-99m HMPAO) SPECT scans using a cross-subject approach in SPM-12. Seeds were chosen to represent regions in a recently published network model of SAD. A second-level regression analysis was performed to further characterize the underlying relationships identified in the group contrasts. Twenty-three SAD participants were included, of which 18 underwent follow-up measures after an 8-week course of citalopram or moclobemide. Fifteen healthy control (HC) scans were included. SAD participants at baseline demonstrated several significant connectivity disturbances consistent with the existing network model as well as one previously unreported finding

(increased connectivity between cerebellum and posterior cingulate cortex). After therapy, the SAD group demonstrated significant increases in connectivity with dorsal anterior cingulate cortex which may explain therapy-induced modifications in how SAD sufferers interpret emotions in others and improvements in self-related and emotional processing.

Keywords: anterior cingulate; pharmacologic effects; phobia, social; SPECT

Introduction

Social Anxiety Disorder (SAD) is characterized by excessive fear of social interactions and of scrutiny by others in which sufferers fear negative evaluation (American Psychiatric Association and DSM-5 Task Force 2013). The disorder is common(Kessler RC et al. 2005; Stein et al. 2010) and frequently results in significant disability (Wittchen and Beloch 1996). There is a growing interest in both anatomical and functional neuroimaging as means to investigate the biology of SAD.

Recent neuroimaging research has established differences in resting-state functional networks in SAD sufferers compared to healthy controls. Ding et al, using brain parcellation and calculating a correlation matrix of all regions, reported increased connectivity in frontal regions and decreased connectivity between several frontal and occipital regions (Ding et al. 2011). Liao et al used a seed-based method with amygdalar seeds and found evidence for disrupted connectivity between amygdala and distributed cortical regions, including default mode network (DMN) nodes (Liao et al. 2010b). Amygdalar connectivity disruptions using seed-based techniques have also been described by Hahn et al (Hahn et al. 2011), Prater et al (Prater et al. 2013) and Pannekoek et al (Pannekoek et al. 2013). The latter study also found dorsal attention network but not DMN disturbances. Arnold-Anteraper et al used seed-based methods and reported connectivity disturbances in subcortical networks (Arnold-Anteraper et al. 2014). Liao et al have used regions of gray matter volume reduction as seeds, including a medial prefrontal cortex seed which showed aberrant connectivity with several DMN regions (Liao et al. 2011). Independent component analysis (ICA) was used by Liao et al who reported disturbances in several components including increased connectivity in the self-referential network and decreased connectivity in the DMN (Liao et al. 2010a). Qiu et al used regional homogeneity (ReHo) analysis and reported several ReHo abnormalities including

reductions in DMN components (Qiu et al. 2011). Finally, Liu et al used graph theory to identify disrupted cortical hubs in right fusiform gyrus and bilateral precuneus (Liu et al. 2015b).

Given the heterogeneity in analysis techniques and number of (occasionally inconsistent) connectivity disturbances reported in resting-state experiments, a recent neuroimaging review and meta-analysis of connectivity findings in SAD by Brühl and colleagues is particularly valuable (Brühl et al. 2014a). In their paper, the authors proposed a network model of SAD that provides a useful basis for generating hypotheses in SAD connectivity research. The model builds on preclinical work in that it implicates several structures of the previously described "fear-circuit"(LeDoux 2000) and proposes that SAD sufferers have disrupted connectivity between widely-distributed, functionally distinct regions of the brain. It is important to note however that this model is based on both resting-state and paradigm-driven activation and connectivity data. While many of the regions in this model have also been implicated in resting state studies in SAD, the applicability of this model to "baseline" mental processing (resting state), and to anxiety-provoking socially-focused experimental paradigms is still uncertain. The investigation of resting-state functional connectivity (RFC) is important since it contextualizes and refines our understanding of localized activation or deactivation (and connectivity) in paradigm-driven functional neuroimaging experiments (Greicius et al. 2003), as well as network models such as that proposed by Brühl.

A limited amount of RFC research has been conducted in SAD, and has exclusively been acquired using functional magnetic resonance imaging (fMRI). The high temporal resolution of this modality is eminently suited to functional connectivity research since it is possible to detect spatially distinct, temporally-correlated voxels or voxel clusters from a relatively short total scan duration. It is also possible to perform functional correlation analyses during the same time period, using positron emission tomography (PET) or single photon emission tomography (SPECT). Here a cross-subject approach is used to determine whether the signal intensity in remote brain regions are correlated across participants. Such a cross-subject approach has been used in prior PET, SPECT, and fMRI experiments, e.g. (Blumenfeld et al. 2004; Lee et al. 2008; Di and Biswal 2012; Zhang et al. 2014). There are two main rationales supporting the use of PET and/or SPECT in connectivity research: Firstly, despite its many advantages, fMRI is prone to susceptibility artefacts which make it more difficult to study specific brain regions potentially significant to psychiatric studies such as the orbitofrontal and inferior and medial temporal cortices (Stenger et al. 2000). SPECT and PET do not suffer

from this problem. Secondly, the BOLD signal obtained in fMRI depends on a combination of several physiological factors (cerebral blood flow; cerebral blood volume concentration of deoxyhaemoglobin) and serves as an indirect measure (Steinbrink et al. 2006); whereas it may be argued that the signal obtained using perfusion SPECT or PET is more physiological, as a 'pure' perfusion measure. PET and SPECT are thus complementary to fMRI in functional brain imaging.

In terms of behavioural correlates; in understanding the mechanisms by which drugs exert their effects; and as a biomarker of treatment effect, the translational relevance of disturbances in RFC in SAD remains largely speculative. There is evidence to suggest that the DMN plays a role in social cognition (Schilbach et al. 2008; Laird et al. 2011; Mars et al. 2012), and that this network may be disordered in SAD (Gentili et al. 2009; Liao et al. 2010a; Liu et al. 2015a). In depression, the DMN's role in maladaptive rumination (also a feature of social anxiety disorder) has previously been reported (Hamilton et al. 2011). This is noteworthy given the frequent comorbidity of depression and SAD (Merikangas and Angst 1995). Very limited research has been conducted that examines the effect of treatment on RFC in SAD. Giménez and colleagues reported attenuation of connectivity in four components (using independent component analysis) using resting state fMRI in SAD patients treated with an 8-week course of paroxetine (a selective serotonin reuptake inhibitor - SSRI) (Giménez et al. 2014). That group reported attenuation (with therapy) in the DMN (produced in right thalamus); in a posterior insula component (produced in right insula as well as perigenual regions); in an anterior paralimbic component (produced in subgenual ACC); and in a fronto-parietal component (in left insula). No studies have been performed in SAD that test the effect of pharmacotherapy on seed-based RFC. Such analyses in healthy volunteers and in depressed patients have reported changes in RFC with therapy (McCabe et al. 2011; van Wingen et al. 2014; Yang et al. 2014; Wang et al. 2015).

The objective of this study was to compare RFC in HCs and in SAD participants at baseline and to investigate the impact of pharmacotherapy on RFC in the SAD group. We hypothesized RFC differences between SAD and HCs would correspond to the existing network model of SAD proposed by Brühl and that pharmacotherapy effects would be consistent with normalization of connectivity disturbances predicted by the model. All participants in this study were included in a prior study conducted by our institution (Warwick et al. 2006).

Methods

Participants

The study was approved by the health research ethics committee of Stellenbosch University (Ref # S14/08/159).

SAD participants: SAD participants had to meet DSM-IV criteria for SAD. They were screened using the Structured Clinical Interview for the Diagnosis of Axis-I disorders (SCID) (First et al. 1996). Left-handed participants as well as those with other primary (dominant) psychiatric disorders or significant medical illnesses/neurological conditions were excluded. Co-morbid anxiety spectrum disorders were not an exclusion criterion if these were considered secondary in terms of temporal course and severity. Highest level of education was recorded for all participants. Technically inadequate scans were excluded. Data for all SAD participants were used in a previous research study by our institution.
Healthy controls: Healthy control participants underwent a psychiatric screening interview using the Mini International Neuropsychiatric Interview (v4.4) (Sheehan et al. 1998), physical examination and MRI scan prior to inclusion. Participants were excluded if they were left-handed, had any psychiatric diagnoses or significant medical/neurological conditions. Highest level of education was recorded in all participants.

Group matching was assessed using appropriate statistical tests, with significance threshold of $p<0.05$: a two-tailed Welch's t-test was used to detect differences in mean age; a Pearson's Chi-square test was used to detect differences in gender proportions; and a Freeman-Halton extension of the Fisher exact test was used to detect differences in highest level of education.

Pharmacotherapy

After baseline measures, SAD participants received an 8-week course of pharmacotherapy with either moclobemide or citalopram (open label). No randomization was applied to assign which medication would be prescribed (the citalopram and moclobemide sub-groups originally consisted of independent datasets from separate studies). Citalopram was initiated

at a dose of 20 mg daily for two weeks followed by 40 mg daily thereafter. Moclobemide was initiated at a dose of 600 mg daily for two weeks followed by 900 mg daily thereafter.

Clinical measures

SAD participants were evaluated with the Liebowitz Social Anxiety Scale (LSAS) (Liebowitz 1987), Montgomery- Åsberg Depression Rating Scale (MADRS) (Montgomery and Asberg 1979), and Sheehan Disability Scale (SDS) (Sheehan 1983) at baseline and after a course of pharmacotherapy. The clinical global improvement (CGI) score (Guy 1976) was used to evaluate treatment response. Statistical significance of changes in clinical scores between baseline and follow-up was tested using a one-tailed, paired student t-test (significance threshold $p<0.05$). Differences in score improvement between the SAD subgroup treated with moclobemide and that treated with citalopram was calculated using a two-tailed Welch's t-test.

SPECT imaging

Single photon emission tomography (SPECT) was performed in the resting state for all scans. After the placement of an intravenous catheter, participants lay in a quiet, dimly lit room with their eyes open, for 30 minutes prior to the injection of the radiopharmaceutical. A dose of 555 MBq of technetium-99 m hexamethylpropylene amine oxime (Tc-99m HMPAO) was administered after which participants lay quietly for (at least) an additional 10 minutes, shortly whereafter imaging was performed. Brain SPECT imaging was conducted using a dual detector gamma camera (Elscint Helix, GE Medical Systems, USA) equipped with fanbeam collimators. A headrest was used for support and comfort. Data were acquired in the step-and-shoot mode (3 degree steps; 15 seconds per step), using a 360 degree circular orbit, with the detectors of the gamma camera as close as possible to the participant's head. A 128 x 128 image matrix was used.

For the purposes of the study, original raw data were reconstructed using optimal reconstruction techniques (Hybrid Recon^{TM} – Neurology v1.1.23, HERMES Medical Solutions, AB, Sweden). Iterative reconstruction (OSEM; 3 iterations; 30 subsets) was performed with uniform attenuation correction (μ_l = 0.15 cm^{-1}, outline threshold 15%, outline

filter FWHM 1 cm), Monte Carlo-based scatter correction, and resolution recovery. Images were then smoothed using a 3D Gaussian post-filter (FWHM 1.2cm). The final reconstructed voxel size was 2.21 x 2.21 x 2.21 mm^3.

Spatial pre-processing

DICOM image files were converted to SPM NIfTI format using MRIConvert v2.0 rev250 (Jolinda Smith, Lewis Centre for Neuroimaging, University of Oregon, USA). Pre-processing of scans was performed using Statistical Parametric Mapping (SPM12, Wellcome Trust Centre for Neuroimaging, UCL, London; http://www.fil.ion.ucl.ac.uk/spm/). Scans were then spatially normalised to the Montreal Neurological Institute (MNI) standard anatomical space with 2 x 2 x 2 mm^3 voxels. The images were then smoothed using a 3D Gaussian kernel with a FWHM of 8 mm. All images' global brain counts were normalized to a mean value of 100 using a custom MATLAB script (P. Dupont).

Analysis

Whole brain, seed-based connectivity analyses were conducted using seeds representative of regions for which a priori interest existed based on the SAD network model of Brühl and colleagues (Brühl et al. 2014a).

For regions that were anatomically distinct (bilateral insula; amygdala; thalamus) seed volumes of interest (VOIs) were extracted from the Automated Anatomical Labelling (AAL) atlas (Tzourio-Mazoyer et al. 2002) using the WFU PickAtlas tool v3.05 (ANSIR Laboratory, Wake Forest University School of Medicine, http://fmri.wfubmc.edu/cms/software) (Maldjian et al. 2003, 2004). To define left and right dorsolateral prefrontal cortex (dlPFC) seeds, we used a method based on that described by Takeuchi and colleagues(Takeuchi et al. 2014a) using the WFU PickAtlas tool to intersect BA46 (extracted from Talairach Demon *Brodmann areas+* atlas) (Lancaster et al. 1997, 2000); respective middle frontal gyri (extracted from Automated Anatomical Labelling (AAL) atlas) (Tzourio-Mazoyer et al. 2002) and gray matter (extracted from Talairach Demon *Type* atlas) (Lancaster et al. 1997, 2000). Each of these regions was dilated by a factor of 3 (to account for reduced spatial resolution of SPECT) before the intersection was applied to derive the final seed VOI. The

remaining seed VOIs consisted of spheres centred on coordinates of interest and were generated by a custom Matlab script (P. Dupont). For the medial prefrontal cortex (mPFC) seed we used the same MNI coordinates as reported by Takeuchi and colleagues (Takeuchi et al. 2014a); this same seed has been used to represent mPFC in several previous studies. A single (midline) seed VOI was also used for posterior cingulate cortex/precuneus (PCC/Precun), centred on the coordinates reported by Greicius and colleagues (Greicius et al. 2003) which is frequently used to probe DMN. Talairach-Tournoux coordinates for this seed were converted to MNI coordinates using BrainMap GingerALE 2.3 (Research Imaging Institute UT Health Science Centre San Antonio, http://www.brainmap.org) (Eickhoff et al. 2009, 2012; Turkeltaub et al. 2012) which uses the **icbm_spm2tal** transform validated by Lancaster and colleagues (Lancaster et al. 2007). While this VOI overlaps bilateral precuneus, we also defined an additional dedicated right precuneus seed centred on a cluster reported by Liu and colleagues in their work on disrupted cortical hubs in SAD (Liu et al. 2015b). Right fusiform gyrus coordinates, also based on a cluster reported by Liu and colleagues (Liu et al. 2015b), were used to generate a right fusiform gyrus seed. The anterior cingulate cortex (ACC) was represented in our analysis by choosing representative seeds from both anterior dorsal (adACC) and subgenual (sgACC) sub-regions. Left and right adACC and sgACC seeds such as those published by Margulies and colleagues (Margulies et al. 2007) and used by several other researchers were insufficiently separated across the midline to use as separate seed VOIs in a SPECT analysis (limited spatial resolution). For this reason, we used single spherical seed VOIs centred on the midline to represent adACC and sgACC regions, effectively combining selected bilateral seeds as published by Margulies. Details of the various seed VOIs can be found in **Table 2.1**.

Group contrasts (SAD baseline vs HC; and SAD baseline vs. after therapy) were performed on a voxel-wise basis using a cross-subject correlation approach in SPM12. Significance of group differences was calculated using a two-sample, two-tailed t-test. Results were thresholded on an uncorrected voxel level of $p<0.001$ and on a cluster-level at $p<0.05$, false discovery rate (FDR) corrected. Only results significant at cluster level were reported. A second-level analysis was performed to interrogate the relationships identified in the seed-based contrast analysis. To do so, the seed and related cluster in question were used as VOIs in a linear regression analysis, again with a two-sample, two-tailed t-test ($p<0.05$) in SPM12.

Results

Demographics

Twenty-three SAD participants were included, of whom 18 also had follow-up (post-treatment) scans. All participants in the final sample were medication-free except for one participant that was on alprazolam 0.25mg per day. Fifteen healthy controls were selected for the final analysis. All controls were medication-free. No statistically significant differences were found between the demographics of the healthy control and SAD groups or between the subgroups of SAD patients treated with citalopram and moclobemide. Demographic data and details of group matching are summarized in **Table 2.2**.

Clinical

Baseline clinical scores and the effect of medication is summarized in **Table 2.3**.
There were no statistically significant differences in baseline or follow-up clinical scores between the SAD subgroup treated with citalopram and that treated with moclobemide. In terms of improvement in clinical scores with therapy, moclobemide resulted in a greater reduction of social anxiety symptomatology as assessed by the LSAS than did citalopram (p=0.04). Differences in other clinical scores between the citalopram and moclobemide-treated SAD subgroups were not statistically significant.

Correlation analysis

Results of the seed-based RFC analyses are summarized in **Tables 2.4** and **2.5**.

SAD baseline vs HC

Compared to the healthy control group, the SAD group at baseline had decreased connectivity between left amygdala and a cluster containing the right middle frontal gyrus. Second-level linear regression analysis between these two regions indicated that this decrease in connectivity represented a switch from a positive correlation (in HC) to a negative correlation (in SAD) (**Fig 2.1**).

Additionally, the SAD group showed decreased connectivity between the midline PCC/precuneus seed and a cluster in left cerebellar exterior (crus 1). This decrease was due to a switch from a positive correlation (in HC) to a negative correlation (in SAD) (**Fig 2**.2).
Increased connectivity (in SAD compared to controls) between right thalamus and a cluster overlapping right middle frontal gyrus and adjacent white matter was due to a switch from a negative correlation (in HC) to a positive correlation (in SAD) (**Fig 2.3**).
Second-level, linear regression analysis of relationships identified in the SAD baseline vs after therapy contrast (using respective seed and cluster) did not yield significant results (even with more liberal p values) in the SAD baseline vs HC contrast.

SAD baseline vs after therapy

Three significant contrasts were identified between the SAD group at baseline and after a course of pharmacotherapy. No decreases in connectivity were identified after therapy.
Pharmacotherapy resulted in an increase in connectivity between the right fusiform gyrus seed and a cluster that involved the medial segment of superior frontal gyrus bilaterally. Second-level regression analysis indicated that this increase was due to a switch from a negative correlation pre-therapy to a positive correlation after therapy (**Fig 2.4**).
After therapy there was an increase in connectivity between the adACC seed and a cluster including right precuneus, which was due to a switch from a negative correlation pre-therapy to a positive correlation after therapy (**Fig 2.5**).
An increase in connectivity (after treatment) between the adACC seed and a cluster in right middle occipital gyrus was likely due to a switch from a negative correlation pre-therapy to a positive correlation after therapy (**Fig 2.6**).
Second-level, linear regression analysis of relationships identified in the SAD baseline vs HC contrast (using respective seed and cluster) did not yield significant results (even with more liberal p values) in the SAD baseline vs after therapy contrast.

Discussion

In this study we identified several RFC differences between the SAD group at baseline and healthy controls, including a novel finding of decreased connectivity between cerebellum and posterior cingulate cortex. Furthermore, we demonstrated that pharmacotherapy has an effect

on RFC in SAD, particularly on connectivity of the anterior-dorsal region of the anterior cingulate cortex. These findings contribute to the limited number of RFC studies in SAD and are largely supportive of the current network model of the disorder, as well as providing novel data on the effects of therapy. The study also provides the first SPECT RFC data in SAD.

Increased connectivity was found between the right thalamus and right middle frontal gyrus in SAD at baseline compared to healthy controls. These findings are consistent with the current network model of SAD (Brühl et al. 2014a), which predicts increased fronto-thalamic connectivity in SAD. Based on fear conditioning models, two routes exist to convey sensory information from the thalamus to the amygdala (LeDoux 1998). Rapid communication is achieved by a direct thalamo-amygdala pathway, whereas an indirect thalamo-cortico-amygdala pathway enables external stimuli to be cognitively appraised and modulated by cortical regions en route to the amygdala. Increased thalamo-cortical connectivity may reflect excessive utilisation of the first part of this slower pathway in SAD, although it is unclear whether this change could be an underlying cause or a response to SAD. The prefrontal cluster identified in this study corresponded most closely to BA47, localized predominantly in the orbital portion of the middle frontal gyrus. This is compatible with the implication of this region in several processes potentially relevant to SAD, namely identification of emotional intonation (Wildgruber et al. 2005); behavioural inhibition (Del-Ben et al. 2005; Völlm et al. 2006); embarrassment at violation of social norms (Berthoz et al. 2002); attribution of intention to others (Brunet et al. 2000); and reward processing (Rogers et al. 1999). Research by Giménez and colleagues in SAD participants has linked connectivity between these regions with the perception of social scrutiny (Giménez et al. 2012).

Decreased connectivity was found between left amygdala and right superior frontal gyrus in SAD at baseline. Although this finding is not consistent with increased connectivity predicted by the Brühl network model for SAD, the authors of that meta-analysis did highlight inconsistency of this relationship in the literature, with fronto-amygdalar connectivity being either increased or decreased in SAD (Brühl et al. 2014a). Certainly decreased functional connectivity between these regions in SAD is consistent with preclinical models of anxiety in which there is failure by frontal cortex to dampen the highly sensitive subcortical (amygdalar) alarm system (i.e. failure of top-down control) (LeDoux 2000; Akirav and Maroun 2007). Inconsistency in connectivity findings between these regions in human SAD

research may be due to the fact that several amygdalo-frontal connectivity disturbances are present in SAD.

The superior frontal gyrus (overlapping BA9/32) has previously been implicated in self-focused reappraisal, i.e. emotionally detaching oneself from negative events by down-regulation of arousal , or what Falquez and colleagues refer to as "adopting the role of a detached third-person observer during the presentation of emotional stimuli" (Falquez et al. 2014). Such a regulatory role over negative emotion for this region is supported by studies that found decreased amygdalar activation during reappraisal (Banks et al. 2007). A negative correlation between these regions in SAD during rest may represent the tendency for these patients to spontaneously engage in emotional distancing; a behaviour reported by some SAD sufferers (Alden and Taylor 2004). While the significance of functional connectivity between contralateral structures (left amygdala; right prefrontal cortex) is uncertain, there is evidence for lateralization of amygdala function, with left amygdala more involved in ongoing appraisal of emotional stimuli and right amygdala preferentially activated by tasks requiring rapid orientation or ambiguous stimuli (Freitas-Ferrari et al. 2010).

Diminished connectivity was found between a posterior cingulate/precuneus seed and left cerebellum in SAD at baseline. While this finding was no longer significant on the seed-based analysis after excluding a participant on low-dose alprazolam, the finding remained highly significant using a seed x cluster linear regression (which demonstrated no outliers) and was likely real. A relationship between these regions may be related to findings in healthy participants that correlated cerebellar crus 1 activity with DMN activity (Buckner et al. 2011) (of which posterior cingulate/precuneus is a critical node) (Greicius et al. 2003); and with other work that suggests the cerebellum modulates DMN function (Bernard et al. 2012). This finding is of interest in SAD given evidence that the DMN plays a role in social cognition (Schilbach et al. 2008; Laird et al. 2011; Mars et al. 2012), and of DMN dysfunction in the disorder (Gentili et al. 2009; Liao et al. 2010a; Liu et al. 2015a). While a few RFC studies have reported cerebellar connectivity disturbances in SAD, as far as the authors are aware, a connectivity disturbance between cerebellum and posterior cingulate/precuneus has not previously been reported. This may in part be due to the limited attention cerebellum has received in investigative hypotheses to date. Our findings support closer scrutiny of cerebellar functioning in SAD, especially in the context of evidence for it playing a role in cognitive emotional processing (Schmahmann 2010), and renewed interest in disturbed cortico-cerebellar connectivity in anxiety states (Caulfield and Servatius 2013).

Evidence exists from neuroimaging research in healthy volunteers and in psychiatric disorders that pharmacotherapy affects RFC (McCabe et al. 2011; van Wingen et al. 2014; Yang et al. 2014; Wang et al. 2015). Only one study in SAD has tested for pharmacological effects on RFC: Giménez and colleagues used independent component analysis to identify paroxetine treatment effects in four different components (Giménez et al. 2014). That group reported reductions in connectivity with therapy in all components (in some cases produced by structures included in our own analysis – right thalamus; sgACC and insula). That we did not identify a treatment effect on connectivity of these regions may be due to differences in analysis methodology. The therapy-related connectivity changes we found were for seed regions outside of the components examined by Giménez and colleagues.

Whether identified using seeds or clusters, our findings on how therapy influenced RFC in SAD all related to connectivity of the dorsal anterior cingulate cortex. A possible mechanism for an increase in connectivity following pharmacotherapy (frequently using selective serotonin reuptake inhibitors - SSRIs) is suggested by studies reporting downregulation of 5-HT_{1A} receptors (Lanzenberger et al. 2007) as well as increased serotonin synthesis and reuptake in dorsal anterior cingulate of untreated SAD patients compared to healthy controls (Frick et al. 2015a). The dorsal anterior cingulate cortex probably has a mainly evaluative role in emotion processing (Etkin et al. 2011), which is consistent with a recent model in which dorsal ACC integrates information about rewards and costs to estimate the value of allocating control (Shenhav et al. 2013).

An increase in connectivity was found between right fusiform gyrus and dorsal anterior cingulate cortex in SAD after therapy. The subregion of right fusiform gyrus we used as our seed VOI closely corresponds to the fusiform face area (FFA) which is involved in the early visual processing of faces (Haxby et al. 2000; Li et al. 2009). Fusiform hyperactivity is a consistent finding that may reflect a specific aspect of SAD, such as altered processing of emotional facial expressions, or generally heightened emotional system reactivity (Frick et al. 2013). Disturbed connectivity of this right fusiform subregion in SAD is suggested by prior resting-state fMRI research (Danti et al. 2010; Liu et al. 2015b), although connectivity abnormalities between right fusiform and dorsal anterior cingulate per se have not been reported. Contrary to our hypothesis, this finding did not represent a normalization of connectivity between these regions as predicted by the Brühl model, which suggests increased connectivity between prefrontal cortex and fusiform in SAD (Brühl et al. 2014a). Increased dorsal anterior cingulate connectivity with fusiform gyrus may therefore represent

a compensatory effect in SAD that is further enhanced by pharmacotherapy. We can speculate that a therapy-induced increase in connectivity between these regions may lead to modification of the process whereby we evaluate emotions in others. Certainly, neuroimaging studies in SAD using emotion recognition paradigms have previously reported differences after therapy (Schneier et al. 2011; Phan et al. 2013; Giménez et al. 2014; Pantazatos et al. 2014).

Our analysis also found an increase in connectivity between the adACC seed and a cluster in right middle occipital gyrus in the SAD group after therapy. This cluster was sufficiently removed from the right fusiform gyrus seed that we considered this to be a separate finding. While this result was no longer significant on the seed-based analysis after excluding the participant on low-dose alprazolam, no clear outlier was seen on the linear regression analysis using seed and cluster as VOIs and using that method the difference remained highly significant even after exclusion and was likely real. Once again, our finding did not represent a normalization of the connectivity disturbance between these regions predicted by the Brühl model (increased connectivity in SAD at baseline) and provides indirect evidence that baseline connectivity between these regions in SAD may be compensatory. Functional connectivity between dorsal anterior cingulate and a region involved in visual function once again highlights the role of visual processing in the disorder. Finally, the study also found an increase in connectivity between dorsal anterior cingulate cortex and the right precuneus in the SAD group following therapy. Once again, this finding was no longer significant on seed-based analysis after excluding a participant on low-dose alprazolam, however clearly persisted on the linear regression analysis. The current SAD network model predicts generally decreased connectivity between prefrontal cortex and precuneus and as such our finding is consistent with a normalization of this relationship with pharmacotherapy. Functional connectivity of the precuneus is complex, likely underlying its many functions in visuo-spatial imagery, episodic memory retrieval, self-related processing and consciousness (Cavanna and Trimble 2006). It is also a component region of the DMN which is active at rest (Greicius et al. 2003). It is possible that a strengthening of this connectivity deficit in SAD with therapy may underlie a synchronous improvement in self-related processing and emotion processing.

Our study suffered from several limitations inherent to the type of functional connectivity analysis employed. The open label nature of the study did not allow control of expectancy effects in the SAD group. It may also be argued that lack of randomization in assignment of

moclobemide or citalopram therapy in the SAD group may introduce bias in our mixed sample but given that participants in the two SAD subgroups (i.e. treated with moclobemide and treated with citalopram) were all treated, were not recruited simultaneously, and did not differ in clinical severity measures at baseline, we do not consider this to be a major problem. The effect of non-randomized assignment is also less relevant in that a comparison of moclobemide and citalopram was not performed since these subgroups were too small. It is possible that RFC changes secondary to therapy were related to improved mood (evidenced by reduction in MADRS scores) or other pharmacotherapy effects rather than improvements in SAD, however we consider this unlikely given that none of the participants suffered from major depression as a dominant disorder and that in both the citalopram and moclobemide treated groups, baseline MADRS scores were in the mild clinical severity range (as per Table 2.3), which further supports the argument that the RFC changes are unlikely to be primarily the result of improvement in depressive symptomatology. Furthermore, while it is possible that non-dominant psychiatric comorbidities may have affected the results, none of the SAD participants had any other dominant psychiatric disorder and we therefore consider this unlikely. Since a cross-subject correlation was used, clinical scores e.g. for depression or anxiety severity, could not be used as covariates or to correlate connectivity differences between groups. Similarly, because a cross-subject (group level) connectivity analysis was used (rather than intra-subject connectivity, as can be performed with fMRI) it was necessary to assume independence between baseline and post-therapy connectivity measures in the SAD group (i.e. a group-level, cross-subject approach prevented the use of a paired t-test which is more sensitive for detecting longitudinal differences). Other potential confounds include the potential effect of prior treatment or length of illness in the SAD group (not recorded). While SAD and HC participants did not undergo identical screening procedures, both diagnostic instruments used are known as accurate structured psychiatric interviews with sound psychometric properties and therefore it is unlikely that this confounded our results.

Our study was significant in that, in addition to finding further support for several connectivity disturbances predicted by the recently published meta-analytic network model for SAD, it identified for the first time decreased connectivity between cerebellum and a core node of the default mode network in the disorder. Our work also adds to the limited literature on the effect of pharmacotherapy on resting-state functional connectivity in SAD; specifically

how therapy increases connectivity between dorsal anterior cingulate cortex and regions involved in self-related processing and the interpretation of facial emotion.

Acknowledgements

The PhD from which this study emanated was funded by the South African Medical Research Council under the MRC Clinician Researcher Programme.
Financial support towards study costs was received from the Nuclear Technologies in Medicine and Biosciences Initiative (NTeMBI) of South Africa.

Profs Stein and Lochner receive funding from the MRC.

Neither funder played any role in study design; collection, analysis, or interpretation of data; in the writing of this article or in the decision to submit it for publication.

Contributors

Data collection: GP Jordaan, JM Warwick
Data collation: A Doruyter
Data processing and analysis: A Doruyter, P Dupont
Manuscript: A Doruyter
Manuscript review: All authors
Supervisors: JM Warwick, C Lochner

Conflicts of interest

None.

Tables and Figures

Table 2.1 Description of seeds used in analysis

Seed	Description [MNI, *xyz*]
Amygdala (L+R)	Anatomical: extracted from AAL atlas
Thalamus (L+R)	Anatomical: extracted from AAL atlas
Insula (L+R)	Anatomical: extracted from AAL atlas
dlPFC (L+R)	Anatomical: intersect of middle frontal gyrus; BA 46; and gray matter (all dilated by factor of 3)
mPFC	Spherical VOI (radius 6mm) centred on [-1 47 -4]
PCC/Precun	Spherical VOI (radius 6mm) centred on [-1 -50 31]
R Precuneus	Spherical VOI (radius 6mm) centred on [3 -48 63]
adACC	Spherical VOI (radius 12mm) centred on [0 19 28]
sgACC	Spherical VOI (radius 12mm) centred on [0 25 -10]
R FFG	Spherical VOI (radius 6mm) centred on [42 -60 -15]

Abbreviations: **MNI** - Montreal Neurological Institute space; **L** – Left; **R** – Right; **AAL** – Automated Anatomical Labelling; **dlPFC** – dorsolateral prefrontal cortex; **VOI** – volume of interest; **BA** – Brodmann Area; **mPFC** – medial prefrontal cortex; **PCC/Precun** – posterior cingulate cortex/precuneus; **adACC** – anterior-dorsal anterior cingulate cortex; **sgACC** – subgenual anterior cingulate cortex; **FFG** –fusiform gyrus.

Table 2.2a Group matching; HC group vs SAD group at baseline

	Group		
	HC	**SAD**	*p*
Total (n)	15	23	
Mean age in years:	37.0 (26.8 – 57.0)	32.8 (17.1 – 48.3)	0.12[†]
Gender:	Male: 10, Female: 5	Male: 17, Female: 6	0.63[‡]
Highest level of education:			
Formal schooling not completed	2	5	0.75[ǂ]
Formal schooling completed	6	10	
Formal schooling + additional qualification	7	8	

[†]Two-tailed Welch's t-test

[‡]Pearson's Chi-square test

[ǂ]Freeman-Halton extension of the Fisher exact test

Table 2.2b Group matching of SAD subgroup treated with citalopram vs SAD subgroup treated with moclobemide

	Subgroup		
	Citalopram	**Moclobemide**	*p*
Total (n)	11	7	
Mean age in years:	32.8 (18.5 – 42.7)	32.3 (23.6 – 42.1)	0.9†
Gender:	Male: 7, Female: 4	Male: 6, Female: 1	0.31‡
Highest level of education:			
Formal schooling not completed	2	1	0.8ǂ
Formal schooling completed	5	5	
Formal schooling + additional qualification	4	1	

†Two-tailed Welch's t-test

‡Pearson's Chi-square test

ǂFreeman-Halton extension of the Fisher exact test

Table 2.3 Effect of medication on mean clinical scores (*±SD),* in SAD participants with statistical measures of group matching

	Subgroup		
	Citalopram (*n*=11)	**Moclobemide (*n*=7)**	*p*[†]
Mean duration of therapy	8.4 weeks (8.0 – 10.9)	8.0 weeks (8.0)	0.15
LSAS			
Baseline	93.1 (±24.0)	112 (±17.6)	0.07
Post-therapy	74.8 (±30.0)	74.6 (±22.4)	0.98
Mean % change	-21.1(±20.3)	-33.8 (±15.4)	**0.04**
p[‡]	**0.003**	**0.0007**	
MADRS			
Baseline	14.7 (±3.4)	10.7 (±7.8)	0.24
Post-therapy	7.0 (±3.8)	4.9 (±2.3)	0.16
Mean % change	-50.2 (±28.9)	-38.5 (±34.1)	0.56
p[‡]	**0.0003**	**0.04**	
SDS			
Baseline	16.8 (±5.2)	19.1 (±4.8)	0.35
Post-therapy	12.2 (±7.5)	16.0 (±3.7)	0.17
Mean % change	-31.3 (±32.4)	-14.6 (±15.3)	0.44
p[‡]	**0.004**	**0.02**	
CGI-S	4.8 (±0.8)	5 (±0.8)	0.64
CGI-I	3.2 (±1.5)	3.4 (±0.5)	0.63

Abbreviations: **LSAS**: Liebowitz Social Anxiety Scale; **MADRS**: Montgomery-Åsberg Depression Rating Scale; **SDS**: Sheehan Disability Scale; **CGI**: Clinical Global Impression; **-S**: Severity; **-I**: Improvement

[†]Two-tailed Welch's t-test

[‡]One-tailed paired Student's *t*-test

Table 2.4 Functional correlation seed-based analysis results (statistically significant contrasts) in the SAD group compared to the HC group

Seed connectivity findings	**Cluster size (mm^3)**	**p***	**Peak voxel location (mm) MNI**		
			x	**y**	**z**
L Amygdala seed showed reduced connectivity with cluster overlapping right SFG/adACC (BA9/ BA32)	776	**0.04**	20	28	36
PCC/Precun seed showed reduced connectivity with cluster in left cerebellar crus 1	594	**0.05**	-48	-78	-44
R Thalamus seed showed increased connectivity with cluster overlapping right MFG and MFGorb (BA47/11)	756	**0.01**	26	42	0

*Cluster-level threshold of $p<0.05$ (FDR corrected), at voxel-level threshold of $p<0.001$ (uncorrected)

Abbreviations: **MNI** - Montreal Neurological Institute space; **L** – Left; **R** – Right; **SFG** – superior frontal gyrus; **PCC/Precun** – posterior cingulate cortex/precuneus; **BA** – Brodmann area; **adACC** – anterior-dorsal anterior cingulate cortex; **MFG** – middle frontal gyrus; **MFGOrb** – middle frontal gyrus, orbital part.

Table 2.5 Functional correlation seed-based analysis results (statistically significant contrasts) in the SAD group after therapy compared to baseline

Seed connectivity findings	**Cluster size (mm^3)**	**p***	**Peak voxel location (mm) MNI**		
			x	**y**	**z**
R FFG seed showed increased connectivity with cluster in bilateral adACC (mSFG; BA32)	668	**0.01**	-6	44	30
adACC seed showed increased connectivity with cluster in right precuneus (BA7)	371	**0.04**	14	-62	42
adACC seed showed increased connectivity with cluster in right MOG (BA19)	390	**0.04**	36	-74	4

*Cluster-level threshold of $p<0.05$ (FDR corrected), at voxel-level threshold of $p<0.001$ (uncorrected)

Abbreviations: **MNI** - Montreal Neurological Institute space; **R FFG** – right fusiform gyrus; **mSFG** – superior frontal gyrus medial segment; **BA** – Brodmann area; **adACC** – anterior-dorsal anterior cingulate cortex; **MOG** – middle occipital gyrus.

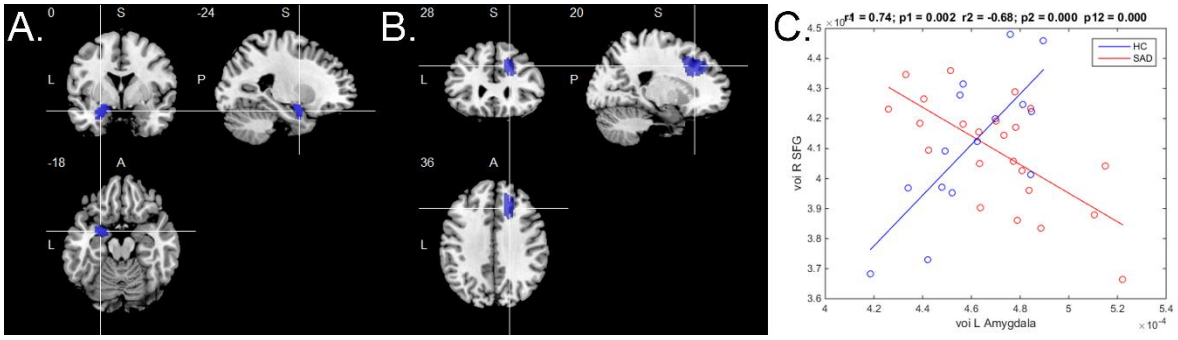

Figure 2.1 Connectivity result 1. Left amygdala seed (x=-24; y=0; z=-18) (**A**) and right superior frontal gyrus (R SFG) cluster (x= 20; y=28; z=36) (**B**) in the SAD baseline vs HC contrast. Results of the regression analysis (**C**) demonstrate that decreased connectivity between these regions in the SAD group compared to healthy controls (p<0.001) was due to a switch from a positive correlation in HC (p=0.002) to a negative correlation in SAD (p<0.001). Axes in arbitrary units.

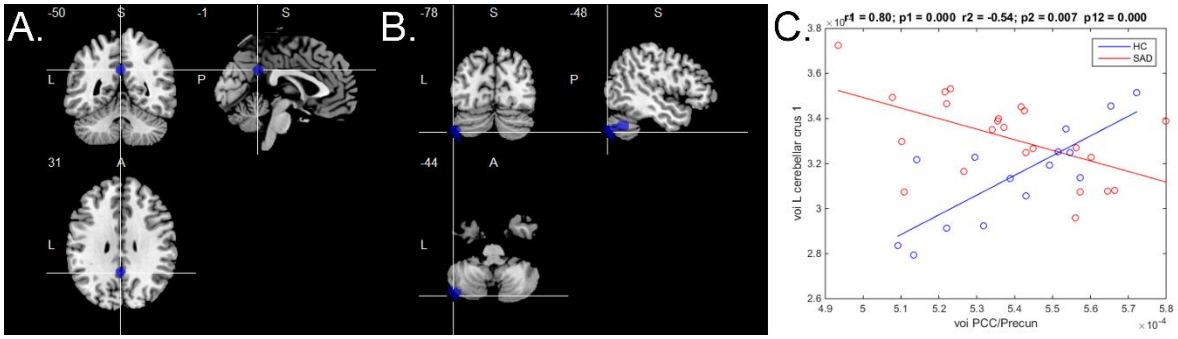

Figure 2.2 Connectivity result 2. Posterior cingulate cortex/precuneus (PCC/Precun) seed (x=-1; y=-50; z=31) (**A**) and left cerebellar crus 1 cluster (x=-48; y=-78; z=-44) (**B**) in the SAD baseline vs HC contrast (cerebellar cluster only appears to extend outside brain on the MRI template used for illustrative purposes). Results of the regression analysis (**C**) demonstrate that decreased connectivity between these regions in the SAD group compared to healthy controls (p<0.001) was due to a switch from a positive correlation in HC (p<0.001) to a negative correlation in SAD (p=0.007). Axes in arbitrary units. While results of seed-based analysis did not meet statistical significance after excluding a patient on low-dose alprazolam (p=0.71), difference on linear regression remained significant (p<0.001).

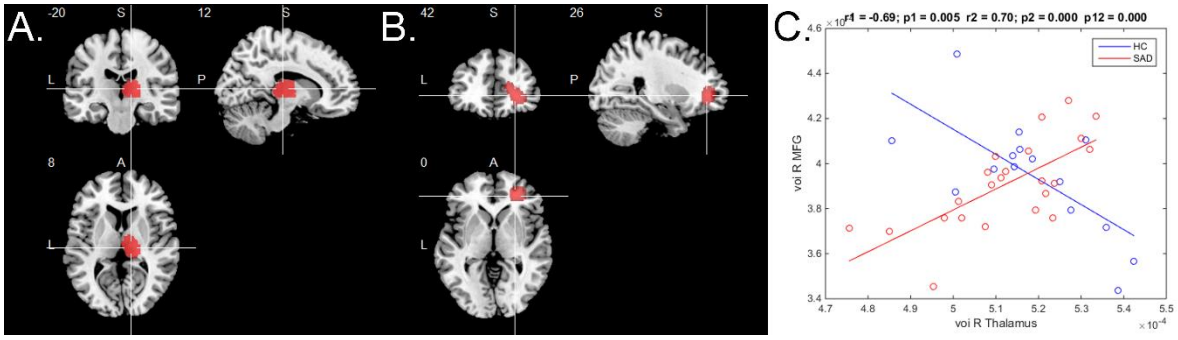

Figure 2.3 Connectivity result 3. Right thalamus seed (x=12; y=-20; z=8) (**A**) and right middle frontal gyrus (R MFG) cluster (x=26; y=42; z=0) (**B**) in the SAD baseline vs HC contrast. Results of the regression analysis (**C**) demonstrate that increased connectivity between these regions in the SAD group compared to healthy controls (p<0.001) was due to a switch from a negative correlation in HC (p=0.005) to a positive correlation in SAD (p<0.001). Axes in arbitrary units.

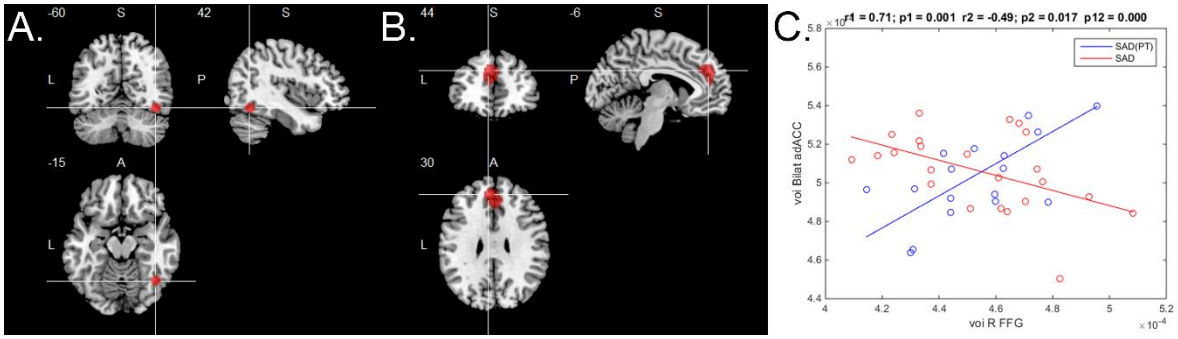

Figure 2.4 Connectivity result 4. Right fusiform gyrus (R FFG) seed (x=42; y=-60; z=-15) (**A**) and bilateral anterior-dorsal anterior cingulate cortex (adACC) cluster (x=-6; y=44; z=30) (**B**) in the SAD contrast before (SAD) and after (SAD(PT)) therapy. Results of the regression analysis (**C**) demonstrate that increased connectivity between these regions after therapy (p<0.001) was due to a switch from a negative correlation in SAD at baseline (p=0.017) to a positive correlation post-therapy (p=0.001). Axes in arbitrary units.

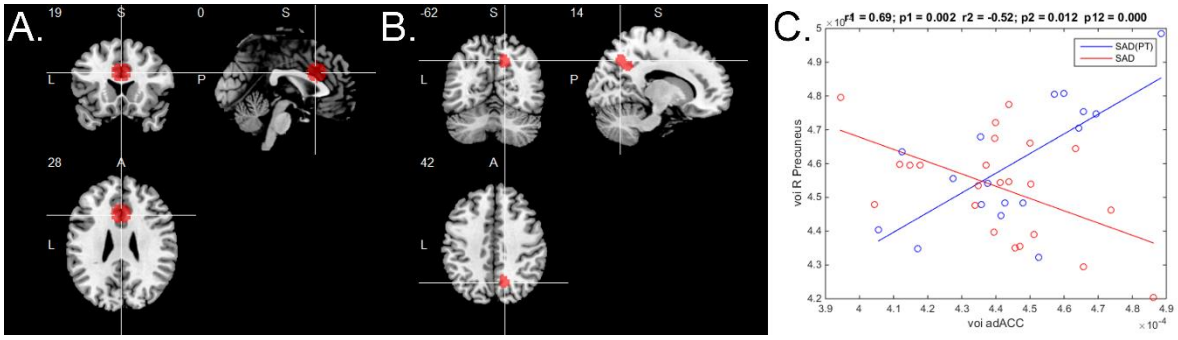

Figure 2.5 Connectivity result 5. Anterior-dorsal anterior cingulate cortex (adACC) seed (x=-5; y=19; z=28) (**A**) and right precuneus cluster (x=14; y=-62; z=42) (**B**) in the SAD contrast before (SAD) and after (SAD(PT)) therapy. Results of the regression analysis (**C**) demonstrate that increased connectivity between these regions after therapy (p<0.001) was due to a switch from a negative correlation in SAD at baseline (p=0.012) to a positive correlation post-therapy (p=0.002). Axes in arbitrary units (arb. unit). While results of seed-based analysis did not meet statistical significance after excluding a patient on low-dose alprazolam (p=0.28), difference on linear regression remained significant (p<0.001).

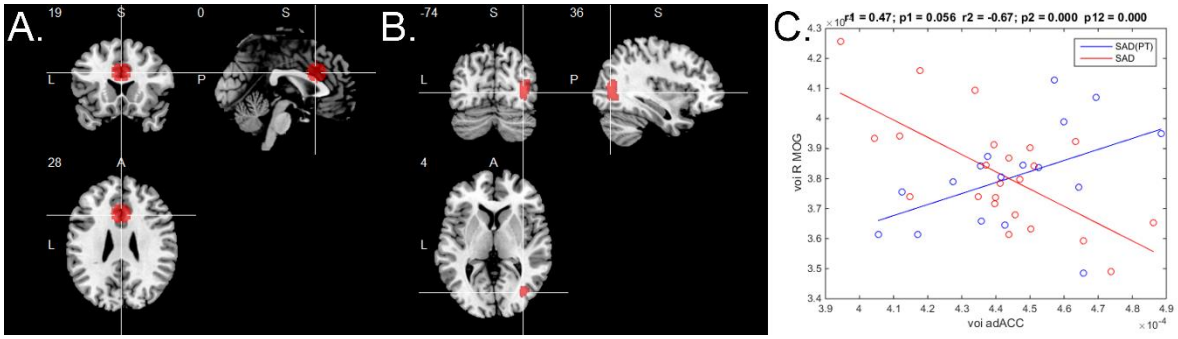

Figure 2.6 Connectivity result 6. Anterior-dorsal anterior cingulate cortex (adACC) seed (x=0; y=19; z=28) (**A**) and right middle occipital gyrus (R MOG) cluster (x=36; y=-74; z=4) (**B**) in the SAD contrast before (SAD) and after (SAD(PT)) therapy. Results of the regression analysis (**C**) demonstrate that the statistically significant (p<0.001) increase in connectivity after therapy was likely due to a switch from a negative correlation in SAD at baseline (p<0.001) to a positive correlation post-therapy (p=0.06; borderline significant). Axes in arbitrary units (arb. unit). While results of seed-based analysis did not meet statistical significance after excluding a patient on low-dose alprazolam (p=0.28), difference on linear regression remained significant (p<0.001).

Resting-state fMRI and social cognition: an opportunity to connect

Authors: Alexander Doruyter[1], Nynke A Groenewold[2], Patrick Dupont [3], Dan J Stein[4], James M Warwick[1]

1 Stellenbosch University Faculty of Medicine and Health Sciences, Division of Nuclear Medicine, Cape Town, South Africa

[2] University of Cape Town Faculty of Health Sciences, Department of Psychiatry, Cape Town, South Africa

3 KU Leuven, Department of Neurosciences, Laboratory of Cognitive Neurology, Leuven, Belgium

[4] MRC Unit on Anxiety & Stress Disorders, University of Cape Town Faculty of Health Sciences, Department of Psychiatry, Cape Town, South Africa

Publication status: Published manuscript (Doruyter et al. 2017d).

Abstract

Many psychiatric disorders are characterized by altered social cognition. The importance of social cognition has previously been recognized by the NIMH Research Domain Criteria project, in which it features as a core domain. Social task-based functional magnetic resonance imaging (fMRI) currently offers the most direct insight into how the brain processes social information, however resting-state fMRI may be just as important in understanding the biology and network nature of social processing. Resting-state fMRI allows researchers to investigate the functional relationships between brain regions in a neutral state: so-called resting functional connectivity (RFC). There is evidence that RFC is predictive of how the brain processes information during social tasks. This is important since it shifts the focus from possibly context-dependent aberrations to context-independent aberrations in functional network architecture. Rather than being analysed in isolation, the study of resting-state brain networks shows promise in linking results of task-based fMRI results, structural connectivity, molecular imaging findings, and performance measures of social cognition – which may prove crucial in furthering our understanding of the social brain.

Keywords:
social cognition; intrinsic functional connectivity; resting functional connectivity; task-free fMRI; resting-state fMRI

Text

Functional magnetic resonance imaging (fMRI) offers unique insights into brain function. A particular avenue of interest is how functional connectivity (FC) techniques are employed to map relationships between spatially distant brain regions during a variety of cognitive tasks (Bressler & Menon, 2010; Fox et al., 2005). The same techniques have been applied to scans acquired during a sustained period of rest, i.e. the resting state (rs-fMRI). Note that while it is possible to generate "pseudo" resting-state data derived from task-based series (Fair et al., 2007), and such techniques make valuable contributions to social cognitive research (e.g. Iacoboni et al., 2004; Spunt, Meyer, & Lieberman, 2015), these data are not entirely equivalent to that obtained with rs-fMRI (Fransson, 2006) and are not the focus of this communication. Alterations in resting functional connectivity (RFC) have been described in multiple psychiatric and neurological disorders (Bressler & Menon, 2010; Buckner, Andrews-Hanna, & Schacter, 2008; Kennedy & Adolphs, 2012). While such work is important, in isolation it has little relevance to understanding the fundamental workings of the brain, disruptions in the context of disorder, or biological basis of treatment effects. A deeper understanding requires insight into how variations in RFC relate to cognitive constructs, operations, and performance (Bilder et al., 2009; Kelly, Biswal, Craddock, Castellanos, & Milham, 2012).

The social brain hypothesis suggests that our brains evolved to navigate complex social systems (Dunbar, 1998). Social cognition, or *"the mental operations that underlie social interactions, including perceiving, interpreting, and generating responses to the intentions, dispositions, and behaviours of others"* (Green et al., 2008) may therefore be considered as fundamental to our nature. Impairments in social cognition are found in most psychiatric conditions (Kennedy & Adolphs, 2012) and constitute a significant component of the morbidity associated with these diagnoses. Recognizing its trans-diagnostic importance, social processing has been included as one of the domains in the NIMH Research Domain

Criteria (RDoC) project for classifying mental illnesses (Cuthbert & Insel, 2013). While the relationship between RFC and social cognition remains relatively understudied, several recent initiatives have begun to address this, with the inclusion of both social cognition measures and rs-fMRI in open databases in which participants also undergo deep phenotypic characterization and genetic sampling (for instance McDonald et al., 2017; Miller et al., 2016). There are numerous advantages to research using such large datasets, including the option to use normative modelling as an alternative to the more traditional clustering used in case-control studies (Marquand, Rezek, Buitelaar, & Beckmann, 2016). In this communication we briefly discuss strategies in which rs-fMRI can contribute to social cognition research with some examples. Further examples are found in **Table 3.1**.

The social cognitive significance of RFC findings is frequently speculated upon when analyses reveal functional connectivity between regions for which there is independent evidence of social function (Schilbach, Eickhoff, Rotarska-Jagiela, Fink, & Vogeley, 2008). Regions implicated in such experiments include the temporoparietal junction, inferior frontal gyrus, anterior insula, anterior cingulate cortex and medial prefrontal cortex (Frith & Frith, 2007; van Veluw & Chance, 2014). Most research attempting to link RFC and social cognition has been directed at identifying overlaps between resting networks identified by independent component analysis (ICA) or seed-based correlation techniques and networks activated by social task fMRI. Observations of similarity between the default mode network (DMN) – an RFC network, and networks activated by social tasks (Buckner et al., 2008) have for example been confirmed by using meta-analytic connectivity modelling approaches (Amft et al., 2015; Jack et al., 2013; Laird et al., 2011; Schilbach, Bzdok, Timmermans, Fox, & Laird, 2012). While informative, conjunction analyses using the data of multiple independent research samples only imply shared spatial distribution of networks. This offers at best indirect evidence of shared function. Two approaches that more directly link social cognition and RFC are outlined below, which allow direct investigation of the relation between RFC and social cognition on an individual subject level.

The first approach combines rs-fMRI and non-imaging phenotypic measures in the same participants. RFC between brain regions on a per-subject level can then be correlated with scores on validated psychological instruments that test social cognitive domains of interest. For example, RFC measures of the medial prefrontal cortex have been correlated with self-reported empathic capacity in healthy volunteers (Takeuchi et al., 2014). The approach of

correlating RFC to phenotypic measures is also well-suited to exploratory multivariate analyses of large datasets, wherein multiple RFC measures can be linked to multiple domains of social cognition. The availability of publicly available, large databases represent great opportunities in this regard (McDonald et al., 2017; Miller et al., 2016; Nooner et al., 2012). At the network level, graph theory metrics from RFC data can be used to mine large datasets for significant correlations (Zanin et al., 2016). While correlations have been performed between graph metrics (e.g. clustering coefficient, characteristic path length, etc.) and more traditional cognitive domains (Alavash, Doebler, Holling, Thiel, & Gießing, 2015; Santarnecchi, Galli, Polizzotto, Rossi, & Rossi, 2014), there are limited studies in which graph metrics have been correlated with social cognition measures. In one such study, decreased network centrality within a fronto-temporo-insular network in patients with probable behavioural variant frontotemporal dementia was associated with impairments in social cognition scores (Sedeño et al., 2016).

In the second approach, rs-fMRI and social-task fMRI are performed in the same participants. In such approaches, RFC is either correlated to regional activations or to FC during social tasks. An example of such a comparative FC approach is to be found in research by Hyatt et al, who related three DMN subnetworks to FC during a mentalizing task in healthy volunteers (Hyatt, Calhoun, Pearlson, & Assaf, 2015). In a fascinating study that offers further evidence of the benefit of large databases, RFC data from the Human Connectome Project were successfully used to train a model to predict individual differences in regional activation on task-based fMRI (including social cognitive tasks) in the same subjects (Tavor et al., 2016). That RFC can be used to successfully predict the brain's activity during tasks is perhaps the most compelling rationale for the value of RFC in social cognition research. This is important since it shifts the focus from possibly context-dependent aberrations (activity or FC on task) to context-independent aberrations in functional network architecture (RFC) when investigating social cognition in the normal or abnormal ranges. The future inclusion of RFC measures in innovative hyperscanning experimental designs, in which multiple subjects are scanned simultaneously, allowing the direct study of social interactions (Montague et al., 2002), or in experience sampling studies, in which subjects undergo intensive longitudinal sampling during daily life social interactions (Hurlburt, 1997), may also be beneficial in contextualizing scan results.

Inclusion of rs- fMRI in addition to task-based fMRI potentially clarifies the spatiotemporal relationships between RFC and task-dependent FC, and allows RFC (sub)networks to be functionally characterized and segregated. While rs-fMRI has its pitfalls (Kelly et al., 2012), the inclusion of rs- fMRI sequences in social cognition research holds several advantages, especially in a multimodal imaging context. In addition to contextualizing findings from task-based fMRI, the combination of RFC with structural and molecular imaging measures in the same subjects has the potential to provide sophisticated models of social cognition in relation to both the architecture and function of the brain in health and disease.

Social cognition is innate to what makes us human. It is clear that the biological basis for social cognitive processing is complex and is best investigated with multiple complementary measures. Recognizing the valuable contributions of previous studies in the field, we suggest there is a compelling case motivating the increased use of rs-fMRI in future social cognition research.

Contributors

Manuscript: A Doruyter
Manuscript review: All authors
Supervisors: JM Warwick

Conflicts of Interest

None.

Acknowledgements

The PhD from which this work emanated was funded by the South African Medical Research Council under the MRC Clinician Researcher Programme.
The authors would like to thank the Nuclear Technologies in Medicine and the Biosciences Initiative (NTeMBI), a national technology platform developed and managed by the South African Nuclear Energy Corporation (Necsa) and funded by the department of Science and Technology.

Neither funder played any role in study design; collection, analysis, or interpretation of data; in the writing of this article or in the decision to submit it for publication.

Table

Table 3.1 Summary of studies that have correlated RFC and social cognition measures.

Study reference	Participants	RFC measure	Social cognition domain	Summary of relevant findings
Research correlating RFC measures with non-imaging measures of social cognition *Non-clinical samples:*				
(Takeuchi et al., 2014)	Healthy adults (n=248)	Seed-based analysis of *a priori* ROIs	Empathizing	Higher empathizing was associated with greater RFC between the mPFC and dorsal ACC; precuneus; and left STS.
(Takeuchi et al., 2013)	Healthy adults (n=248)	Seed-based analysis of *a priori* ROIs	Emotional processing	The intrapersonal factor of TEI was negatively correlated with RFC between mPFC and right dlPFC. The interpersonal factor of TEI was positively correlated with RFC between mPFC and lingual gyrus. Total TEI was positively correlated with RFC between mPFC and the precuneus as well as between the left AI and the middle part of the right dlPFC.
(Wu et al., 2016)	Healthy adults (n=258)	Seed-based analysis of *a priori* ROIs	Emotional processing	Women with higher trait-level emotion regulation exhibited stronger negative RFC between right CM and mSFG as well as

				stronger positive RFC between CM and AI and STG. Men with higher trait-level emotion regulation exhibited weaker negative RFC of right CM-mSFG and positive RFC of right CM-left AI, right CM-right AI/STG, and right CM-left STG.
(Cox et al., 2012)	Healthy adults (n=38)	Seed-based analysis of experimentally-derived ROIs (regions demonstrating correlation between fALFF and empathy scores)	Empathizing	Dominance of affective empathy was associated with greater RFC among social–emotional regions. Dominance of cognitive empathy was associated with greater RFC among regions implicated in interoception, autonomic monitoring and social–cognitive processing.
(Marchetti et al., 2015)	Healthy adults (n=670)	ROI x ROI correlation of atlas-derived parcellations (Harvard-Oxford atlas)	ToM	In participants with high ToM scores, a network with greater RFC with a dominance of the left hemisphere; as well as an increased within-lobe RFC in frontal and insular lobes was identified.
Clinical samples:				
(Cao et al., 2015)	Oesophageal cancer with ToM deficits (n=25) Oesophageal cancer controls (n=25)	ROI x ROI correlation of *a priori* ROIs	ToM	In the ToM deficit group, reduced RFC was found between several DMN regions.

(Caminiti et al., 2015)	bvFTD (n=12) HC (n=30)	Components identified on ICA	ToM	In the bvFTD group, higher affective mentalizing performance correlated with greater RFC between medial prefrontal sectors of DMN and attentional/performance monitoring networks, as well as with increased RFC between components of the executive, sensorimotor and fronto-limbic networks.
(Sedeño et al., 2016)	Probable bvFTD (n=14) HC (n=12) Frontoinsular stroke (n=10)	ROI x ROI correlations of atlas-derived parcellations (AAL atlas). Network centrality within different networks	Emotional processing and ToM	In the bvFTD group, decreased network centrality in frontotemporoinsular network was associated with impaired social cognition.
(Peeters et al., 2015)	Psychotic disorder (n=63) Unaffected siblings (n=73) HC (n=59)	Seed-based analysis of *a priori* ROIs	Emotional processing and ToM	In the total sample, reduced dlPFC-insula RFC was associated with lower social cognition scores.
(Fox et al., 2017)	Schizophrenia (n=28) HC (n=32)	Inter-component connectivity metrics calculated from components identified on ICA	Emotional processing and ToM	In the schizophrenia group, social cognition did not mediate the association between DMN connectivity and social functioning
(Abram et al., 2017)	Schizophrenia (n=28) HC (n=31)	Inter-component connectivity metrics calculated from	Empathizing	In the schizophrenia group, the medial-fronto-temporal metric and an orbito-fronto-

		components identified on ICA		temporal metric were related to cognitive empathizing.
(Jastorff et al., 2016)	bvFTD (n=14) HC (n=19)	Seed-based analysis of experimentally-derived ROIs (regions in which VBM results correlated with non-imaging task measure)	Emotional processing	In the bvFTD group, there was reduced RFC between several ROIs defined on the basis of the emotional processing measure: between ATL and mid and posterior temporal cortex, IFG, and mOFC. Left IFG demonstrated reduced connectivity with contralateral AI, contralateral amygdala and contralateral ATL.
(Mothersill et al., 2016)	Schizophrenia or schizoaffective disorder (n=27) HC (n=25)	Seed-based analysis of *a priori* ROIs	ToM	In the schizophrenia/schizoaffective disorder group, higher ToM scores were associated with increased RFC between left precuneus and right middle cingulate/right inferior frontal gyrus and between left TPJ and right calcarine gyrus/right lingual gyrus. Lower ToM scores were associated with higher RFC between left precuneus and right insula/left STG.
(Serra et al., 2016)	DM1 (n=20) HC (n=18)	ROI x ROI correlation of atlas-derived parcellations (AAL atlas)	ToM	In the DM1 group, ToM deficits were associated with abnormal connectivity between the left inferior temporal and fronto-cerebellar nodes.
(Wang, Song, Zhen, & Liu, 2016)	Healthy adults (n=268)	Seed-based analysis of experimentally-derived ROIs (regions identified on localizer fMRI)	ToM	Individuals with stronger within-network connectivity of the right pSTS performed better on the ToM task. Further, RFC between the right pSTS and right OFA, EVC, and

				bilateral STS were positively correlated with the scores of ToM. RFC of EVC-pSTS and OFA-pSTS contributed independently to ToM ability.
(Joshua T. Kantrowitz et al., 2015)	Schizophrenia or schizoaffective disorder (n=84) HC (n=66)	Seed-based analysis of experimentally-derived ROIs (regions identified on localizer fMRI)	Emotional processing	In the schizophrenia group, decreased auditory-insula RFC was associated with reduced scores of auditory emotion regulation.
(Sawaya et al., 2015)	MDD (n=21) HC (n=21)	Seed-based analysis of *a priori* ROIs	Emotional processing	There was a positive correlation between emotional intelligence score and RFC between BA25 and BA24.
(J. T. Kantrowitz, Hoptman, Leitman, Silipo, & Javitt, 2014)	Schizophrenia (n=76) HC (n=72)	Seed-based analysis of *a priori* ROIs	Social perception	In the schizophrenia group, sarcasm discrimination correlated with RFC within primary auditory regions. For controls, sarcasm discrimination correlated with RFC within core-mentalizing regions.
(Dodell-Feder, Delisi, & Hooker, 2014)	Familial high risk of schizophrenia (n=20) HC (n=17)	ROI x ROI correlation of *a priori* ROIs	Empathizing	Across all participants, no RFC between ROIs predicted empathic subscores.
(Fan et al., 2013)	Schizophrenia (n=27) HC (n=15)	Seed-based analysis of *a priori* ROI	Emotional processing	In the schizophrenia group, RFC between vmPFC and right middle temporal lobe; parahippocampal cortex and amygdala was

				positively correlated with the performance of emotional regulation.
Research correlating RFC measures with fMRI task-based measures of social cognition *Non-clinical samples:*				
(Hyatt, Calhoun, Pearlson, & Assaf, 2015)	Healthy adults (n=53)	Components identified on ICA	ToM	Spatial correlation between subnetworks that supported mentalizing and DMN subnetworks derived from rs-fMRI.
(Simmons & Martin, 2012)	Healthy adults (n=25)	Seed-based analysis of experimentally-derived ROIs (regions identified on localizer fMRI)	Social knowledge	RFC of social knowledge regions different to RFC of tool knowledge regions (domain-specific networks).
(Tavor et al., 2016)	Human Connectome Project subjects (n=98)	Components identified on ICA	ToM	RFC and structural data used to train a model that successfully predicted social-task based activations.
(Andrews-Hanna, Saxe, & Yarkoni, 2014)	Healthy adults (n=33)	Seed-based analysis of experimentally-derived ROIs (significant clusters on task-fMRI)	ToM	Left TPJ exhibited positive correlations with a network of medial and lateral regions throughout the DMN.
(Kanske, Böckler, Trautwein,	Healthy adults (n=178)	Seed-based analysis of experimentally-derived ROIs (significant clusters on task-fMRI)	Empathizing and ToM	Separable networks were demonstrated for empathy and ToM on task-based fMRI. These distinct networks could be replicated in RFC analysis.

& Singer, 2015)				
(Bzdok et al., 2013)	Healthy adults (n=139)	Seed-based analysis of experimentally-derived ROIs (significant clusters on MACM analysis of task-fMRI)	ToM	Convergent connectivity results across task-based FC and RFC of the vmPFC and dmPFC seed ROIs.
(Morawetz et al., 2016)	Healthy adults (n=60)	Seed-based analysis of *a priori* ROIs	Emotional processing	Greater RFC between ventrolateral prefrontal cortex and the amygdala was associated with emotion regulation success.
Clinical samples:				
(Alaerts et al., 2014)	ASD (n=15) HC (n=15)	Seed-based analysis of experimentally-derived ROIs (significant clusters on task-fMRI)	Emotional processing	In the ASD group, pSTS hypoactivity (on task) was related to reduction in RFC of pSTS and both measures were predictive of emotion recognition performance.
(Radke et al., 2017)	MDD (n=22) HC (n=22)	Seed-based analysis of experimentally-derived ROIs (significant clusters on task-fMRI)	Emotional processing	Differences on task-based fMRI did not extend to RFC.
(Ho et al., 2015)	MDD (n=26) HC (n=37)	Seed-based analysis of experimentally-derived ROIs (significant clusters on task-fMRI)	Emotional processing	In the MDD group, there was increased FC between PCC and subcallosal cingulate during emotional face processing and at rest.

(Mier et al., 2016)	Schizophrenia (n=22) HC (n=22)	Seed-based analysis of experimentally-derived ROI (significant cluster on task-fMRI)	ToM and emotional processing	In the schizophrenia group, reduced FC between right and left pSTS was revealed for affective ToM but not at rest.
(Prater, Hosanagar, Klumpp, Angstadt, & Phan, 2013)	SAD (n=20) HC (n=17)	Seed-based analysis of experimentally-derived ROIs (significant clusters on task-fMRI)	Emotional processing	In the SAD group, reduced FC between amygdala and rostral ACC and dlPFC while viewing fearful faces and at rest.

Note: in this table we have focused on empathizing, and the social cognitive domains defined by Green et al (Green et al., 2008), namely theory-of-mind; emotional processing; social knowledge; social perception; and attributional style (none). Other topics, such as self-referential processing; self-other processing; moral competence; agreeableness; etc. while relevant to social cognition, have not been included here.

Abbreviations: **(d/v)mPFC**: (dorso-/ventro-)medial prefrontal cortex; **(m)SFG**: (medial) superior frontal gyrus; **(p)STS**: (posterior) superior temporal sulcus; **(R)FC**: (resting) functional connectivity **AAL**: automated anatomical labelling; **ACC**: anterior cingulate cortex; **AI**: anterior insula; **ASD**: Autism spectrum disorder; **ATL**: anterior temporal lobe; **BA24/25**: Brodmann Areas 24/25; **bvFTD**: behavioural variant of fronto-temporal dementia; **CM**: centromedial amygdala; **dlPFC**: dorsolateral prefrontal cortex; **DM1**: Myotonic dystrophy type-1; **DMN**: default mode network; **EVC**: early visual cortex; **fALFF**: fractional amplitude of low-frequency fluctuations; **fMRI**: functional magnetic resonance imaging; **HC**: Healthy controls; **ICA**: independent component analysis; **IFG**: inferior frontal gyrus; **MACM**: meta-analytic connectivity modelling; **MDD**: Major Depressive Disorder; **mOFC**: medial orbitofrontal cortex; **mSFG**: medial superior frontal gyrus; **OFA**: occipital face area; **PCC**: posterior cingulate cortex; **ROIs**: regions of interest; **SAD**: Social Anxiety Disorder; **STG**: superior temporal gyrus; **TEI**: trait emotional intelligence; **ToM**: Theory-of-mind; **TPJ**: temporoparietal junction.

Disruptions in the theory of mind network in social anxiety disorder

Authors: Alex Doruyter[1], Patrick Dupont[2], Lian Taljaard[3], Dan J Stein[4], Christine Lochner[3], James M Warwick[1]

[1]Stellenbosch University Faculty of Medicine and Health Sciences, Division of Nuclear Medicine, Cape Town, South Africa.
[2]KU Leuven, Department of Neurosciences, Laboratory of Cognitive Neurology, Leuven, Belgium.
[3]MRC Unit on Risk and Resilience in Mental Disorders, Department of Psychiatry, Faculty of Medicine and Health Sciences, Stellenbosch University, Cape Town, South Africa.
[4]MRC Unit on Risk and Resilience in Mental Disorders, Department of Psychiatry, Faculty of Health Sciences, University of Cape Town, Cape Town, South Africa.

Publication status: Unpublished manuscript; being prepared for journal submission.

Abstract

Introduction: Social anxiety disorder (SAD) is associated with deficits in emotional processing and attribution. Given evidence that causal attribution of social events relies heavily on theory of mind (ToM) and given the spatial homology between the default mode network (a resting-state network) and the ToM network, a case can be made for studying the neural correlates of social attribution in SAD using resting-state fMRI. In addition, relatively little is known about the effect of pharmacotherapy on resting-state networks in SAD or about the behavioural correlates of any therapy-induced changes.
Methods: A graph theory approach was used to compare resting-state graph metrics within the ToM network in patients with a primary diagnosis of SAD (n=12) and a group of case-matched healthy controls (n=12) (effect of group: SAD vs HC) as well as in a subset of SAD participants (n=9) before and after a 8-9 week course of moclobemide (600mg daily) (effect of condition: baseline vs post-therapy). Clinical measures of disease severity, depressive symptoms, and disease improvement were also collected. Subject-specific graph metrics were correlated with individual scores on the Internal, Personal and Situational Attributions

Questionnaire (IPSAQ) at baseline. An exploratory analysis that investigated the nodal graph metrics and partial correlations of five a priori nodes within the ToM network was also performed.

Results: Compared to HCs, SAD participants exhibited reduced global efficiency and increased clustering coefficients within the ToM network as well as demonstrating evidence of disrupted social attributional style. No statistically significant relationship could be identified between individual graph metrics and IPSAQ scores. After therapy, SAD participants exhibited several changes in social attribution scores but no changes in graph metrics. In the exploratory nodal level analysis we found no group difference in graph metrics of the a priori nodes but did find changes in nodal metrics after therapy. Differences in partial correlations of several a priori nodes were detected for both comparisons.

Conclusion: We report the first evidence of disrupted global efficiency and clustering coefficients within the ToM network in SAD, supporting existing work of resting functional connectivity disruptions in the disorder. While findings of social attribution bias in SAD were consistent with previous studies, we were unable to correlate these changes with disrupted graph metrics. We found no evidence that moclobemide therapy resulted in network-level modifications within the ToM network in SAD but did provide novel evidence of altered attributional style post-therapy. Exploratory analysis of several a priori nodes within the ToM network with a putative role in social attribution yielded findings which merit further research.

Keywords: social anxiety disorder, graph theory, social attribution, attributional style, therapy, resting functional connectivity, resting-state fMRI

Introduction

Social anxiety disorder (SAD) is characterized by excessive fear and anxiety about, and avoidance of, social and/or performance situations (American Psychiatric Association and DSM-5 Task Force 2013). Several deficits have been identified in how people with SAD process social information (Plana et al. 2014). One domain of social cognition that remains relatively understudied in SAD is how sufferers attribute socially-relevant outcomes (i.e. causal attribution, or social attributional style).

There is evidence that SAD participants are prone to social attributional bias (Heimberg et al. 1989) and that SAD participants exhibit deficits in two related social cognitive domains, namely social interpretation (Amir et al. 1998; Stopa and Clark 2000; Franklin et al. 2005) and theory of mind (ToM) (Hezel and McNally 2014; Washburn et al. 2016). The neural correlates of social attribution in healthy volunteers has been studied using task-based functional magnetic resonance imaging (fMRI) and has implicated several brain regions including the temporoparietal junction, precuneus, superior temporal sulcus and medial prefrontal cortex (Seidel et al. 2010; Kestemont et al. 2012, 2015). These activations share considerable spatial homology with the ToM network which is activated by ToM tasks, and with the default mode network (DMN) which is active at rest (Laird et al. 2011). As previously posited, such similarities provide indirect evidence that a functionally distinct network, which is also active at rest, underlies the social cognitive processes of both ToM and social attribution (Mars et al. 2012). Disrupted resting functional connectivity (RFC) within the DMN or of its core nodes has previously been reported in SAD (Liao et al. 2010a; Liu et al. 2015b; Doruyter et al. 2016; Cui et al. 2017). There is limited evidence that pharmacotherapy affects RFC of the DMN in SAD (Giménez et al. 2014; Doruyter et al. 2016; Yuan et al. 2016).

The neural bases for deficits in social attribution in SAD are unknown and represent a target for further research. While such neural correlates can be investigated directly using social attribution task-based fMRI, they can also be studied by correlating resting-state fMRI (rs-fMRI) findings with behavioural measures. One technique well-suited to describing characteristics of complex brain networks is graph theory (Bullmore and Sporns 2009). Graphs can be constructed using either binary techniques (whereby edges are categorized as being either present or absent depending on weight) or weighted techniques (whereby edges are weighted along a continuum, depending on the strength of the connection between nodes) (Rubinov and Sporns 2010). There is evidence to suggest that weighted graphs are more robust than binary graphs since the threshold for binarization is largely arbitrary and binary graphs may not be reproducible at the single subject level (Wang et al. 2014). Graph metrics may be used to characterize global graph properties (the network as a whole) and also local properties, down to the individual nodal level. In addition to analysing graphs at the group level, it is possible to construct individual (subject-specific) weighted graphs, the metrics of which can then be correlated with clinical measures. Only a few experiments using graph theory have been conducted in SAD (Liao et al. 2010a; Zhu et al. 2017; Yun et al. 2017),

none of which limited their analysis to a distinct functional network or investigated the behavioural correlates of graph findings. While there is evidence that pharmacotherapy improves symptoms in SAD, no research has investigated whether pharmacotherapy has any effect on social attributional style or resting graph metrics in the disorder.

We hypothesized the following: firstly, compared to controls, SAD participants would demonstrate differences in graph metrics of the ToM network at rest; secondly, the SAD group would exhibit evidence of social attribution bias; and thirdly, that a correlation would be found between disrupted graph metrics and social attribution scores. Finally, we also hypothesised that pharmacotherapy would modify graph metrics and improve any social attribution deficits in the SAD group.

Methods

The study was approved by the health research ethics committee of Stellenbosch University (ref # S14/09/191).

Participants

Patients with SAD were recruited through the MRC Unit on Risk and Resilience in Mental Disorders. Volunteers were invited to join the study in advertisements on local radio stations and in print media, as well as online and through email campaigns. Potential volunteers were screened in an interview setting. Participants had to be between the ages of 18 and 55 years of age; right-handed; and fluent in English. SAD participants had to meet DSM-5 criteria for SAD and not have any comorbid mood or anxiety disorders, substance use or psychotic disorders. Volunteers were excluded from participation if they had any metal implants or claustrophobia that would preclude MRI; had any current or prior neurological illness, any current or prior psychiatric condition, or prior head injury resulting in loss of consciousness; had any serious medical conditions; or were heavy caffeine users (>600mg per day). All SAD participants were free of psychotropic medication (other than the study medication) at study visits. SAD participants already on medication were not excluded from the study, provided they were willing to taper and discontinue their medication and then commence with moclobemide 600mg after a suitable washout period. SAD participants who could not safely

stop medications known to interact with moclobemide were excluded. SAD and healthy control (HC) participants were matched for age and sex.

Screening, clinical and social cognition measures

All participants were telephonically screened. HC participants subsequently attended a total of 3 study visits, which included a comprehensive clinical interview; as well as separate visits for neuroimaging and social cognition measures. SAD participants attended 5 study visits, comprising a visit for the clinical interview; a visit for neuroimaging; a visit for the social cognition measure; a follow-up neuroimaging session; and a final visit in which the social cognition measure was repeated. All participants underwent a structured clinical interview for DSM-IV (SCID) (First et al. 1996) and completed the Edinburgh Handedness Inventory (Oldfield 1971) as part of the screening process. A separate checklist was used to ensure SAD participants also met criteria on DSM-5. In addition, participants completed the Liebowitz Social Anxiety Scale (LSAS) (Liebowitz 1987) and Beck Depression Inventory (BDI-II) (Beck et al. 1996) to assess the severity of social anxiety and depressive symptoms, respectively.

At each study visit participants completed the state version of the State Trait Anxiety Inventory (STAI-S) which measures levels of anxiety at the time of the measure (Spielberger 1983). The efficacy of pharmacotherapy was studied with the Clinical Global Impressions Improvement scale (CGI-I) (Guy 1976).

Social attributional style was measured with the Internal, Personal, and Situational Attributions Questionnaire (IPSAQ). This measure was completed once by healthy controls and twice (at baseline and post-therapy) by SAD participants. Participants were asked to read an equal number of negative (16) and positive (16) hypothetical scenarios in which they imagine themselves interacting with someone else. They were then asked to record what caused the event and then record whether the cause was “something about you”; “something about the other person or other people”; or “something about the situation (circumstances or chance)”. The attributions recorded in the responses were categorized as either internal, external (personal) or external (situational) (Kinderman and Bentall 1996). Several derived measures were also calculated. Externalizing bias (EB) was calculated by subtracting the

number of internal attributions for negative events from the number of internal attributions for positive events and is indicative of either a self-serving bias (positive score) or self-effacing bias (negative score). Personalizing bias for negative events (PBn) was calculated by dividing the number of personal attributions for negative events by the sum of both personalizing and situational attributions for negative events and represents the degree to which participants attribute negative events to external personal (scores greater than 0.5), rather than external situational causes (scores less than 0.5). Similarly, personalizing bias for positive events (PBp) was calculated by dividing the number of personal attributions for positive events by the sum of both personalizing and situational attributions for positive events and represents the degree to which participants attribute positive events to external personal (scores greater than 0.5), rather than external situational causes (scores less than 0.5) (Kinderman et al. 1998).

Pharmacotherapy

After baseline measurements were completed, SAD participants commenced with a course of moclobemide according to clinical prescribing guidelines for SAD (300 mg PO once daily for 3 days, followed by 300 mg PO twice daily thereafter). After at least 8 weeks of therapy, follow-up measures were completed whereafter participants either opted to continue on moclobemide or discontinue the medication in favour of other management strategies. SAD participants were closely monitored for adverse effects during the trial period and for symptoms of discontinuation in the event that the study medication was stopped.

Neuroimaging

SAD participants were scanned both at baseline and at the end of therapy. Participants were instructed not to ingest any caffeine-containing food or beverages in the 2 hours preceding the scan. MRI scanning was initially performed on a 3 tesla (3T) Siemens Magnetom Allegra camera (Siemens Medical Systems, Erlangen, Germany). Midway through the project, this scanner was decommissioned and imaging was switched to a 3T Siemens Magnetom Skyra. Acquisition parameters across the two systems were optimized to reduce scanner-related bias. Scan parameters for the functional resting-state T2-weighted sequence on the Allegra system: single-shot gradient echo planar imaging (EPI); 300 volumes; repetition time (TR) = 1600

ms; echo time (TE) = 23 ms; flip angle = 73°; number of slices = 30; slice gap = 0.2 mm; field of view = 255 x 255 mm; voxel size = 4mm x 4mm x 4mm. On the Skyra system: same settings except TR = 1740 ms. Additional structural scans (T1-weighted ME-MPRAGE; T2; FLAIR) were acquired for anatomical co-registration and to exclude relevant intracranial pathology.

Before imaging, participants completed the STAI-S measure and received an explanation of the scanning procedure. They were instructed to lie still and to keep their eyes open during the scan. After being comfortably positioned in the scanner participants viewed a black screen with the word "RELAX", centred in their field of view. After a few seconds this screen was replaced by a blank black screen and the scan session was commenced. After the scanning patients were debriefed on their experience and questioned as to whether they kept their eyes open during the functional sequence.

Pre-processing

In addition to radiologist review for structural abnormalities, all scans were reviewed visually for artefacts. DICOM images were converted to NIfTI format and pre-processing was performed using SPM12 (http://www.fil.ion.ucl.ac.uk/spm/) and MATLAB (Mathworks R2014b). Functional images were realigned and checked for significant motion using a custom script. Functional scans in which there was more than 2 mm translation overall; or more than 1 mm momentary translation; or more than 2° rotation were excluded from the analysis. Functional scans were slice time corrected and co-registered to the T1-weighted structural image using the normalized mutual information estimation option. For follow-up scans of the same participants (SAD group) a second co-registration was performed in which follow-up scans were co-registered to the baseline structural scan. The SPM Segment function was used to extract tissue classes from the structural scan and calculate a deformation field to a standardized template (SPM Average sized template). Functional images were then warped using the relevant deformation field and written to a final voxel size of 4x4x4 mm. No additional smoothing was performed. All images were bandpass filtered at a frequency range of 0.009 – 0.1 Hz.

Network nodes

Procedures for node definition and graph analysis were performed using customized scripts for SPM12 and MATLAB. For nodes in the ToM network, we first created 17 volumes of interest (VOIs; spheres with radii of 6mm). These VOIs were centred on activation peaks for ToM tasks reported in a meta-analysis by Bzdok et al. (Bzdok et al. 2012), the names, abbreviations, and MNI coordinates of which appear in **Table 4.1** and are illustrated in **Figure 4.1**.

Five of these VOIs, i.e. left and right temporoparietal junction (L TPJ, R TPJ); left and right posterior superior temporal sulcus (L pSTS; R pSTS), and precuneus (Precun) were selected to represent regions of a priori interest in social attribution (Kestemont et al. 2016), for a secondary exploratory analysis of individual nodal graph metrics and connectivity.

Subject-specific VOIs were then generated by calculating the intersection of the relevant spherical VOI and corresponding gray matter map. In the event that the final subject-specific VOI was smaller than 10 voxels, additional neighbouring voxels were included to form a single cluster, until the minimum VOI size threshold was reached. The time series of every VOI was then extracted and corrected by regressing out white matter and CSF signal, as well as the 6 motion regressors. The partial correlation coefficient between the averaged (across voxels) time series of each node-pair was calculated for each participant and transformed to a Z-score using a Fisher's r-to-Z transform for partial correlations.

Graph construction

We performed weighted, undirected graph constructions at two levels: at the group level, and at the individual level. At the group level, edges (a) were defined by weights obtained after transforming the absolute value of the average Z-scores Z_{ij} (across subjects in the group) to a weight using the power law transformation $w_{ij} = (2\varphi(Z_{ij}) - 1)^4$where φ is the cumulative distribution function of the standard normal distribution (Wang et al. 2017). The graphs were constructed for each participant group. A comparable method was used to construct weighted graphs on the individual level (subject-specific). Metrics derived from these graphs were used for correlation with clinical measures.

Graph measures

We calculated the following graph metrics at both group and individual levels:

Global metrics

Mean clustering coefficient (C) is a measure of network segregation (based on the number of triangles in the network, with a high value implying network segregation). The mean clustering coefficient reflects on average, how clustered connectivity is around individual nodes in the network. The method for calculation of the mean clustering coefficient for weighted graphs was as described by Wang et al (Wang et al. 2017).

Mean characteristic path length (λ) is the average shortest path length (where length refers to the number of connections linking any two nodes) between all network nodes. It is a measure of network integration in connected networks.

Mean global efficiency (E) is related to the average inverse shortest path length between all network nodes. Like characteristic path length, it is a measure of network integration.

Mean betweenness centrality (BC) refers to the fraction of all shortest paths that pass through a node in the network. It is a measure of the average importance of nodes within the network. Both binary and weighted networks were calculated.

λ, E and BC were calculated as described by Rubinov and Sporns (Rubinov and Sporns 2010).

Local nodal metrics

As a secondary, exploratory analysis, individual nodal metrics were calculated for five VOIs, selected a priori as regions for which there was evidence in social attribution (references on calculation methods in parentheses).

Nodal clustering coefficient (C_i) (Wang et al. 2017).
Nodal characteristic path length (λ_i) (Rubinov and Sporns 2010).
Nodal local efficiency (E_{loci}) (Wang et al. 2017).
Nodal betweenness centrality (BC_i) (Rubinov and Sporns 2010).

Global and nodal graph metrics were normalized by the average value obtained in 10 equivalent random graphs, i.e. graphs with the same number of nodes and the same distribution of weights but which are randomly assigned to each node-pair.

Statistical analysis

Two broad comparisons were made. In the first, we compared two groups: SAD and HCs participants (effect of group: SAD vs HC). In the second comparison we investigated the effect of therapy within the SAD group (effect of condition: baseline vs post-therapy).

All statistical analyses were performed using MATLAB (Mathworks R2014b). A statistical threshold for significance of p = 0.05 was used throughout. No corrections for multiple testing were applied.
Group matching for age was tested using a two-tailed Welch's t-test while matching for education level was tested with the Freeman-Halton extension of the Fisher exact test.
Differences in clinical scores and social cognition scores were tested with a two-tailed Welch's t-test (effect of group: SAD vs HC comparison) and a single-tailed paired t-test (effect of condition: SAD baseline vs post-therapy).
Differences in group-level graph metrics for both comparisons (effect of group; effect of condition) were evaluated using non-parametric group-membership permutation testing. These methods have an advantage over parametric methods in that they better account for complexity within networks (Simpson et al. 2013). As part of this analysis, the graph constructs were compared to 500 randomly generated equivalent graphs and compared to 500 random assignments to group or condition.
Individual (subject-specific) graph measures shown to be disrupted in the group comparison were correlated with social attribution measures found to be statistically different in the group comparison using simple linear regressions. These were conducted for both HC and SAD

groups combined and for the SAD group. Similar analyses were used to test whether disease severity (LSAS) had any effect on these measures in the SAD group.
A secondary, exploratory analysis comparing local nodal graph metrics of five VOIs (for which there was strong a priori evidence of relevance to social attribution) was performed using two-tailed Welch's t-tests (effect of group: SAD vs HC comparison) and two-tailed paired t-tests (effect of condition: baseline vs post therapy). The same tests were used to detect differences in partial correlations between these nodes and other nodes within the ToM network.

Results

Participants

Fifteen participants with SAD and 15 age- and sex-matched healthy controls (HC) were recruited.

In the group analysis, the rs-fMRI of two SAD participants and one HC (and their matched counterparts) were excluded due to excessive motion while in the scanner. Final group size was thus SAD (n=12) and HC (n=12).

In the condition (effect of therapy) analysis, baseline and follow-up measures were available for 12 SAD participants, however three participants were excluded due to excessive motion during either the baseline or follow-up scan. One SAD participant included in this analysis was excluded from the SAD vs HC analysis due to excessive motion of their matched control. Final group size in this comparison was thus (n=9).

Demographics

The demographics of participants appear in **Table 4.2**. No significant differences were detected between groups in terms of age and sex.

In the effect of therapy analysis, the 9 SAD participants consisted of 5 males and 4 females with a mean age of 30 years (range: 21.4 – 42.6).

Clinical characteristics

In the group (SAD vs HC) comparison, SAD participants had a significantly higher mean (±SD) LSAS score of 87.5 (±26.7) compared to the HC participants' 19.0 (±10.6) ($p<0.0001$). Mean (±SD) BDI-II score in the SAD group at baseline was 12.1 (±8.8) compared with 4.0 (±5.1) in the HC group, which also reflects a significant difference ($p=0.013$). Despite not having any psychiatric comorbidity based on the SCID-assessment, several participants fell into the clinical ranges for depression based on self-report BDI-II scores: one participant in the HC group met BDI-II criteria for mild depression, while in the SAD group there were 3 participants whose depressive symptoms were mild, 1 with moderate depressive symptoms, and 1 with severe depressive symptoms. There were no significant intragroup differences in STAI-S scores across baseline visits. There were significant intergroup differences in STAI-S scores across baseline visits: in the effect of group (SAD vs HC) comparison, SAD participants had significantly higher state anxiety compared to HCs ($p < 0.0001$).

In the effect of condition (baseline vs post-therapy) comparison SAD participants received a mean of 8.9 weeks (range: 8.0 – 12.1) of moclobemide therapy between baseline and follow-up measures. The effects of therapy on clinical measures are summarized in **Table 4.3**. There were no significant difference in STAI-S scores across baseline visits, nor across follow-up visits. There was however a significant reduction in state anxiety scores when comparing STAI-S scores pre-treatment to STAI-S scores post-treatment ($p=0.0001$).

Social cognition

On the IPSAQ, SAD participants were more likely than HCs to attribute negative items to an internal cause and less likely to attribute negative items to a situational cause. This also resulted in lower EB scores in the SAD group. When SAD participants did attribute negative events to external causes, these were more frequently personal as opposed to situational, as reflected by the higher PBn score in the patient group. There was no correlation between disease severity as measured by the LSAS and EB ($p=0.91$) or PBn ($p=0.496$) scores in the SAD group.

After pharmacotherapy, SAD participants attributed fewer positive events to an external personal cause, as reflected by the significant reduction in their PBp score. There were no other statistically significant changes in IPSAQ scores from pre- to post-therapy.

Results of the IPSAQ scores for the two comparisons are summarized in **Table 4.4**.

Graph measures

Global metrics

Partial correlation matrices used for the global graph analysis are presented in **Figure 4.2**.

In the effect of group (SAD vs HC) comparison, SAD participants exhibited reduced global efficiency (E) ($p = 0.02$) and increased clustering coefficients (C) ($p=0.04$) within the ToM network when compared to controls.
For SAD participants, no statistically significant differences in graph metrics were detected when comparing baseline to post-therapy conditions. A summary of group differences in graph metrics is presented in **Table 4.5.**

Local nodal metrics and connectivity of a priori VOIs

In the effect of group (SAD vs HC) comparison, no significant differences were detected in nodal graph metrics of the selected a priori VOIs.

In the effect of condition (baseline vs post-therapy) comparison, SAD participants exhibited a reduction in local efficiency of the left temporoparietal junction ($p=0.042$), as well as an increase in the node degree of the right posterior superior temporal sulcus ($p=0.047$).

Significant differences in partial correlations, between selected a priori nodes and other nodes within the network for both comparisons are summarized in **Table 4.6**.

Correlates between subject-specific graph metrics and social attribution scores

No significant correlations between disrupted graph metrics (E, C) and either externalizing bias (EB), or personalizing bias (PBn) were found.

Discussion

A graph theory approach was used to compare resting-state graph metrics within the ToM network in patients with SAD and a group of case-matched healthy controls, as well as for a subset of SAD participants before and after an 8-9 week course of moclobemide. In addition, an exploratory analysis that investigated the nodal graph metrics and partial correlations of five a priori nodes within the ToM network was performed. We found evidence of social attribution bias and differences in graph metrics within the ToM network at rest in SAD. No statistically significant relationship could be identified between disrupted graph metrics and social attribution scores, either in the SAD group alone or in the larger group (HC and SAD participants combined). A secondary analysis of graph metrics of five a priori nodes potentially relevant to social attribution and of the partial correlations between these a priori nodes and other nodes in the ToM network, found several differences between SAD and HC groups. Compared to baseline, SAD participants after a course of moclobemide demonstrated changes in social attributional style, but no changes in graph metrics within the ToM. There were however changes in local nodal graph metrics and partial correlations of a priori nodes after therapy.

In our study we found that SAD participants were more likely than HCs to attribute negative scenarios to themselves (internal attribution), which was also manifested by lower EB scores (reflecting a self-effacing bias, attributing negative events more and positive events less to oneself) in the patient group. When SAD participants in our sample did attribute negative events to external causes, they were more likely to attribute them to personal rather than situational causes (as manifest by the higher PBn scores in the SAD group). Attributions have previously been defined as causal statements; i.e. any statement that includes or implies the *cause* of an event (Green et al. 2008). Typically such attributional statements are categorized as either *external situational* (something about the situation resulted in the outcome); *external personal* (something that someone else did resulted in the outcome); or *internal* (something I

did resulted in the outcome) (Kinderman and Bentall 1996). Our findings are consistent with work by Heimberg et al who reported that compared to controls, SAD participants more frequently attributed negative events and less frequently attributed positive events to internal causes (Heimberg et al. 1989). Our results are also consistent with earlier experiments on social interpretation in SAD which found that not only were SAD participants more likely to classify ambiguous social scenarios as negative (Stopa and Clark 2000; Franklin et al. 2005) but they were more likely to do so when the scenarios were self-relevant (Amir et al. 1998). There are no studies that have directly investigated social attribution in SAD using task-based fMRI, as has for example been performed in depressed patients (Seidel et al. 2012; Hao et al. 2015). A task-based fMRI experiment that used a ToM task has however been performed in SAD. Sripada et al reported differences in brain activation in SAD participants (n=26) compared to HCs (n=26) while mentalizing during a simulated economic exchange task (trust game). In that study, SAD participants showed reduced activation in medial prefrontal cortex during mentalizing (Sripada et al. 2009). As already discussed, there is a rationale for investigating the neural correlates of ToM and related processes such as social attribution using RFC measures on rs-fMRI. Several studies have investigated RFC within the DMN/ToM network in SAD which have found various disruptions in connectivity in SAD participants (Liao et al. 2010a; Liu et al. 2015b; Doruyter et al. 2016; Cui et al. 2017), although one study (Pannekoek et al. 2013) reported no difference between patients and HCs. None of these studies correlated RFC findings with behavioural measures.

We found that in SAD, there was reduced mean global efficiency (a measure of how integrated a network is) and increased mean clustering coefficient (a measure of how segregated individual network nodes are from one another) within the ToM network at rest. Graph analysis, which focuses on various characteristics of complex networks, is a promising tool for studying interactions within distributed brain regions (Wang et al. 2014) yet only limited research using graph theory has been conducted in SAD. In one study, researchers compared whole brain, voxel-to-voxel resting functional connectivity strength (FCS) in SAD and HC groups and defined network hubs as regions with the highest FCS (Liu 2011). That study found disruptions in SAD in two cortical hubs, one of which was the precuneus, which is commonly considered as the core node of the DMN (Greicius et al. 2003) and by extension the ToM network. This is consistent with our own finding of a reduction in global efficiency within the ToM network at rest. Two other studies that used all 90 regions from the automated anatomical labelling atlas (AAL), to construct graphs in both SAD and HC groups

reported abnormalities relating to the middle temporal gyrus (Yun et al. 2017) and the temporal pole (mid) (Zhu et al. 2017) which are also nodes of the ToM network. Unlike these previous studies, rather than using all voxels in the brain, or a large number of atlas-based parcellations, our graph analysis was confined to a much more limited set of nodes (Stanley et al. 2013), to probe a specific network.

While we found independent evidence of ToM network disruption and social attribution bias in SAD, we were unable to detect any correlation between either of the graph metrics identified as disrupted in SAD and individual IPSAQ scores, either in the SAD group or when combining both HC and SAD participants used in the group comparison. Only limited research has investigated the social cognitive correlates of RFC findings in SAD. Prater et al performed both rs-fMRI and an emotional processing task fMRI (viewing of fearful faces) and reported reduced FC between amygdala and rostral anterior cingulate and dorsolateral prefrontal cortex both at rest and during the task (Prater et al. 2013). That study directly linked RFC with brain activation during complex social cognitive processes. Resting graph metrics are also suited to investigating the neural underpinnings of social cognition as shown by a study that correlated network centrality with impairments in emotional processing and ToM in patients with behavioural variant frontotemporal dementia (Sedeño et al. 2016). Ours is the first study investigating the relationship between graph metrics and a social cognition measure in SAD.

This is the first report to focus on the effects of pharmacotherapy on graph metrics in SAD. We did not identify any changes to graph metrics within the ToM network in a group of SAD participants treated with moclobemide, despite clinical evidence of therapeutic effect. We did however find evidence in our exploratory analysis that such effects might exist. That therapy might have an effect on resting graph measures within the ToM network in SAD is suggested by evidence of therapy effects on RFC of regions overlapping with this network's distribution. Our group has for example previously reported on changes in perfusion SPECT-based RFC of the anterior cingulate and precuneus after pharmacotherapy in SAD (Doruyter et al. 2016), while other groups have reported therapy-related RFC changes in dorsomedial prefrontal cortex and dorsal anterior cingulate (Giménez et al. 2014; Yuan et al. 2016). The use of a graph approach to understanding the impact of pharmacotherapy is promising, and is being applied to other disorders (Shin et al. 2014; Wang et al. 2015, 2016; Haneef et al. 2015; Hadley et al. 2016).

In our secondary, exploratory analysis we identified several group differences in partial correlations of several a priori nodes within the ToM network. We also found changes to both nodal graph metrics and partial correlations of these nodes after therapy. In addition to their involvement in ToM, these regions all share a putative role in social attribution (Kestemont et al. 2016). We limited ourselves to these five regions in this analysis, since it was not possible to correct for multiple comparisons. While the results of this exploratory enquiry are interesting, they were not the primary aim of the experiment. Our findings may serve to generate hypotheses for future experiments.

Our study had several limitations. Despite screening for depressive symptoms, six participants, all but one from the SAD group, scored in the clinical range on the self-report BDI-II questionnaire. While we cannot exclude the possibility that the effects seen were driven by depressive symptoms, rather than social anxiety, this is unlikely given that in all cases SAD was the dominant condition in terms of severity, and none of the patients were diagnosed with major depressive disorder using the SCID. Furthermore, it may be argued that this distinction is in many respects artificial, given the frequent comorbidity of SAD and depression (Ohayon and Schatzberg 2010) and evidence that they stem from a shared underlying genetic vulnerability (Langer and Rodebaugh 2014). Another limitation of our study was the small group sizes, potentially increasing the risk of over-representing the contribution of statistical outliers, and reducing sensitivity for small effect sizes. Two approaches in our study design partly mitigate against the risk of false positives imposed by small group sizes: first, we carefully matched (on a per subject level) our SAD and HC samples, thus reducing the risk of outliers; and second, we limited our analysis to RFC in a set of confined regions in a network with strong internodal correlations, making the risk of false positives much lower than in a whole-brain analysis (Cremers and Roelofs 2016). Such measures do not however address the reduction in sensitivity inherent to analyses using small groups, and as such our negative result for the effect of condition (baseline vs post-therapy) comparison might simply imply that the effect sizes of any changes in graph metrics after therapy were too small to detect with our sample sizes. Our choice of moclobemide as a therapeutic agent might be criticized given that most guidelines currently recommend a selective serotonin reuptake inhibitor (SSRI) as first-line pharmacological intervention (National Collaborating Centre for Mental Health (UK) 2013). It should be noted however that the rationale for this recommendation is largely based on the observation that

monoamine oxidase inhibitors (MAOIs) as a class are associated with more drug interactions, dietary restrictions and side effects; and not based on evidence of their therapeutic inferiority to other pharmacological interventions. Moclobemide is a reversible MAOI which does not have the same risk profile or dietary restrictions as other members of its class and several studies have confirmed its safety and tolerability (Stein et al. 2002; Bonnet 2003). There is no evidence that when used at therapeutic doses, moclobemide is inferior to SSRIs when treating SAD and it remains an established therapeutic option in managing SAD. The final limitation of our study relates to the fact that because we did not include a placebo group in our therapy effect comparison, or obtain repeat measures in our HC group, we were not able to distinguish true therapeutic effects from expectancy effects or effects related to subject familiarity with the measures at follow up.

Conclusion

The study findings were concordant with existing evidence on social attribution bias in SAD, providing further support for social cognitive deficits in the disorder. In addition, disrupted RFC within the ToM network in SAD, as evidenced by differences in global efficiency and clustering coefficient supports existing work suggesting RFC disruptions in the DMN in SAD. We were however unable to link individual graph metrics to behavioural measures of social attribution. Our study adds to the existing knowledge of how pharmacotherapy affects social attribution in SAD although we could not detect changes in global graph metrics within the ToM network. Exploratory analysis of several a priori nodes within the ToM network with a putative role in social attribution, yielded findings which merit further research.

Contributors

Data collection: A Doruyter, L Taljaard, C Lochner
Data processing and analysis: A Doruyter, P Dupont
Manuscript: A Doruyter
Manuscript review: All authors
Supervisors: JM Warwick, C Lochner

Conflicts of Interest

None.

Acknowledgements

The PhD from which this study emanated was funded by the South African Medical Research Council (MRC) under the MRC Clinician Researcher Programme.
Study costs were funded by the Nuclear Technologies in Medicine and the Biosciences Initiative (NTeMBI), a national technology platform developed and managed by the South African Nuclear Energy Corporation (Necsa) and funded by the department of Science and Technology; and the Harry Crossley Foundation.

Profs Stein and Lochner receive funding from the MRC.

None of the funders played any role in study design; collection, analysis, or interpretation of data; in the writing of this article or in the decision to submit it for publication.

Tables and Figures

Table 4.1 Network nodes used to construct graphs. A sphere of r=6mm was centred on each coordinate to generate the relevant VOI. Coordinates from (Bzdok et al. 2012). The 5 a priori nodes are indicated in **bold text**.

MNI coordinates			Abbreviation	Region
x	y	z		
0	52	-12	vmPFC	Ventromedial prefrontal cortex
2	58	12	fPOC	Frontopolar cortex
-8	56	30	dmPFC1	Dorsomedial prefrontal cortex 1
4	58	25	dmPFC2	Dorsomedial prefrontal cortex 2
2	-56	30	**Precun**	Precuneus
56	-50	18	**R TPJ**	Right temporoparietal junction
-48	-56	24	**L TPJ**	Left temporoparietal junction
54	-2	20	R TPO	Right temporal pole
-54	-2	-24	L TPO	Left temporal pole
52	-18	-12	R MTG	Right middle temporal gyrus
-54	-28	-4	L MTG1	Left middle temporal gyrus 1
-58	-12	-12	L MTG2	Left middle temporal gyrus 2
50	-34	0	**R pSTS**	Right posterior superior temporal sulcus
-58	-44	4	**L pSTS**	Left posterior superior temporal sulcus
54	28	6	R IFG	Right inferior frontal gyrus (Area 45)
-48	30	-12	L IFG	Left inferior frontal gyrus
48	-72	8	R MTV5	Right MT/V5 (middle temporal visual area 5)

Table 4.2 Demographics and group matching in the SAD vs HC baseline analysis

	Group		
	HC	**SAD**	**p**
Total (n)	12	12	-
Mean age in years	31.0 (21.2 – 46.8)	30.5 (21.0 – 45.6)	0.88[a]
Sex	Female: 8, Male: 4	Female: 8, Male: 4	-
Highest level of education:			
Formal schooling incomplete	1	1	0.07[b]
Additional training college or technical qualification	0	4	
Additional University degree	11	7	

[a] Two-tailed Welch's t-test

[b] Freeman-Halton extension of the Fisher exact test

Table 4.3 Clinical measures in SAD participants (n=12) used for the effect of therapy analysis, mean and standard deviation (SD):

	Condition				
	Baseline		**Post-therapy**		
	mean	*SD*	*mean*	*SD*	*p*[*]
LSAS	88.9	30.3	68.0	40.9	**0.02**
BDI-II	10.8	6.7	9.3	7.9	0.37
CGI-S	4.67	1.4	3.25	2.1	**0.04**
CGI-I			2.75	1.0	

[*] single-tailed paired student t-test

Table 4.4a IPSAQ scores for the SAD vs HC comparison, mean and standard deviation (SD):

	Group				
	HC		**SAD**		
	mean	*SD*	*mean*	*SD*	*p**
Positive items					
Internal	6.92	2.54	7.83	3.01	0.429
Personal	4.33	2.10	4.58	2.39	0.788
Situational	4.75	2.30	3.58	2.81	0.278
Negative items					
Internal	3.58	2.61	8.25	4.14	**0.004**
Personal	5.83	2.92	5.00	2.30	0.446
Situational	6.58	3.06	2.75	2.83	**0.004**
EB	3.33	3.58	-0.42	4.96	**0.046**
PBn	0.47	0.21	0.72	0.21	**0.009**
PBp	0.48	0.18	0.56	0.25	0.390

*Two-tailed Welch's t-test

EB: Externalizing bias; **PBn**: personalizing bias, negative; **PBp**: personalizing bias, positive.

Table 4.4b IPSAQ scores for the therapy effect comparison, mean and standard deviation (SD):

	Condition				
	Baseline		**Post-therapy**		
	mean	*SD*	*mean*	*SD*	*p*[*]
Positive items					
Internal	7.33	2.60	6.67	3.16	0.284
Personal	5.11	2.42	3.33	2.92	**0.007**
Situational	3.56	2.51	6.00	4.44	0.071
Negative items					
Internal	7.89	4.11	5.33	3.87	0.064
Personal	5.44	2.24	6.11	3.98	0.313
Situational	2.67	3.04	4.56	5.27	0.163
EB	-0.56	5.79	1.33	3.81	0.080
PBn	0.73	0.21	0.64	0.37	0.234
PBp	0.59	0.25	0.38	0.32	**0.010**

[*] single-tailed paired student t-test

EB: Externalizing bias; **PBn**: personalizing bias, negative; **PBp**: personalizing bias, positive.

Table 4.5a Differences in graph metrics in the group comparison (HC minus SAD), normalized values only.

	Group		
	HC	**SAD**	*p*
C	0.958	1.022	**0.04**
λ	1.038	1.844	0.13
E	1.004	0.993	**0.02**
BC	1.018	0.998	0.28

Abbreviations: **C**: clustering coefficient; **λ**: characteristic path length; **E**: global efficiency; **BC**: betweenness centrality.

Table 4.5b Differences in graph metrics in the **effect of condition** comparison (SAD participants: baseline minus post-therapy), normalized values only.

	Condition		
	Baseline	**Post-therapy**	*p*
C	0.958	1.022	0.09
λ	1.038	1.844	0.29
E	1.004	0.993	0.42
BC	1.018	0.998	0.50

Abbreviations: **C**: clustering coefficient; **λ**: characteristic path length; **E**: global efficiency; **BC**: betweenness centrality.

Table 4.6a Significant group differences in partial correlations between a priori nodes (in **bold**) and other ToM network nodes in the SAD group, compared to HCs.

	Group					
	HC		**SAD**			
	mean	*SD*	*mean*	*SD*	*t*	*p*
Reduced functional connectivity in SAD						
Precun and L IFG	-1.65	1.49	-6.53	3.86	4.09	**0.001**
Increased functional connectivity in SAD						
R pSTS and vmPFC	-2.33	5.43	2.16	4.24	-2.26	**0.03**

Abbreviations: **Precun**: precuneus; **L IFG**: left inferior frontal gyrus; **R pSTS**: right posterior superior temporal sulcus; **vmPFC**: ventromedial prefrontal cortex. Further information on nodes appears in **Table 4.1**.

Table 4.6b Significant therapy-related differences in partial correlations between a priori nodes (in **bold**) and other ToM network nodes in the SAD participants post-therapy, compared to baseline.

	Condition					
	Baseline		**Post-therapy**			
	mean	*SD*	*mean*	*SD*	*t*	*p*
Reduced functional connectivity post-therapy						
R TPJ and **L TPJ**	6.27	3.37	4.57	2.84	3.02	**0.02**
Increased functional connectivity post-therapy						
R pSTS and fPOC	-1.08	3.74	2.79	2.19	-2.8	**0.02**
Precun and L IFG	-6.94	3.63	-2.15	4.89	-2.55	**0.03**
R TPJ and L MTG2	-0.37	2.53	4.13	4.26	-2.41	**0.04**
L TPJ and R TPO	-2.42	3.74	1.02	4.28	-3.00	**0.02**
L pSTS and L TPO	-3.29	4.71	1.82	4.75	-2.56	**0.03**

Abbreviations: **R TPJ**: right temporoparietal junction; **L TPJ**: left temporoparietal junction; **R pSTS**: right posterior superior temporal sulcus; **fPOC**: frontopolar cortex; **Precun**: precuneus; **L IFG**: left inferior frontal gyrus; **L MTG2**: left middle temporal gyrus 2; **R TPO**: right temporal pole; **L pSTS**: left posterior superior temporal sulcus; **L TPO**: left temporal pole. Further information on nodes appears in **Table 4.1**.

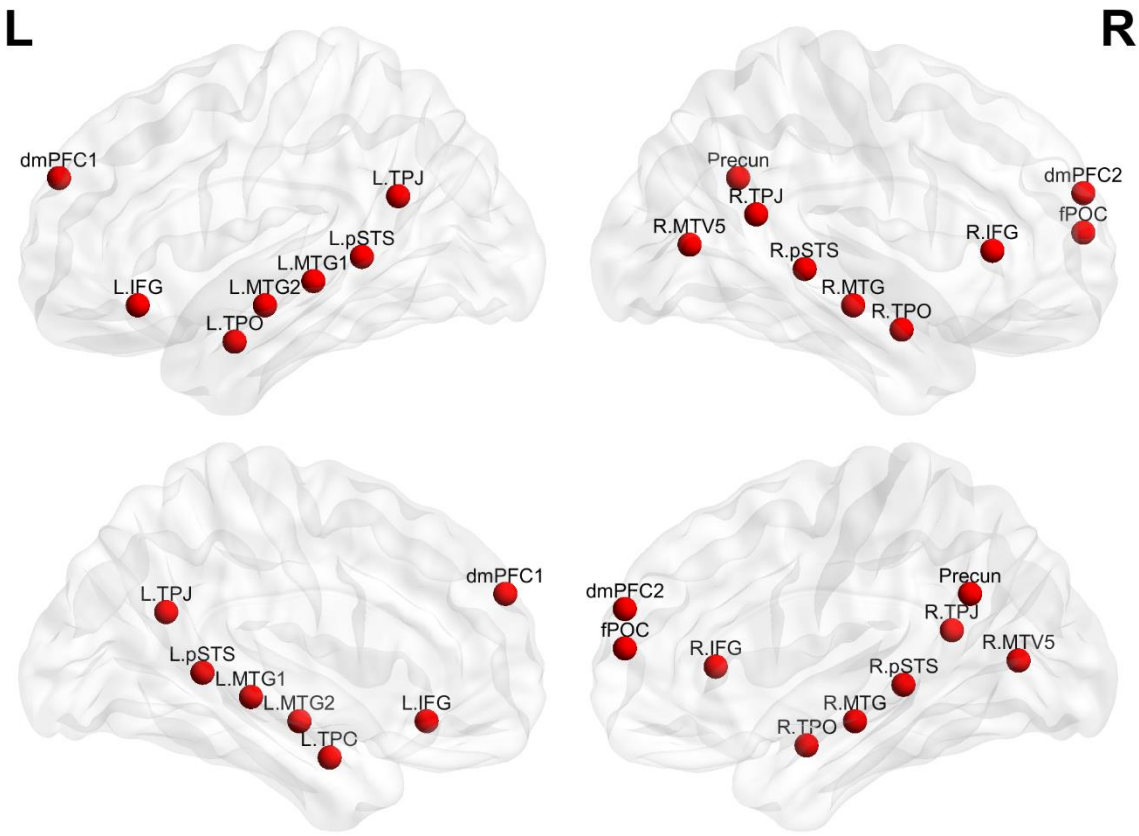

Figure 4.1 Selected network nodes for the ToM network. Full names and MNI coordinates appear in Table 4.1. *BrainNet Viewer (http://www.nitrc.org/projects/bnv/)* (Xia et al. 2013).

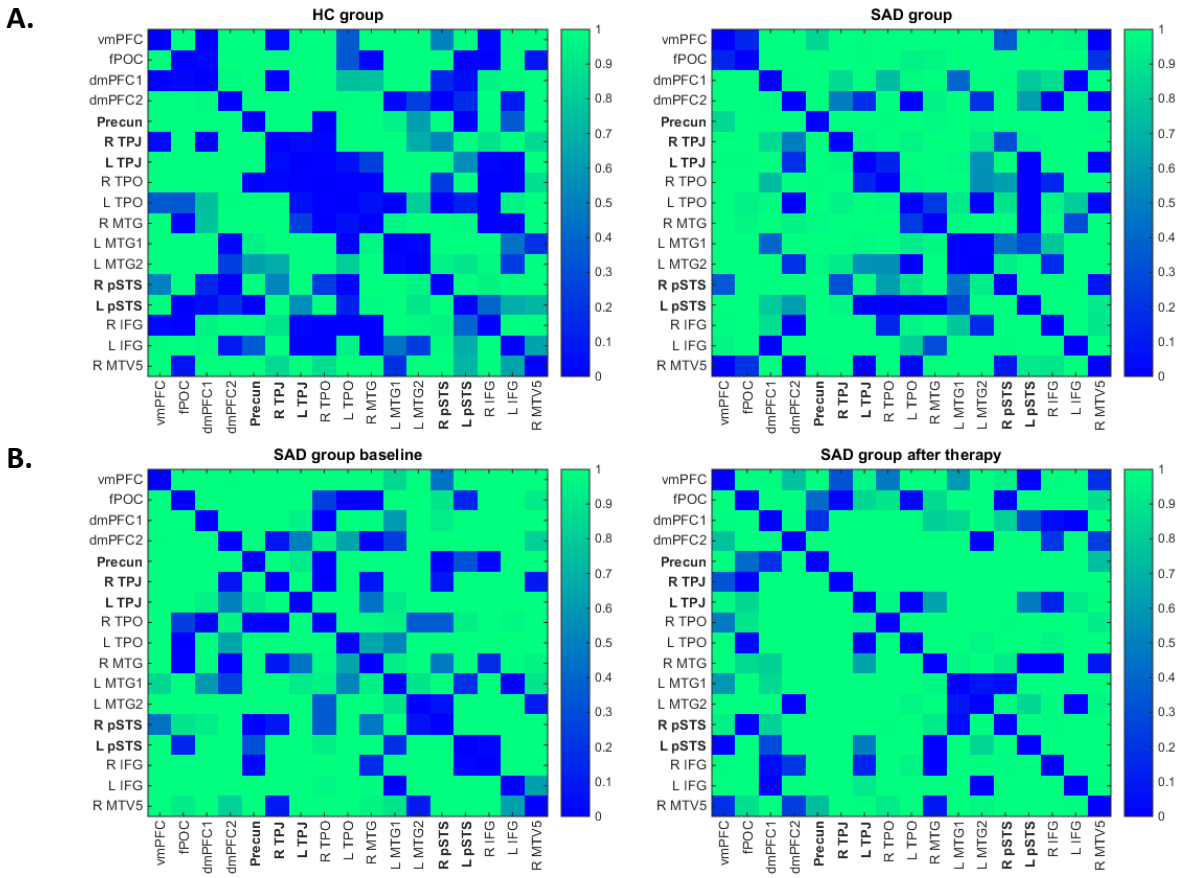

Figure 4.2 Relevant partial correlation matrices for groups used in the group (**SAD vs HC)** comparison (**A**) and in the condition (**therapy effect)** comparison (**B**). Each matrix element is colour-scaled to mean group partial correlation coefficient for the relevant node-pair. The 5 a priori nodes are indicated in **bold text**.

Resting regional brain metabolism in social anxiety disorder and the effect of moclobemide therapy

Authors: Alex Doruyter[1], Patrick Dupont[2], Lian Taljaard[3], Dan J Stein[4], Christine Lochner[3], James M Warwick[1]

[1]Division of Nuclear Medicine, Faculty of Medicine and Health Sciences, Stellenbosch University, Cape Town, South Africa. ORCID ID: 0000-0001-9294-1737
[2]Laboratory of Cognitive Neurology, Department of Neurosciences, KU Leuven, Leuven, Belgium.
[3]MRC Unit on Risk and Resilience in Mental Disorders, Department of Psychiatry, Faculty of Medicine and Health Sciences, Stellenbosch University, Cape Town, South Africa.
[4]MRC Unit on Risk and Resilience in Mental Disorders, Department of Psychiatry, Faculty of Health Sciences, University of Cape Town, Cape Town, South Africa.

Publication status: Published manuscript (Doruyter et al. 2017b)

Abstract

Introduction: While there is mounting evidence of abnormal *reactivity* of several brain regions in social anxiety disorder (SAD), and disrupted *functional connectivity* between these regions at rest, relatively little is known regarding resting regional neural activity in these structures, or how such activity is affected by pharmacotherapy.
Methods: Using 2-deoxy-2-(F-18)fluoro-D-glucose positron emission tomography, we compared resting regional brain metabolism between SAD and matched healthy control groups; and in SAD participants before and after moclobemide therapy. Voxel-based analyses were confined to a predefined search volume. A second, exploratory whole-brain analysis was conducted using a more liberal statistical threshold.
Results: Fifteen SAD participants and fifteen matched controls were included in the group comparison. A subgroup of SAD participants (n=11) was included in the therapy effect comparison. No significant clusters were identified in the primary analysis. In the exploratory analysis, the SAD group exhibited increased metabolism in left fusiform gyrus and right temporal pole. After therapy, SAD participants exhibited reductions in regional metabolism

in a medial dorsal prefrontal region and increases in right caudate, right insula and left postcentral gyrus.
Conclusion: This study adds to the limited existing work on resting regional brain activity in SAD and the effects of therapy. The negative results of our primary analysis suggest that resting regional activity differences in the disorder, and moclobemide effect on regional metabolism, if present, are small. While the outcomes of our secondary analysis should be interpreted with caution, they may prove valuable in formulating future hypotheses or in pooled analyses.

Keywords: social anxiety disorder; moclobemide therapy; positron emission tomography; fluorodeoxyglucose; regional metabolism; resting state

Introduction

Several brain regions are consistently implicated in SAD. Functional disruptions in amygdala, insula, precuneus, fusiform gyrus, thalamus and striatum have been demonstrated in SAD by task-based fMRI work that reported abnormal reactivity (to task) in these regions and resting-state fMRI work that reported abnormal functional connections of these structures (Freitas-Ferrari et al. 2010; Arnold-Anteraper et al. 2014; Brühl et al. 2014a; Manning et al. 2015). There is mounting evidence that pharmacotherapy to some degree reverses some of these abnormalities or results in compensatory changes in reactivity or connectivity (Brühl et al. 2014a). Moclobemide is a selective monoamine oxidase A (MAO-A) inhibitor approved for the therapy of SAD in several countries, including in South Africa. It has a similar tolerability profile to SSRIs, and some evidence indicates that they may be as efficacious as these more widely used agents (National Collaborating Centre for Mental Health (UK) 2013), and studies show it is a safe and well-tolerated therapeutic option in SAD (Stein et al. 2002; Bonnet 2003).

Relatively little is known about regional brain activity at rest in SAD. Only three studies investigating resting regional brain activity in SAD have been published (Stein and Leslie 1996; Warwick et al. 2008; Evans et al. 2009), of which only one (Evans et al. 2009) used FDG PET. None of these studies have been performed using a case-control study design. Findings of these studies have been inconsistent, and have thus far failed to document

abnormality in several regions implicated by MRI-based work. Similarly, the effects of pharmacotherapy on resting regional brain activity in SAD have been investigated in only a handful of studies (van der Linden et al. 2000; Warwick et al. 2006; Evans et al. 2009; Crippa et al. 2011). While MAO-A inhibitors rapidly raise central concentrations of several neurotransmitters relevant to anxiety and depression, the clinical effects take several weeks to manifest. This suggests that the anxiolytic effects of moclobemide are likely the result of mechanisms of neural adaptation that remain poorly-understood, rather than simply increases in neurotransmitters (Bonnet 2003). Only one SAD study (Warwick et al. 2006) has investigated the effect of moclobemide on resting regional brain activity.

The investigation of resting regional neural activity in SAD, as well how this may be impacted by moclobemide therapy merits further investigation. Using FDG PET, we compared a group of non-medicated SAD participants to a group of case-matched healthy controls, and obtained follow-up measures in the SAD group after a course of moclobemide therapy. We hypothesized that there would be regional differences in resting metabolism in SAD compared to healthy controls and that a course of moclobemide would result in alterations in resting regional metabolism in regions previously implicated in SAD.

Methods

Ethical approval

The study was approved by the health research ethics committee of Stellenbosch University and was performed in accordance with the ethical standards of the 1964 Declaration of Helsinki and its later amendments, the guidelines of the International Conference on Harmonisation Good Clinical Practice (ICH/GCP, 2002) and the Medical Research Council of South Africa's guidelines (2002) on the ethical conduct of research studies in humans. Informed consent was obtained from all individual participants included in the study.

Participants

SAD participants were recruited through the MRC Unit on Risk and Resilience in Mental Disorders. Healthy controls (HCs) were invited to join the study in various advertisements on

local radio stations and in print media, as well as online and through email campaigns. Volunteers were screened in an interview setting to assess their suitability for inclusion. Participants had to be between the ages of 18 and 55 years of age; right-handed; and fluent in English. SAD participants had to meet DSM-V criteria for SAD and not have any comorbid mood or anxiety disorders, or psychotic or substance disorders. Volunteers were excluded from participation if they had any metal implants or claustrophobia that would preclude MRI; had any current or prior neurological or psychiatric illness (healthy controls), or prior head injury resulting in loss of consciousness; had any serious medical conditions; or were heavy caffeine users (>600mg per day). All participants were free of psychotropic medication (other than the study medication) at study visits. SAD participants already on medication were not excluded from the study, provided they were willing to taper and discontinue their medication and then commence the study after a suitable washout period. SAD participants who could not safely stop medications known to interact with moclobemide were excluded. SAD and HC participants were matched for age and sex.

Screening and clinical measures

In total, HC participants attended three study visits. Including visits for follow-up measures, the SAD participants attended five study visits. All participants underwent a structured clinical interview for DSM-IV (SCID) (First et al. 1996) and completed the Edinburgh Handedness Inventory (Oldfield 1971) as part of the screening process. In addition, participants completed the Liebowitz Social Anxiety Scale (LSAS) (Liebowitz 1987) and Beck Depression Inventory (BDI-II) (Beck et al. 1996) to assess the severity of social anxiety and depressive symptoms respectively.

At each FDG PET scanning visit participants completed the state version of the State Trait Anxiety Inventory (STAI-S) which measures levels of anxiety at the time of the measure (Spielberger 1983). The efficacy of pharmacotherapy was studied with the Clinical Global Impressions Improvement scale (CGI-I) (Guy 1976).

Pharmacotherapy

After baseline measurements were completed, SAD participants commenced a course of moclobemide according to clinical prescribing guidelines for SAD (300 mg PO once daily for 3 days, followed by 300 mg PO twice daily thereafter). After at least 8 weeks of therapy, follow-up measures were completed whereafter participants either opted to continue on moclobemide or discontinue the medication in favour of other management strategies. SAD participants were closely monitored for adverse effects during the study and for symptoms of discontinuation in the event that the study medication was stopped.

Neuroimaging

PET and MR imaging were performed on separate days and repeated in the SAD group after therapy.

Prior to the FDG PET scan appointment, participants were given verbal and written instructions on correct preparation. Subjects were requested to remain fasting (nil per mouth other than plain unflavoured water and permitted medications) for a minimum of 6 hours prior to the injection time. After the placement of an intravenous cannula and blood glucose check, participants were seated in a comfortable chair, in a dimly lit cubicle and instructed to relax with their eyes open. During the subsequent 20-30 minutes, participants sat quietly without engaging in activities such as reading or electronic device use and without conversation. After this time, a technologist injected a ±150 MBq dose of FDG through the pre-sited cannula. After a further 20 minutes of relaxation, the cannula was removed and participants encouraged to make use of the toilet before being placed on the scanner bed of a Philips Gemini TF PET/CT camera (Philips Medical Systems, Best, the Netherlands). Head restraints were used and participants were reminded to remain still throughout the entire acquisition. At approximately 30 minutes post-injection brain scanning was commenced. This consisted of a low-dose CT scan (16-slice; 0.5 sec rotation; 140 kVp; 20mAs) for attenuation correction, followed by 30 minutes of dynamic PET scanning. PET data were acquired over a FOV of 18 cm (90 slices with 2mm separation); voxel size: 2x2x2 mm. Scatter and CT-based attenuation correction were applied during reconstruction. List mode data were re-binned into 15 frames of 2 minutes each.

MRI scanning was performed on either a 3T Siemens Magnetom Allegra or 3T Siemens Magnetom Skyra camera (Siemens Medical Systems, Erlangen, Germany). Acquisition parameters across the two systems were selected to minimise scanner-related bias. Scan parameters for a T1-weighted ME-MPRAGE acquisition on the Allegra system: four coil; repetition time (TR) = 2530 ms; echo time (TE) = 1.533-6.57 ms; flip angle = 9°; slices = 160; slice gap = 0.5 mm; field of view = 256 x 256 mm; voxel size = 1x1x1 mm; duration = 10min 49 sec. On the Skyra system: same settings except TE = 1.69-7.27 ms; parallel imaging mode (iPAT) active. Additional structural scans (T2; FLAIR) were acquired to exclude relevant intracranial pathology.

Before PET imaging, participants completed the STAI-S measure to measure state anxiety.

Pre-processing

All DICOM scans were reviewed visually for artefacts. DICOM images were converted to NIfTI format using the dcm2nii program packaged with MRIcron version 1 June 2015 (Chris Rorden, http://people.cas.sc.edu/rorden/mricron/index.html). Further pre-processing was performed using SPM12 (http://www.fil.ion.ucl.ac.uk/spm/) and MATLAB (Mathworks R2014b). PET frames were realigned and checked for significant motion using a custom script. PET frames in which there was more than 2 mm translation or more than 2° rotation in reference to the first frame or serial frames were excluded from the analysis. Consecutive frames that met these criteria were summed and the resultant image checked for correct registration with the low-dose CT used for attenuation correction. Summed PET images were required to have a minimum of 100 million counts for inclusion. Summed FDG scans for each participant were co-registered to the subject-specific T1-weighted structural image using the mutual information estimation option. For follow-up scans in the same participants (SAD group) a second co-registration was performed in which follow-up scans were co-registered to the baseline structural scan. The T1-weighted structural image was segmented using the SPM segmentation function. During this step, the forward and inverse deformation field between the subject space and MNI space was calculated. PET images were then warped to MNI space using the forward deformation field and written to a final voxel size of 2x2x2 mm^3. Finally, PET images were normalized to a total global count value of 100 using a

customized script, before being smoothed with a 3-D Gaussian filter with a 12 mm isotropic kernel. Pre-processing steps are illustrated in **Fig 5.1**.

Statistical analysis

Two principal comparisons were made. In the first, we compared two groups: HCs and SAD participants (effect of group: HC vs SAD). In the second comparison we investigated the effect of therapy within the SAD group (effect of condition: baseline vs post-therapy). All statistical analyses were performed in MATLAB (Mathworks R2014b).

Group matching for age was tested using a two-tailed Welch's t-test. Differences in level of education level were tested with the Freeman-Halton extension of the Fisher exact test. Differences in clinical scores were tested with a two-tailed Welch's t-test (HC vs SAD comparison) and single-tailed paired t-test (for the therapy effect comparison in the SAD group).

For the brain analyses, a voxel-level statistical threshold for significance of p = 0.001 (uncorrected) and a cluster-level threshold of 0.05 (family-wise error corrected) was used. To increase power, the analyses were confined to a subset of regions of a priori interest through the use of an inclusive mask. These regions were identified as potentially important in SAD in a previous meta-analysis of MRI studies (Brühl et al. 2014a). We also included cerebellum as an additional region of interest in this mask given evidence of its potential role in anxiety disorders (Caulfield and Servatius 2013; Phillips et al. 2015) and social cognition (van Overwalle et al. 2015). The mask was generated by first summing and then binarizing regions of interest defined in the WFU PickAtlas tool v3.05 (ANSIR Laboratory, Wake Forest University School of Medicine, http://fmri.wfubmc.edu/cms/software) (Maldjian et al. 2003, 2004). Further details on the mask image can be found in **Table 5.1** and **Fig 5.2**. In addition to our primary analysis, we also performed a second, explorative whole-brain analysis at the same liberal statistical threshold used by Evans et al, i.e. at a voxel-level uncorrected threshold of p=0.001 and a cluster extent threshold of 15 voxels.
FDG images for the group and therapy condition comparisons were compared using two-sample t-tests and paired t-tests respectively (unequal variance). As an exploratory measure in the SAD participants, subject-specific regional metabolism values were extracted for any

clusters identified in the effect of group analyses and correlated with disease severity scores (LSAS) using linear regression. Similarly, subject-specific regional metabolism values were extracted from the baseline SAD scans for any clusters identified in the effect of condition (therapy) analyses and correlated with the percentage change in disease severity with therapy (Δ%LSAS). A statistical threshold of p=0.05 was used in the linear regressions.

Results

Groups

Fifteen (n=15) participants with SAD and fifteen (n=15) case-matched healthy controls (HC) were recruited in the study.

In the effect of group comparison (HC vs SAD), all scans were suitable for analysis (n=15 both groups).

In the effect of condition comparison (baseline vs post-therapy), of the original group of fifteen, one SAD participant could not be scanned due to a PET scanner problem; two patients withdrew from the study due to lack of early therapeutic effect; and one participant withdrew due to scheduling issues. Follow-up measures for a treated SAD group were thus available in eleven (n=11) participants.

Demographics

The demographics of participants and matching in the group analysis appear in **Table 5.2**. While no significant differences were detected in terms of age, there was a statistically significant difference in level of education (p=0.04). SAD duration varied between 3.1 years and 33.1 years (mean 13.5 years).

In the effect of therapy analysis, the 11 SAD participants consisted of 6 males and 5 females with a mean age of 30.5 years (range: 21.5 – 42.7).

Clinical

In the group comparison, the SAD group had a mean LSAS score of 91.1 (range: 57-135, SD: 25.4) and a mean BDI-II score of 14.8 (range: 2-35, SD: 10.9). The HC group, by comparison had a mean LSAS of 16.2 (range: 0-45, SD: 11.2) and a mean BDI-II score of 3.7 (range: 0-16, SD: 4.6).The difference in LSAS and BDI-II scores between the groups was significant ($p<0.001$ and $p=0.002$ respectively).

SAD participants in the effect of condition (effect of therapy) analysis demonstrated an overall improvement in clinical scores after a mean duration of therapy of 9.2 weeks (range: 8.3 – 11.1). Changes in clinical scores are summarized in **Table 5.3**. No major adverse events occurred during the study.

At the time of PET scanning SAD participants had higher state anxiety on the STAI-S (mean: 44, SD: 15.8) than HC participants (mean: 27.7, SD: 9.5) which was significantly different ($p=0.002$). In the effect of therapy comparison there was no statistically significant difference in STAI-S scores at baseline (mean: 40, SD: 15.7) and at follow-up (mean: 30.8, SD: 8.0) ($p=0.37$).

Regional metabolism

No clusters were identified in our primary analysis confined to regions of a priori interest.

In the second, explorative whole brain analysis at a more liberal statistical threshold, several clusters were identified. In the group comparison, SAD participants demonstrated hypermetabolism in a left fusiform gyrus cluster as well as in a right temporal pole cluster. In the therapeutic condition comparison, SAD participants after therapy demonstrated a metabolism decrease in bilateral superior frontal gyrus (medial regions); and an increase in metabolism in the insula, left postcentral gyrus and right caudate. No significant correlation between extracted cluster values and LSAS or Δ%LSAS were demonstrated on the linear regressions. Differences in whole brain regional metabolism for the group and therapy condition comparisons are summarized in **Table 5.4** and illustrated in **Fig 5.3** and **5.4**.

Discussion

In this study we compared resting regional metabolism between SAD and healthy control groups, as well as investigating whether there were any differences in regional resting metabolism in the SAD group after a course of moclobemide therapy. Confining our analysis to regions of a priori interest, we detected no significant differences in these comparisons. We then performed a second, exploratory analysis of whole brain differences. In that analysis, we observed several differences for each comparison. No correlations were found between regional metabolism within clusters and either disease severity or improvement in disease severity.

Nuclear neuroimaging offers alternative windows into biological processes to those available through magnetic resonance imaging (MRI). One such process is regional glucose metabolism. Since the vast majority of the brain's energy demands are met by glucose, the molecular imaging of glucose metabolism offers an attractive target to research.

Positron emission tomography (PET) using 2-deoxy-2-(F-18)fluoro-D-glucose (FDG) is effectively an in vivo measurement of hexokinase activity within the brain (Hertz and Dienel 2002). Due to neurometabolic coupling, FDG PET studies provide a summed representation of brain activity during the 15-20 minutes it takes for most of the uptake to occur, in the interval between injection and scanning. Despite this sacrifice in temporal resolution, there are strong rationales for the use of nuclear techniques such as FDG PET as a complementary tool to fMRI in neuropsychiatric research. Foremost amongst these is PET's robustness with respect to susceptibility artefacts (Devlin et al. 2000); its resilience to small amounts of head motion and its more direct measurement of biological processes. While fMRI's better temporal resolution makes it ideal for studying resting-state *networks* it is at a disadvantage in measuring *regional* brain activity while at rest. We have previously motivated the importance of understanding baseline (resting) conditions in psychiatric disorders (Doruyter et al. 2017c) and in this sense, nuclear techniques such as FDG PET, that offer insight into regional neural activity at rest, are well-suited to provide biological information complementary to that obtained with fMRI.

In our primary analysis we did not detect any differences in regional resting metabolism between control and SAD groups, nor in the SAD group before and after a course of pharmacotherapy. This is in contrast to previous studies on resting regional brain activity which did report group differences (Warwick et al. 2008; Evans et al. 2009) and others that reported a change in regional brain activity in SAD participants after therapy (van der Linden et al. 2000; Warwick et al. 2006; Evans et al. 2009; Crippa et al. 2011). There are several possible methodological reasons for this inconsistency. The first reason relates to differences in study design. Early studies on resting regional activity in SAD (Stein and Leslie 1996) and the effect of pharmacotherapy in the disorder (van der Linden et al. 2000) used ROI-based techniques rather than voxel-based analyses and are therefore not comparable to subsequent studies including our own. Neither of the two previous studies that used voxel-based approaches to compare SAD and HC groups (Warwick et al. 2008; Evans et al. 2009) used case-control matching, as we did. While case-control approaches have their problems (Marquand et al. 2016), it can be argued that they remain the optimal study design for studies with small group sizes, since they reduce intergroup heterogeneity that may give rise to false positives. The second reason relates to differences in the analysis methods, principally in the statistical threshold used. Other studies have consistently set their statistical threshold at a more liberal level of $p<0.001$ uncorrected at the voxel level, sometimes combined with a cluster size threshold of 10-15 voxels. Without correcting for the effects of multiple comparisons (for example through the use of family-wise error correction or false-discovery rate correction), the risks of false positives at these statistical thresholds are high, and the results should be treated with caution (Bennett et al. 2009). As long as too much emphasis is not placed on the results of individual experiments conducted at these liberal thresholds, these studies remain valid and their findings contributory when replicated. In line with this we performed our own exploratory analysis. Even when using a more liberal statistical threshold, there are two additional considerations that should be born in mind when comparing our results to those of previous studies. Firstly, while there is a tight coupling between neuronal activity and metabolism, and neuronal activity and blood flow, the relationship between regional metabolism and blood flow is not absolute and imaging of these processes (glucose metabolism in the case of FDG PET; regional perfusion in the case of Tc-99m hexamethyl propylene amine oxime single photon emission tomography), is not expected to yield identical results (Wehrl et al. 2013); and secondly, the effects of different therapeutic agents (in our effect of condition analysis) are unlikely to be identical, given their different mechanisms of action.

In our secondary analysis at a more liberal statistical threshold, we identified several differences in the group analysis. The finding of increased resting glucose metabolism in a fusiform gyrus cluster in SAD was interesting given several fMRI experiments that reported aberrant resting functional connectivity of this region in SAD (Ding et al. 2011; Qiu et al. 2011; Manning et al. 2015; Liu et al. 2015b; Zhu et al. 2017). The cluster identified in our analysis closely corresponded to the posterior fusiform face area/FFA-1, which is a component of the distributed region of cortex involved in the visual processing of faces (Weiner and Grill-Spector 2012). Other work has implicated this region as playing a potential role in social interpretation (Schultz et al. 2003). Neither Warwick et al, nor Evans et al found any abnormality in the fusiform gyrus in SAD participants in their group comparison although the study by Warwick et al did find a positive correlation between resting fusiform perfusion and disease severity (Warwick et al. 2008). We also identified a cluster of increased regional resting glucose metabolism in the right temporal pole in our SAD group. This finding is consistent with MRI-based research that has found both reduced grey matter volume (Brühl et al. 2014b) and disrupted resting functional connectivity (Zhu et al. 2017) of this region in the disorder. That resting neural activity in this region may be abnormal is interesting, given the temporal pole's importance in conceptual information processing (Frith 2007; Olson et al. 2007); theory of mind (Frith and Frith 2006; Spreng et al. 2009; Bzdok et al. 2012); causal attribution (Kestemont et al. 2015); self-other referential processing (Murray et al. 2012); and empathy (Schulte-Rüther et al. 2007; Takeuchi et al. 2014b). Activity in the temporal pole has also been linked to anticipatory anxiety in both healthy (Chua et al. 1999) and SAD samples (Tillfors et al. 2002) scanned with O-15 water PET. No abnormality in resting regional activity was reported in this region in the studies by Evans et al and Warwick et al. We were unable to detect a correlation between regional resting activity in either of these clusters and disease severity, which might have strengthened the evidence (albeit indirectly) of their intrinsic abnormality in SAD. Importantly, we were unable to replicate the findings of either Warwick et al or Evans et al in our group comparison.

We also performed an exploratory analysis to look for differences in regional resting activity between baseline and post-therapy scans in our SAD participants who were treated with a course of moclobemide therapy. In this analysis we found a decrease in resting activity to several medio-frontal regions after therapy. Again, such a finding has not been reported in nuclear neuroimaging experiments that investigated the effect of moclobemide (Warwick et

al. 2006) or other therapies (Warwick et al. 2006; Evans et al. 2009; Crippa et al. 2011) on resting regional brain activity in SAD. Nevertheless, our finding is plausible, given this region's importance in subjective experience of fear (Etkin et al. 2011). It may be that reduced activity after therapy in this region is related to reductions in anxiety. It is also of interest that dorsal medial prefrontal cortex has high cortical expression of MAO-A receptors, the target for moclobemide therapy (Tong et al. 2013). Our finding of an increase in resting right insular activity after therapy is apparently at odds with that of Warwick et al, who reported decreased resting perfusion in bilateral insula after courses of both moclobemide and citalopram. Certainly, the findings by Warwick et al of changes in bilateral insula makes it unlikely that those results were spurious. Whether our own result represents a false positive, or a more complex physiological process is present that explains this disparity is uncertain. Therapy-related increase in resting regional caudate activity in our study has also not been reported by the few comparable experiments conducted, but is interesting given evidence of increased striatal dopamine transporter binding after escitalopram therapy in SAD (Warwick et al. 2012). Our finding of increased metabolism within the primary somatosensory cortex, in left postcentral gyrus cluster after therapy is of uncertain significance.
We failed to detect any correlation between resting metabolic activity within any of these clusters on the baseline scans), and degree of improvement on the disease severity measure.

This study has a number of limitations. Firstly, we could not correct for two potential confounders: our SAD group was generally more anxious while being scanned (on STAI-S), and several SAD participants scored in the clinical range for depression. Due to the high risk of multicollinearity, we opted not to use STAI-S or BDI scores as nuisance regressors, since doing so would likely regress out the effect of group. Our approach of avoiding correction for these potential confounds may draw the criticism that our results are not specific to SAD (and may represent effects of either depression or anxiety related to scanning), however it is our view that this is unlikely, given that in all cases SAD was the dominant condition in terms of severity. Moreover, SCID-assessments did not suggest any comorbidity. Also, it may be argued that this distinction is artificial, given the frequent comorbidity of SAD and depressive symptomatology (Ohayon and Schatzberg 2010), and evidence that they stem from a shared underlying genetic vulnerability (Langer and Rodebaugh 2014). A second limitation, inherent to our study design, was related to our investigation of therapy effect. Since we did not perform follow-up imaging in the HC group, we cannot exclude the possibility that familiarity with the procedure (and not SAD improvement) resulted in the regional metabolic

changes seen on our exploratory analysis. Also, since there was no placebo arm, we cannot be certain whether regional metabolic changes were driven by moclobemide or the result of a non-specific expectancy effect.

Conclusion

This study adds to the limited existing work on resting regional brain activity in SAD and the effects of therapy. The negative results of our primary analyses with a strict statistical threshold, suggest that both resting regional activity differences in the disorder, as well as therapy effects on regional resting metabolism, if present, are small. At a more liberal statistical threshold, in line with previous studies, we identified several findings of interest, mostly in biologically relevant regions. While the outcomes of such a secondary analysis should be interpreted with caution, they may prove valuable in formulating future hypotheses or in pooled analyses. Our findings are complementary to research performed using fMRI and contribute to current understanding of baseline neurobiology in SAD.

Contributors

Data collection: A Doruyter, L Taljaard, C Lochner
Data processing and analysis: A Doruyter, P Dupont
Manuscript: A Doruyter
Manuscript review: All authors
Supervisors: JM Warwick, C Lochner

Conflicts of Interest

None.

Acknowledgements

The PhD from which this study emanated was funded by the South African Medical Research Council (MRC) under the MRC Clinician Researcher Programme.
Study costs were funded by the Nuclear Technologies in Medicine and the Biosciences Initiative (NTeMBI), a national technology platform developed and managed by the South African Nuclear Energy Corporation (Necsa) and funded by the department of Science and Technology; and the Harry Crossley Foundation.

Profs Stein and Lochner receive funding from the MRC.

None of the funders played any role in study design; collection, analysis, or interpretation of data; in the writing of this article or in the decision to submit it for publication.

Tables and Figures

Table 5.1 Regions of a priori interest used to generate the mask image used in the primary analysis (from WFU PickAtlas tool v3.05)

Description	Atlas	Union of (region labels)
anterior cingulate cortex	IBASPM 116	Cingulum_Ant (L+R)
cerebellum	IBASPM 116	All cerebellar regions including vermis
dorsolateral prefrontal cortex	IBASPM 116	Frontal_Mid (L+R)
fusiform gyrus	IBASPM 116	Fusiform (L+R)
insula	IBASPM 116	Insula (L+R)
medial temporal cortex	IBASPM 116	Hippocampus (L+R); Parahippocampal (L+R); Amygdala (L+R)
posterior cingulate cortex	IBASPM 116	Cingulum_Post (L+R)
precuneus	IBASPM 116	Precuneus (L+R)
striatum	IBASPM 71	caudate nucleus (L+R); putamen (L+R); nucleus accumbens (L+R)
thalamus	IBASPM 116	Thalamus (L+R)
ventromedial prefrontal cortex	IBASPM 116	Frontal_Mid_Orb (L+R); Rectus (L+R)

Table 5.2 Demographics and group matching in the HC vs SAD baseline analysis

	Group		
	HC	**SAD**	*p*
Total (n)	15	15	-
Mean age in years	30.6 (21.2 – 46.9)	30.5 (21.0 – 45.7)	0.97*
Gender	Female: 9, Male: 6	Female: 9, Male: 6	-
Highest level of education: *Formal schooling incomplete*	1	1	**0.04****
Additional training college or technical qualification	0	5	
Additional University degree	14	9	

* Two-tailed Welch's t-test

** Freeman-Halton extension of the Fisher exact test

Table 5.3 Clinical measures in SAD participants (n=11) included in the effect of therapy analysis.

	Condition				
	Baseline		**Post-therapy**		
	mean	*SD*	*mean*	*SD*	*p**
LSAS	90.4	27.4	70.3	35.0	**0.002**
BDI-II	14.8	10.9	11.9	8.8	0.13
CGI-S CGI-I	4.6	1.3	3.5 2.9	1.9 0.9	**0.02**

* single-tailed paired student t-test

Table 5.4 Significant regions identified in the secondary, whole brain analyses

	Number of voxels	*t*	Local maxima			Region
			x	*y*	*z*	
Effect of group HC > SAD	*Nil*					
HC < SAD	59	4.31	-34	-46	-22	Left fusiform gyrus
	26	3.96	36	16	-34	Right temporal pole (mid)
Effect of condition *(treated SAD group, n=11)*						
Baseline > Post-therapy	271	7.49	-16	62	30	Frontal superior left
	134	6.48	-2	38	54	Frontal superior medial left
	27	5.90	-12	28	60	Frontal superior medial left
		4.57	-6	24	56	Frontal superior medial left Supplementary motor area left
	56	5.78	10	70	18	Frontal superior medial right
	80	4.84	8	56	42	Frontal superior medial right
Baseline < Post-therapy	59	5.16	46	16	-6	Insula right
	18	5.04	-58	-6	22	Postcentral left
	42	4.72	10	12	6	Caudate right
		4.64	12	2	6	Caudate right

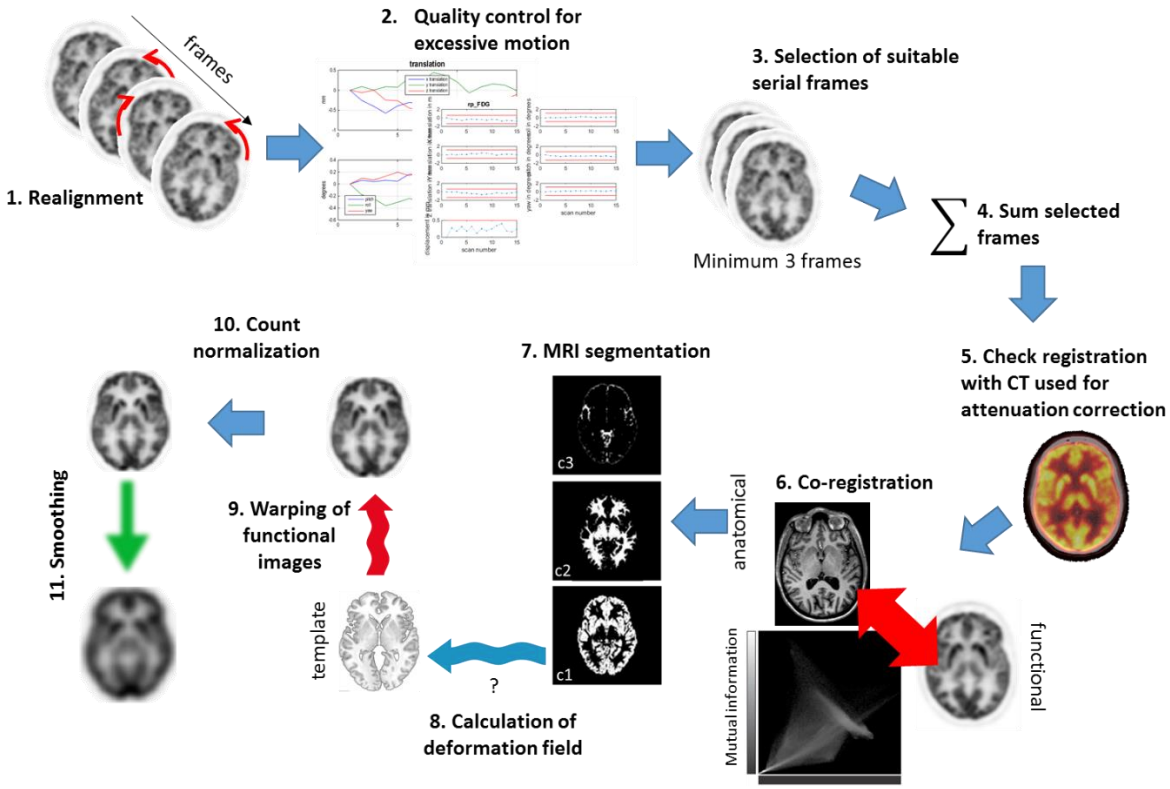

Figure 5.1 Pre-processing steps performed.

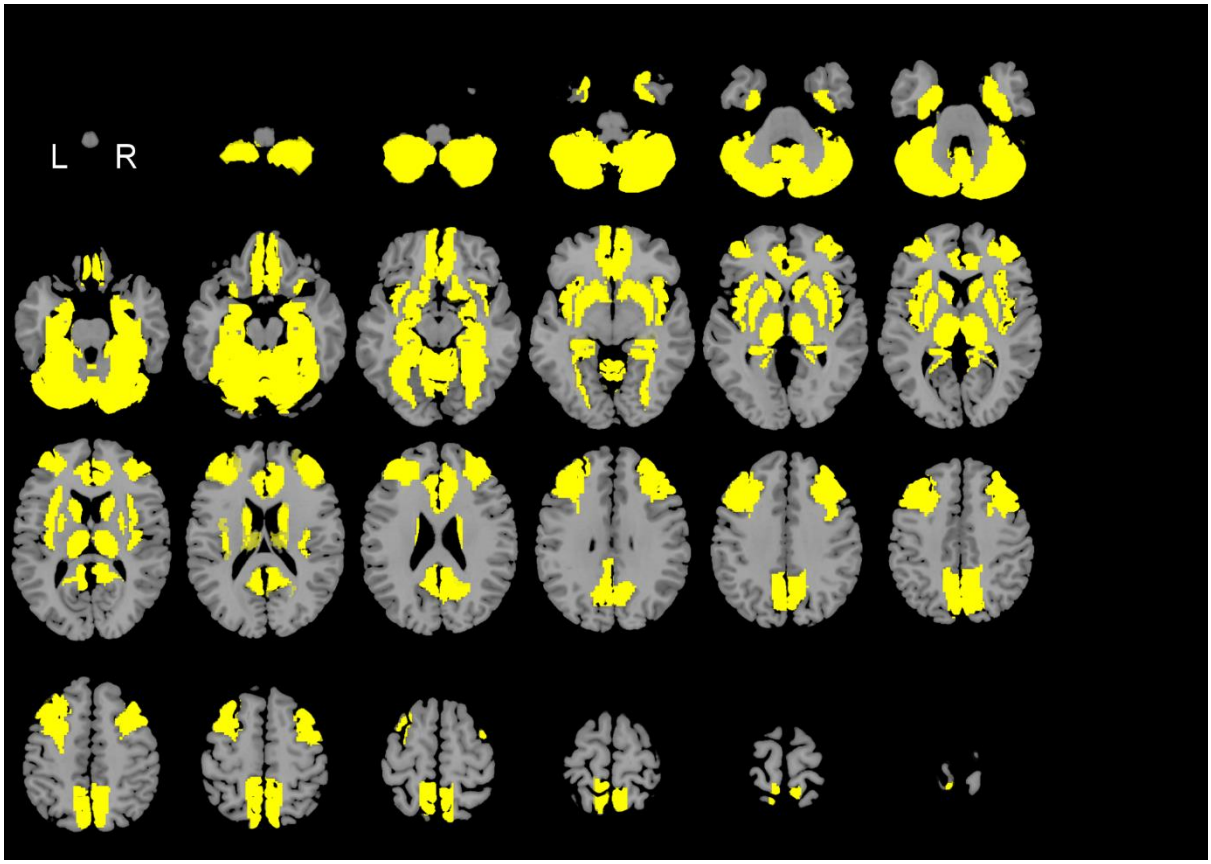

Figure 5.2 Mask image used in the primary analysis. The mask was generated by summing and binarizing a priori regions of interest in **Table 5.1**. *Image generated in MRIcroGL (http://www.mccauslandcenter.sc.edu/mricrogl/).*

a.

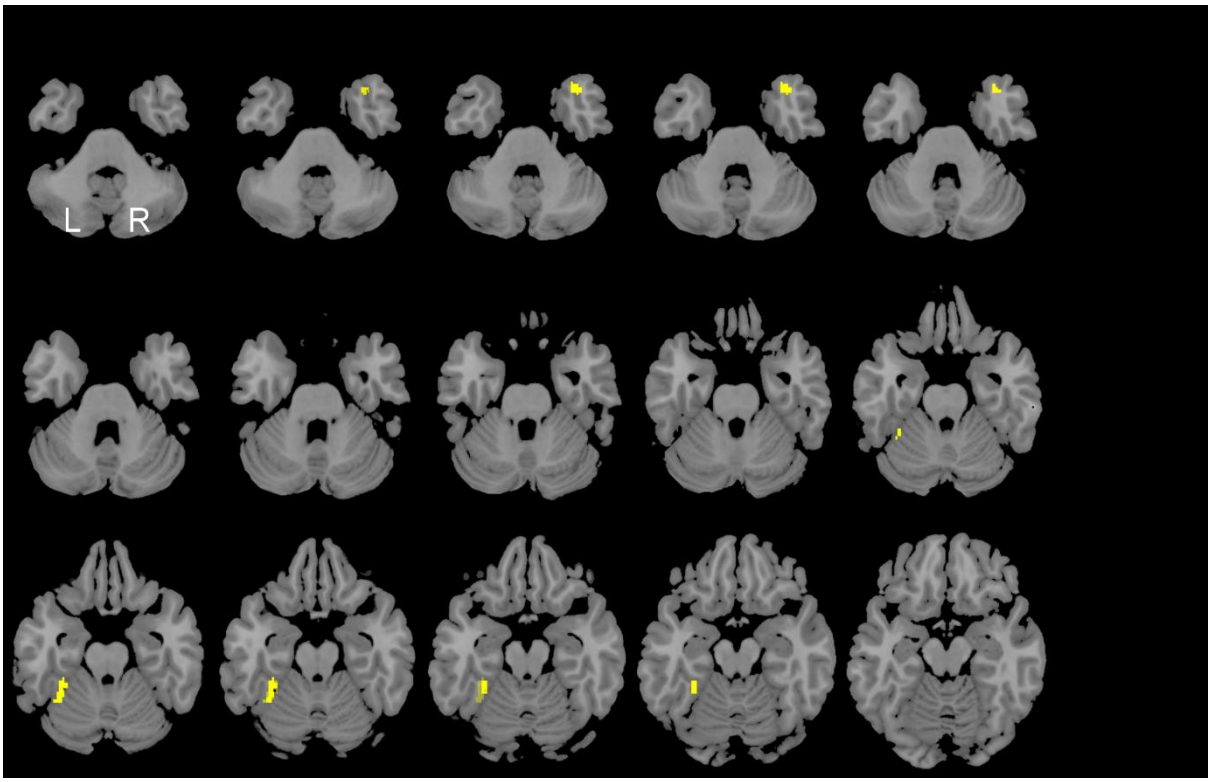

b.

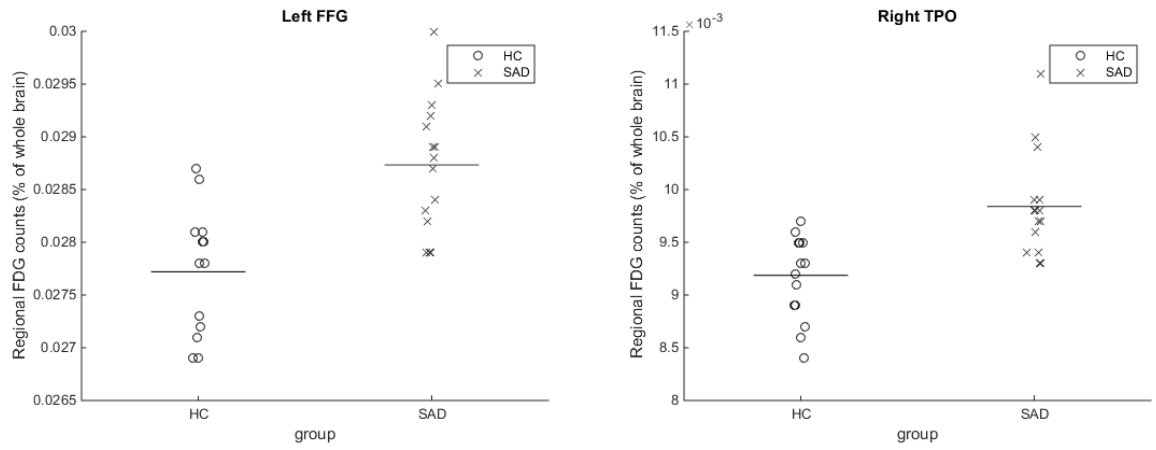

Figure 5.3 Effect of group in the secondary analysis. **(a)** Voxels showing significantly higher FDG activity in SAD participants compared to healthy controls. Slices between z= -38 and z = -16. *Image generated in MRIcroGL (http://www.mccauslandcenter.sc.edu/mricrogl/).* (**b**) Scatter plots of extracted cluster values per group for left fusiform gyrus (left) and right temporal pole (right) (x-position jittered for better visualization of similar y-values). Cluster sizes 59 and 26 voxels respectively. *Image generated in Matlab (Mathworks R2014b).* *Abbreviations*: **FFG**: fusiform gyrus; **TPO**: temporal pole.

a.

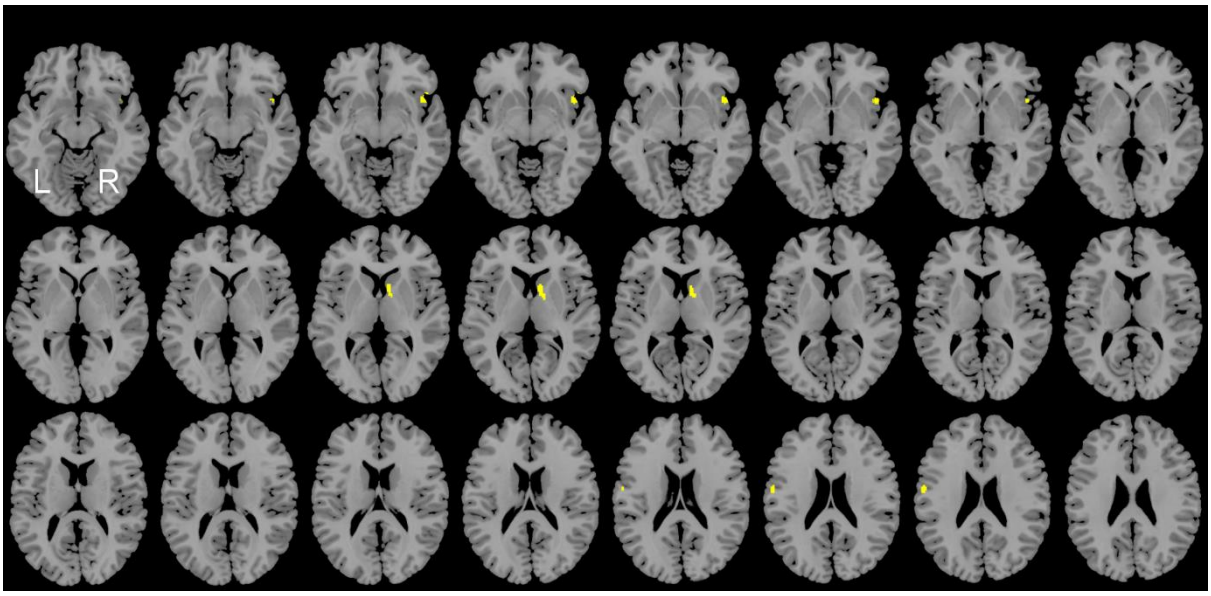

b.

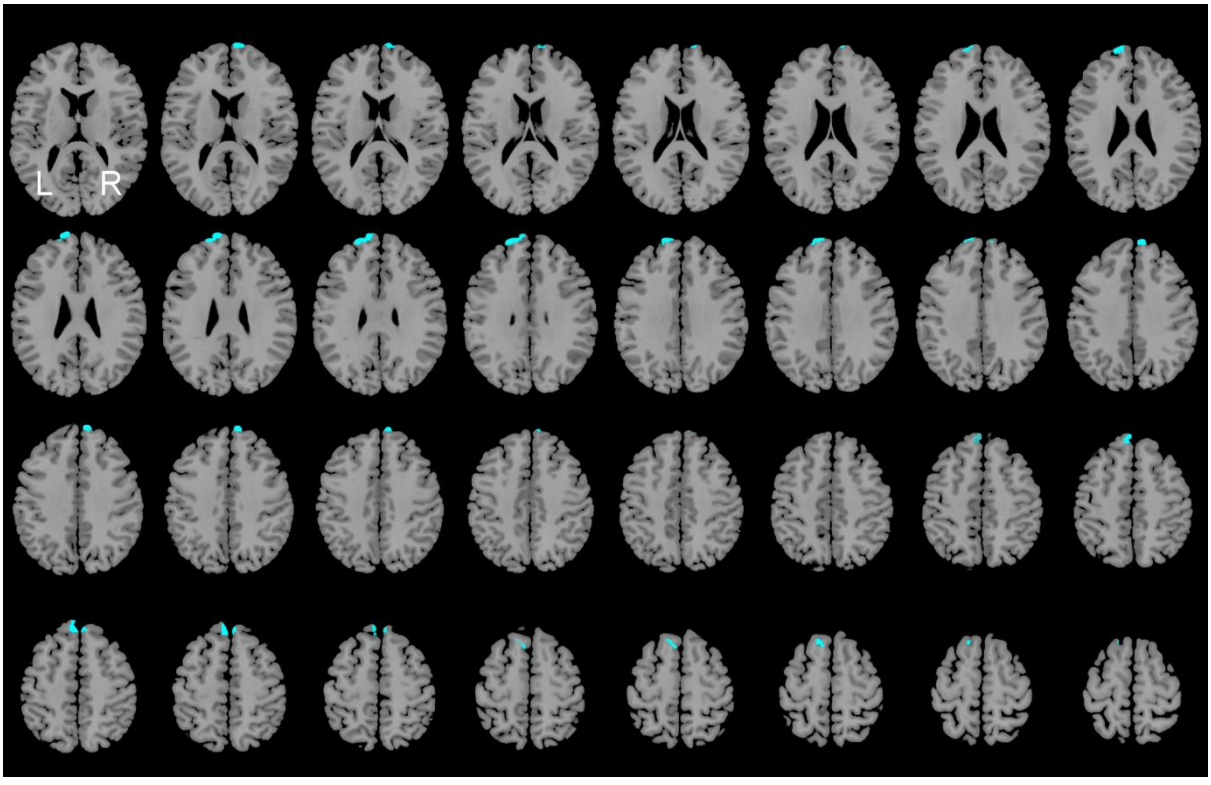

Figure 5.4 Effect of condition in the secondary analysis. Voxels showing increases (**a**) and decreases (**b**) in FDG activity in SAD participants following a course of moclobemide. Slices between z = -12 and z = 25 (a), and z = 14 and z = 63 (b). *Image generated in MRIcroGL (http://www.mccauslandcenter.sc.edu/mricrogl/).*

Reward processing in social anxiety disorder: An fMRI investigation

Authors: Alex Doruyter[1], Patrick Dupont[2], Lian Taljaard[3], Dan J. Stein[4], Christine Lochner[3], James Warwick[1]

[1]Division of Nuclear Medicine, Faculty of Medicine and Health Sciences, Stellenbosch University, Cape Town, South Africa.
[2]Laboratory of Cognitive Neurology, Department of Neurosciences, KU Leuven, Leuven, Belgium.
[3]MRC Unit on Risk and Resilience in Mental Disorders, Department of Psychiatry, Faculty of Medicine and Health Sciences, Stellenbosch University, Cape Town, South Africa.
[4]MRC Unit on Risk and Resilience in Mental Disorders, Department of Psychiatry, Faculty of Health Sciences, University of Cape Town, Cape Town, South Africa.

Publication status: Unpublished manuscript: Data collection extended.

Abstract

Introduction: Reward processing is a key construct in translational neuroscience, and may be key to understanding approach-avoidance decision-making. There is emerging evidence that social anxiety disorder (SAD) may be associated with disruptions in reward processing. Little is yet known about what aspects of reward processing may be disrupted in SAD, and whether reward processing in SAD is altered by pharmacotherapy.
Methods: Patients with a primary diagnosis of SAD as well as age- and gender-matched healthy controls (HC) were recruited. All participants underwent functional magnetic resonance imaging during a modified monetary incentive delay task. SAD participants then received a minimum of 8 weeks of moclobemide therapy before undergoing repeat scanning. Group (SAD vs HC at baseline) and condition (SAD at baseline vs post-therapy) comparisons were performed in an event-related design, and both reward anticipation and reward outcome analysed.
Results: Activation of reward centres known to be important in the processing of reward anticipation and reward outcome could not be demonstrated in either group. No main effect of group or of condition could be demonstrated in either the primary or secondary analysis.

Conclusion: While the negative findings here may reflect a lack of statistical power, they may be consistent with the view that alterations of reward processes in SAD are restricted to social reward. Further research to address whether social reward processing is present in SAD, and is altered by pharmacotherapy, may be useful.
Keywords: reward, monetary reward, social anxiety disorder, functional magnetic resonance imaging.

Introduction

Reward processing is a key construct in translational neuroscience (Cuthbert and Insel 2013). In both animals and humans, reward circuitry is distributed across specific brain regions, including nucleus accumbens, caudate, putamen, and orbitofrontal cortex (Haber and Knutson 2009; Liu et al. 2011). Several fMRI-based experiments have demonstrated that tasks that involve social interactions result in very similar activations in these reward centres to those elicited by other reward types such as money, food, sex and drugs of addiction (Koob and Le Moal 1997; Schultz 1997; Rilling et al. 2002; Zink et al. 2004; Delgado et al. 2005; McClure et al. 2007; Spreckelmeyer et al. 2009). The observation that individuals with social anxiety disorder (SAD) tend to avoid social interactions (and the sense of reward these interactions may confer) has led some researchers to posit that disrupted reward processing may be a feature of the condition (Stein 1998; Mathew et al. 2001).

There is indirect evidence of disrupted reward processing in SAD. Resting functional connectivity (performed on resting-state fMRI) within the reward circuit has been shown to be altered in SAD (Arnold-Anteraper et al. 2014; Manning et al. 2015). There is also evidence from nuclear neuroimaging studies that implicate aberrant dopamine (a core neurotransmitter system in reward) signalling in the disorder (Tiihonen et al. 1997; Schneier et al. 2000; van der Wee et al. 2008b; Plavén-Sigray et al. 2017) although conflicting evidence exists in this regard (Schneier et al. 2009). Also contributory, given the hypothesis of a social anxiety spectrum (Stein et al. 2004; Kashdan 2007), is evidence of abnormality in reward processing in non-clinical social anxiety samples, predominantly in paediatric populations (Kashdan 2007; Caouette and Guyer 2014).

Direct investigation of reward processing in SAD has also been undertaken. Task- or questionnaire-based studies have found no evidence of abnormality in reward dependence

(Kampman et al. 2014) or in temporal discounting of reward (Steinglass et al. 2017) in SAD. Neuroimaging studies have largely relied on the Monetary Incentive Delay Task (MID) (Knutson et al. 2000), a task that allows assessment of neural processing of both anticipation and outcome of monetary reward (Knutson and Heinz 2015), or on variations of the MID task which employ social rewards (Spreckelmeyer et al. 2009), to study reward processing in SAD. This work has consistently demonstrated abnormalities in reward processing in SAD.

Nevertheless, there are inconsistencies in the data, with results that appear to vary on the basis of which component (anticipation, outcome) of reward processing is disrupted, the valence of reward (positive or negative) affected, and the specificity of dysfunction in terms of reward type (monetary, social) (Guyer et al. 2012; Richey et al. 2013, 2017; Cremers et al. 2015). Whether aberrant reward processing in SAD is specific to social reward, or whether there exists a more general dysfunction that extends to the processing of other reward types such as monetary reward remains undecided. In addition, while there is indirect evidence that pharmacotherapy influences striatal dopaminergic function (Warwick et al. 2012), no studies have previously investigated the effect of pharmacotherapy on reward processing in SAD.

In this study, we used a modified version of the MID task to investigate whether SAD was associated with dysfunction in the processing of monetary reward. We hypothesized that there would be differences in reward processing between SAD participants at baseline and matched healthy controls (HCs), as well as in the SAD group before and after a course of pharmacotherapy.

Methods

The study was approved by the Health Research Ethics Committee of Stellenbosch University.

Participants

Volunteers were recruited through the MRC Unit on Risk and Resilience in Mental Disorders. Advertisements calling for both SAD and HC research participants were placed in local print media and online; as well as through local radio stations. Volunteers were eligible

if they were between the age of 18 and 55 years old; right-handed; and fluent in the language of the measuring instruments (English). SAD participants had to meet DSM-V criteria for the disorder and had to be free of comorbid mood or anxiety disorders; psychotic disorders; and substance use disorders. SAD participants were not taking any psychotropic medications at commencement of the trial and were not on any other medications that interacted with the study medication (i.e. moclobemide). Volunteers were excluded from the study if there were any contraindications to MRI (metal implants, claustrophobia); had any current or prior neurological illness; prior head injury resulting in loss of consciousness; or serious medical condition. Case-control matching for age and sex was performed.

Screening and clinical measures

Clinical evaluation and neuroimaging were performed on separate days. All participants underwent a structured clinical interview for DSM-IV (SCID) (First et al. 1996) and completed the Edinburgh Handedness Inventory (Oldfield 1971) as part of their screening. Participants also completed questionnaires used to measure the severity of depressive and social anxiety symptoms, namely the Beck Depression Inventory (BDI-II) (Beck et al. 1996) and Liebowitz Social Anxiety Scale (LSAS) (Liebowitz 1987).

On the day of scanning, all participants completed the state version of the State Trait Anxiety Inventory (STAI-S) which measures levels of anxiety at the time of the measure (Spielberger 1983).

Pharmacotherapy

Both healthy controls and SAD participants completed baseline clinical and neuroimaging measures. Following this, SAD participants commenced a course of moclobemide therapy according to recommended guidelines for SAD (300 mg PO daily for 3 days, followed by a 300 mg PO twice daily for a minimum of 8 weeks). At least 8 weeks after commencing therapy, clinical measures and neuroimaging (including task) were repeated in the SAD group. During this time they were closely monitored for adverse effects of the therapy. After completing the study, SAD participants were monitored for discontinuation symptoms in the event that they chose not to continue with maintenance therapy.

Neuroimaging

Imaging was performed during a dedicated study visit. SAD participants repeated the neuroimaging session after a course of moclobemide.

MRI scanning was initially performed on a 3 tesla (3T) Siemens Magnetom Allegra camera (Siemens Medical Systems, Erlangen, Germany). Midway through the project, this scanner was decommissioned and imaging was switched to a 3T Siemens Magnetom Skyra. Acquisition parameters across the two systems were optimized to reduce scanner-related bias. Scan parameters for the functional T2-weighted sequence on the Allegra system: single-shot gradient echo planar imaging (EPI); 382 volumes; repetition time (TR) = 1600 ms; echo time (TE) = 23 ms; flip angle = 73°; number of slices = 30; slice gap = 0.2 mm; field of view = 255 x 255 mm; voxel size = 4mm x 4mm x 4mm. On the Skyra system: the same settings were used except TR = 1740 ms. Additional structural scans (T1-weighted ME-MPRAGE; T2; FLAIR) were acquired for anatomical co-registration and to exclude significant intracranial pathology.

Before imaging, participants received an explanation of the scanning procedure and on how to perform the monetary incentive delay (MID) task. Participants were informed before the task that all money they won during the task was real and would be paid to them after the scanning session, in addition to the money they received to cover travel costs.

fMRI task

Participants completed a single run of an adapted version of the original MID task (Knutson et al. 2000). This task has been well-validated in probing monetary reward processing and had been previously set up at our site for other research projects (du Plessis et al. 2015). During the task, participants performed 60 trials, in each of which they were presented with five serial images: an anticipation cue consisting of either a neutral (n=30) or smiling (n=30) face; a fixation star; a target during which a button should be pressed; a fixation point; and a feedback screen, which informed participants of their success or failure and on any reward gained. This was followed by a variable inter-trial delay before the next trial began.

Participants were informed that only trials preceded by a smiling face were potentially rewarding but that they should push the button with their right index finger when they saw the target, regardless of trial type. When participants pushed the button while the target was still on screen, a "correct" response was recorded; otherwise an "incorrect" response was recorded. The feedback screen indicated to the participant whether they had had pressed the button in time (green text) or not (red text) as well as whether they had won any money, together with a running total. Potentially rewarding and neutral trials were randomly interspersed. Participants were warned prior to the task that timings would vary and that they would not be able to time their responses. The anticipation cue, and feedback screen were displayed for standard durations of 750 ms and 1000 ms respectively while display duration of the fixation star (mean 3286 ms, range: 779-6729 ms), and inter-trial interval (mean: 3535 ms, range: 1029-6979 ms) were varied in order to reduce collinearity of reward anticipation and reward feedback. Target display duration was varied to favour either trial success or trial failure (half of all neutral and potential reward trials each), by respectively adding 200 ms or subtracting 150 ms from the participant's fastest response time recorded during a preceding practice session. Display of the fixation point varied such that the duration of target and fixation point display together equalled 1000 ms. The complete task thus consisted of 60 trials, each of which had a mean duration of 9571 ms (range: 4946-16107), resulting in a total task duration of 9 min 35 sec.

Correct responses to potentially rewarding trials were rewarded with R10 (ten South African rand), resulting in a target reward amount for the entire task of R150.

A schematic representation of the reward task is presented in **Fig 6.1**.

Pre-processing

Anatomical scans were reviewed for structural abnormalities by a qualified radiologist. All images were reviewed for artefacts. DICOM files were converted to NIfTI format before undergoing further pre-processing in SPM12 (http://www.fil.ion.ucl.ac.uk/spm/) and MATLAB (Mathworks R2014b). After realignment of functional images, a custom script was used to check for significant motion. Only functional sequences in which there was less than 2 mm translation overall; less than 1 mm momentary translation; and less than 2° rotation

were included in the analysis. Functional scans were time slice corrected and the ME-MPRAGE image was co-registered to the mean functional image using normalized mutual information estimation. A second co-registration was performed in which follow-up images were co-registered to baseline images for the SAD group. The SPM Segment function was used to extract tissue classes from the structural scan and calculate a deformation field to the standardized SPM Average sized template. This deformation field was then used to warp the functional images, which were written to a final voxel size of 4x4x4 mm^3. The final functional images were smoothed using an isotropic 3D Gaussian kernel with FWHM = 8 mm.

A schematic diagram of pre-processing steps appears in **Fig 6.2**.

Analysis

Two types of analysis were performed. In the first, we compared two groups: SAD and HC participants (effect of group: SAD vs HC). In the second, we compared the effect of therapy within the SAD group (effect of condition: baseline vs post-therapy).

Statistical analysis was performed in Matlab (Mathworks 2104b). Group matching for age was tested using a two-tailed Welch's t-test. Group differences in level of education level was tested with the Freeman-Halton extension of the Fisher exact test. Differences in clinical scores were tested with a two-tailed Welch's t-test (SAD vs HC comparison) and single-tailed paired t-test (for the therapy effect comparison in the SAD group).

Behavioural data were analysed using SPSS (IBM SPSS Statistics, Version 25). Mixed design (for effect of group: SAD vs HC) and two-way repeated measures (for effect of condition: baseline vs post-therapy) analyses of variance (ANOVA) were performed to test for effects of valence (reward vs neutral) and either group (SAD vs HC) or condition (baseline vs post-therapy) on response accuracy and reaction time. Differences in total reward amount for the task were compared using a two-tailed Welch's t-test (SAD vs HC comparison) and single-tailed paired t-test (therapy effect comparison in the SAD group).

Time series data of the functional scans were analysed using a general linear model regression analysis with an event-related design in SPM12 (first level analysis). Similar to previous studies using this task (Hoogendam et al. 2013; du Plessis et al. 2015), our design model consisted of 6 factors representing haemodynamic responses to 1.) anticipation of reward; 2.) anticipation neutral; 3.) feedback of reward; 4.) feedback of missed reward; 5.) feedback correct neutral; 6.) feedback of missed neutral. Onset of the factors modelling anticipation were set to correspond to the presentation of the anticipation cue; while feedback onsets were set to the time of presentation of the target. Motion parameters obtained during alignment were included as nuisance regressors. A default high-pass filter cut-off of 128 seconds was used. Two contrasts (and their reverse) were defined: 1.) anticipation reward vs anticipation neutral (reward anticipation); and 2.) feedback reward vs feedback correct neutral (reward outcome).

Random effects analyses (second level) were performed using the contrast images generated during the first-level (subject-specific) analysis. These analyses were restricted to a limited set of brain regions known to play a role in reward processing, including striatum, nucleus accumbens, orbitofrontal cortex and anterior cingulate cortex. Similar to a previous study (Cremers et al. 2015), an inclusive mask for these regions was generated by summing the reverse inference statistical map obtained from the Neurosynth meta-analytic database (Yarkoni et al. 2011) for the terms “reward”, “reward anticipation” and “monetary reward”. This summed image was then binarized and clusters smaller than 10 voxels removed to generate the final mask. Generation of the mask image is illustrated in **Fig 6.3**. Since functional-anatomical variability in our groups could potentially result in effects just outside the mask region (and which would then be missed), we also performed a second, whole brain analysis in order to identify any activations in known reward structures.
In our primary analysis we used a statistical threshold of p=0.001 (uncorrected) at the voxel level, and p=0.05 (family-wise error corrected) at the cluster level. In our secondary, exploratory analysis of whole brain we used an uncorrected voxel-level threshold of p=0.001.

Results

Participants

Fifteen participants with SAD and 15 age and sex-matched HCs were recruited.

In the group (SAD vs HC) analysis, 2 of the SAD participant scans (as well as those of matched counterparts) and 5 of the HC participant scans (and their SAD counterparts) were excluded due to excessive motion. The final group size was thus 9 matched SAD participants and healthy controls.

In the effect of condition (baseline vs post-therapy) analysis, two SAD participants were excluded due to excessive motion on the baseline scan. Another two patients withdrew from the study due to lack of early therapeutic effect; and one participant withdrew due to scheduling issues (new job). Baseline and follow-up measures were thus available for 10 SAD participants.

Demographics

The demographics of participants included in the group analysis appear in **Table 6.1**. No significant differences were found in age, gender or level of education.

In the effect of condition (baseline vs post-therapy y) analysis, the 10 SAD participants consisted of 5 females and 5 males with a mean age of 29.2 years (range: 21 – 39).

Clinical characteristics

In the group (SAD vs HC) comparison, SAD participants had a mean LSAS score (±SD) of 88.6 (±25.0) compared to the HC participants, who had a mean LSAS of 18.0 (±13.2). This difference was statistically significant ($p<0.0001$). Despite not meeting diagnostic criteria for major depressive disorder (MDD) on the SCID, several SAD participants (n=5) fell into the clinical ranges for depression based on their BDI-II scores: one who met criteria for mild depression, 3 with moderate depression, and 1 with severe depression. BDI-II scores were

significantly higher in the SAD group (14.4 ±9.0) than in the HC group (2.0 ±2.1) (p=0.003). SAD participants were significantly more anxious than controls immediately before scanning, with a mean STAI-S score of 48.9 (±14.9) compared to 25.6 (±5.6) respectively (p=0.001).

In the effect of condition (baseline vs post-therapy) comparison, SAD participants received a mean of 8.9 weeks (range: 8.0 – 12.1 weeks; mode: 8.0) of moclobemide therapy at a fixed dosage of 600mg daily between baseline and follow-up measures. Differences between pre- and post-therapy clinical measures are summarized in **Table 6.2**. STAI-S scores at time of scanning were significantly higher at baseline (43.6 ±13.9) than after therapy (34.1 ±8.4) (p=0.007).

Reward processing: behavioural results

In the SAD vs HC comparison, there were no significant main effects of group or valence nor was there evidence of a group-by-valence interaction on response time or on accuracy. In the baseline vs post-therapy comparison effect of valence on response accuracy [$F(1, 9) = 6.68$, $p = 0.03$], reflecting higher accuracy across both conditions when completing potentially rewarding trials. No other significant effects of condition or valence, nor evidence of condition-by-valence interactions, were found on accuracy or response time. There was no significant difference between groups (SAD vs HC) or conditions (baseline vs post-therapy) in total reward amount won in the task.

Reward processing: fMRI results

No activations related to reward anticipation or reward outcome were observed within the a priori regions of interest in either group, or in the SAD group after therapy. No significant differences were observed between groups or conditions. In our second, exploratory analysis, in which we looked for activations in reward structures that may have been obscured by masking, the SAD group exhibited activation in anterior cingulate cortex during reward outcome, but again, no significant group or condition effects were detected.

Discussion

In this study, we investigated whether there was any difference in how participants with SAD anticipated and subsequently processed reward feedback when compared to a group of healthy controls. We also tested whether reward anticipation and processing of reward outcome differed after a course of moclobemide in the SAD participants. We did not detect any significant activations during reward anticipation or reward outcome in regions of a priori interest in either the HC group or the SAD group. Nor did we identify any group or condition effect in these regions. While an exploratory (whole-brain) analysis did detect activations (in the HC group: in precuneus, during reward anticipation; in the SAD group, in anterior cingulate cortex during reward outcome), no differences were detected in either group or condition comparisons in this analysis either.

While our negative findings in both the group and condition analyses may point to the absence of an effect, the lack of any activation in reward regions in either our SAD or HC groups suggests there may be technical reasons for these results. The detection of statistically significant activations depends on two factors: sample size and effect size. In terms of sample size, not only were our final group sizes smaller than anticipated due to excessive motion on a high proportion of scans, but we only performed one run of the task per participant, reducing our statistical power still further. In terms of effect size, it has been shown that this is influenced by the size of the financial reward (Wu et al. 2014), and it may be that the relatively low reward amount (R10) used in our experiment contributed to the absence of detectable activations. Given that a previous study at our centre (du Plessis et al. 2015) detected reward activations when using a single run of the same MID task (with group sizes of 16-18 participants) and the same reward amount, we plan to conduct a repeat analysis once we have included more participants. Data collection for this experiment has therefore been extended.

In addition to being underpowered, our study had some other limitations. The first is that our modified MID task can only investigate components of positively-valenced monetary reward. Other groups have designed MID-based tasks that include both positive and negative rewards and have combined social and monetary rewards in the same task (Richey et al. 2017). Such approaches are accepted to be more powerful in that they make full benefit, through mixed effects models, of disruptions in several reward components as well as interactions between

monetary and social reward processing. Unfortunately we lacked the resources to set up such a task in our setting, and thus chose to use an existing version of the task that had been trialled successfully (du Plessis et al. 2015). Another limitation relates to the design of the therapy effect component of our experiment. Once again, due to resource limitations, we used an uncontrolled design, whereas such research is optimally performed in a randomised control trial. Consequently, even if an effect was present when comparing post-therapy scans to baseline scans in the SAD group, we would be unable to distinguish a therapy-specific effect from a placebo effect. Our study is however predominantly exploratory in nature and should suspected therapy-related effects be identified in a future analysis using a larger group, this will motivate for future experiments with more targeted designs.

Nevertheless, our study had several strengths. Firstly, we have used case-control matching (unlike previous studies). This is arguably the recommended approach to limit false positives due to group heterogeneity. We have also chosen to focus on a relatively understudied component of reward processing in SAD for which there is currently conflicting evidence of abnormality, motivating for further study. In the context of accumulating evidence for disrupted reward processing in SAD, the distinction between general reward system dysfunction and an isolated specific (social) reward system dysfunction is an important one. For example, the former scenario suggests a model of SAD in which core reward circuitry (principally dopaminergic system) is affected as a "final common pathway" resulting in the aberrant processing of multiple reward types. In contrast, if reward processing dysfunction is limited to social reward, it might support a model in which this final common pathway is intrinsically normal, but "upstream" modulatory systems such as the oxytocinergic or endocannabinoid systems, which have been implicated in the experience of social reward (Skuse and Gallagher 2011; Harari-Dahan and Bernstein 2014; Karhson et al. 2016; Wei et al. 2017), are not. These two models would have different implications for developmental theories in SAD, for research into comorbid substance and mood disorders, and for current and novel therapeutic targets.

Conclusion

While there is emerging evidence of aberrant reward processing in SAD, it is uncertain whether reward processing in general is affected in SAD, or whether dysfunction is limited to

specific reward types. Using a modified version of the MID task, we performed an investigation of monetary reward processing in the SAD. We found no differences in monetary reward processing between SAD and HC groups, nor evidence that therapy with moclobemide influences monetary reward processing in SAD. Given the limitation of our small sample sizes, we plan to repeat our analyses once additional data are collected. Knowledge on disruptions in reward processing, as well as on the specificity of such disruptions to reward type, has potentially important implications in our understanding of the neurobiology of SAD and in the investigation of future therapeutic targets.

Contributors

Data collection: A Doruyter, L Taljaard, C Lochner
Data processing and analysis: A Doruyter, P Dupont
Manuscript: A Doruyter
Manuscript review: All authors
Supervisors: JM Warwick, C Lochner

Conflicts of Interest

None.

Acknowledgments

The PhD from which this study emanated was funded by the South African Medical Research Council (MRC) under the MRC Clinician Researcher Programme.
Financial support towards study costs was received from the Nuclear Technologies in Medicine and the Biosciences Initiative (NTeMBI), a national technology platform developed and managed by the South African Nuclear Energy Corporation (Necsa) and funded by the department of Science and Technology. The authors would also like to acknowledge contributions to study costs received from the Harry Crossley Foundation. Profs Stein and Lochner receive funding from the MRC. No funders played any role in study design; collection, analysis, or interpretation of data; in the writing of this article or in the decision to submit it for publication.

The authors would like to thank Dr Stéfan Du Plessis from the Department of Psychiatry, Stellenbosch University, for his assistance and advice in the set-up and analysis of the MID task.

Tables and Figures

Table 6.1 Demographics and group matching in the SAD vs HC baseline analysis.

	Group		
	HC	**SAD**	*p*
Total (n)	9	9	-
Mean age in years	30.3 (21.2 – 46.8)	30.1 (21.0 – 45.6)	0.96[a]
Sex	Female: 7, Male: 2	Female: 7, Male: 2	-
Highest level of education: *Formal schooling incomplete* *Additional training college or technical qualification* *Additional University degree*	 0 0 9	 1 2 6	 0.10[b]

[a] Two-tailed Welch's t-test

[b] Freeman-Halton extension of the Fisher exact test

Table 6.2 Clinical measures in SAD participants (n=10) used for the effect of therapy analysis.

	Condition				
	Baseline		**Post-therapy**		
	mean	*SD*	*mean*	*SD*	*p*[*]
LSAS	97.6	25.3	76.7	34.7	**0.003**
BDI-II	16.3	10.3	13.6	8.0	0.18
CGI-S CGI-I	4.5	1.4	4.0 3.0	1.5 0.9	0.13

[*] single-tailed paired student t-test

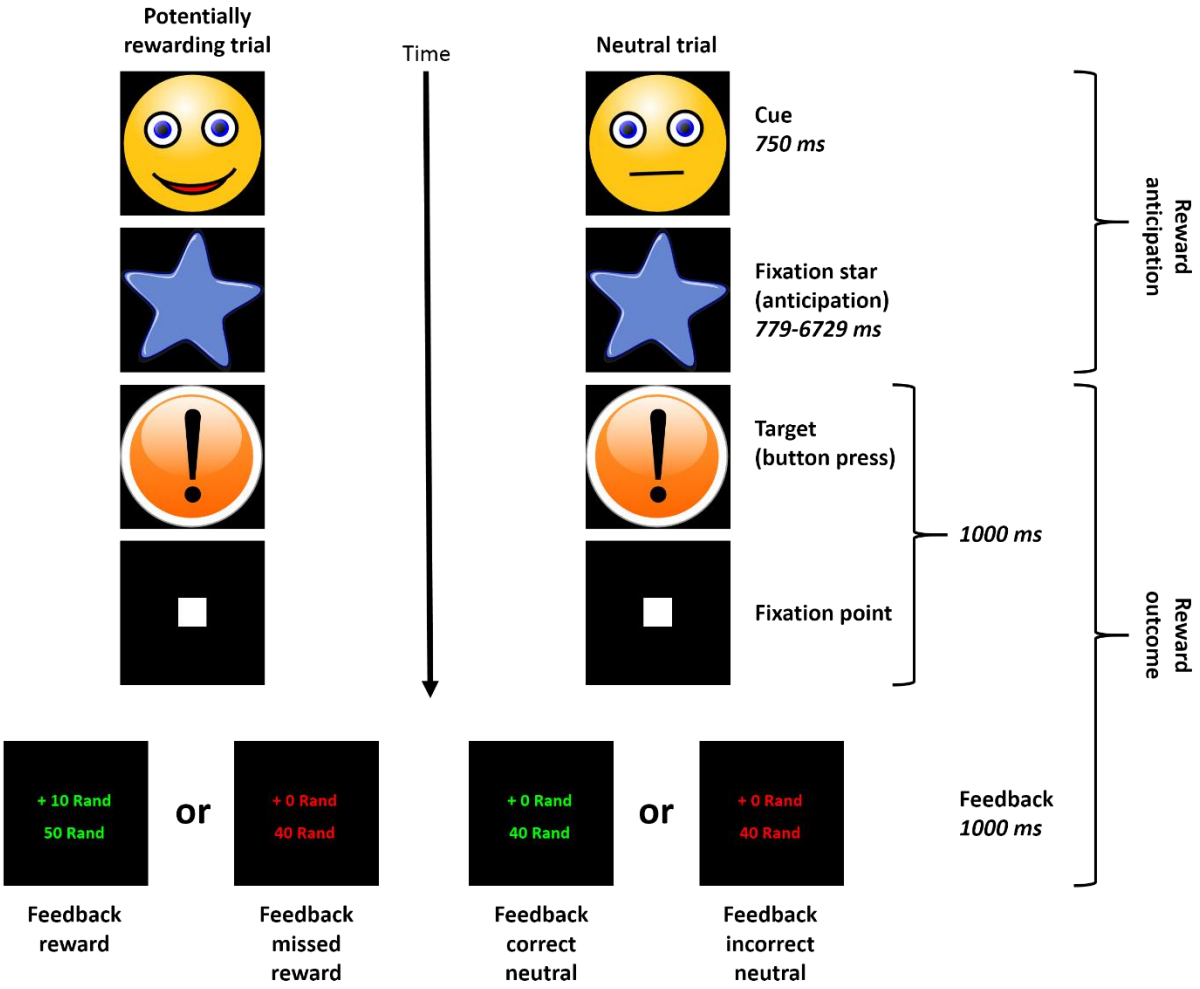

Figure 6.1 Schematic representation of the adapted monetary incentive delay task (Knutson et al. 2001) used in this study. *Graphic adapted from Hoogendam et al* (Hoogendam et al. 2013).

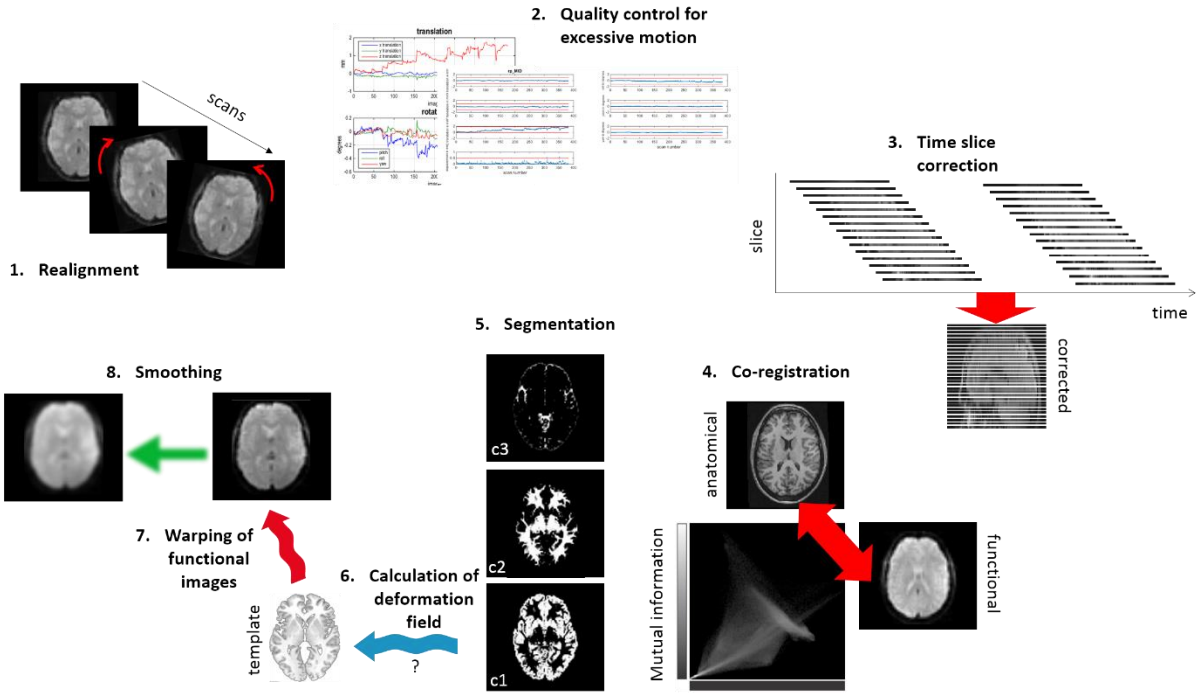

Figure 6.2 Pre-processing steps performed.

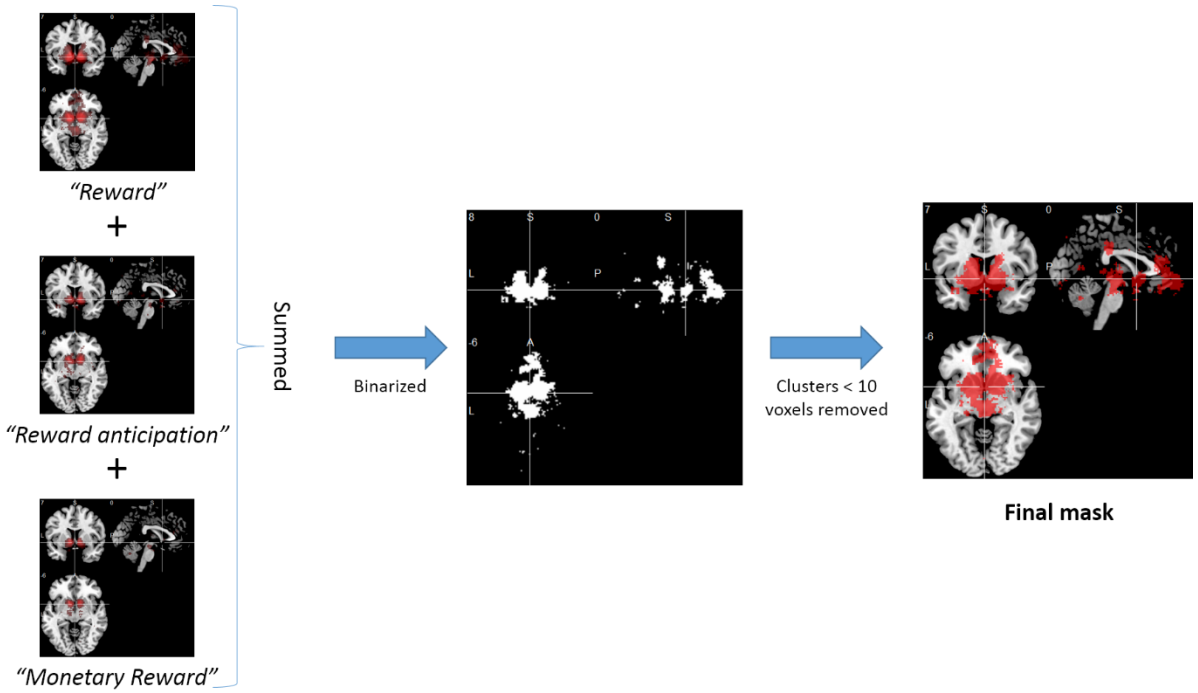

Figure 6.3 Generation of mask. Analysis was confined to brain regions known to play a role in reward processing. For this purpose, an inclusive mask was generated by summing the reverse inference statistical maps obtained from the meta-analytic database Neurosynth (Yarkoni et al. 2011) using the search terms "reward"; "reward anticipation" and "monetary reward". This summed image was then binarized and clusters smaller than 10 voxels were removed to generate the final mask image.

Conclusion

Summary of findings

In this thesis are presented the findings of several neuroimaging experiments in social anxiety disorder (SAD).

In a retrospective experiment using single photon emission tomography, as hypothesized, several differences in perfusion-based, resting functional connectivity (RFC) in SAD were detected, which were broadly consistent with a network model of the disorder. This is important, since concordant findings using a nuclear imaging technique strengthen the evidence supporting the contemporary network model of SAD, which is based on fMRI experiments. The experiment also reported a novel finding of disturbed RFC of the cerebellum, a structure that is not currently included in network models of SAD, but for which there is independent evidence of dysfunction in anxiety disorders. It was also hypothesized that changes in RFC would be detected in the SAD group post-therapy. The finding that RFC of the anterior cingulate cortex strengthened after pharmacotherapy suggests the importance of this region in the therapeutic response, although further research will be needed to confirm that this is indeed a therapy effect and whether such a finding can be directly correlated with clinical improvements with treatment. The finding of increased RFC between anterior cingulate and both fusiform gyrus and middle occipital gyrus post-therapy was interesting given that the current network model predicts increased RFC between these regions in SAD at baseline. That this connectivity should strengthen after therapy, coupled with an overall reduction in anxiety severity, invites speculation that this baseline disturbance may represent a compensatory effect, enhanced by therapy.

In a second experiment it was hypothesized that an SAD group would demonstrate differences in resting graph metrics within the theory-of-mind network, would display evidence of social attribution bias on a psychological measure, and that these findings would be correlated. In line with these hypotheses, the SAD group demonstrated several differences to controls in terms of both resting graph metrics within the theory of mind network as well as evidence of social attribution bias. No correlation between imaging findings and behavioural measures could be demonstrated however. While the absence of such a

correlation may indicate the absence of a relationship, this might also be explained by a small sample size and the high-interconnectedness of the network under study. It was also hypothesized that moclobemide therapy would influence resting graph metrics and social attributional style. While no changes in graph metrics within this network were detected in response to moclobemide therapy, there was evidence of altered attributional style after treatment. This work was important for several reasons. Firstly, it strengthened the limited evidence of social attribution biases in SAD and presented new evidence that pharmacotherapy might change these. Secondly, it sought to investigate the neuroimaging correlates of a behavioural measure. Although no correlation was identified in this study, it is important that such work is conducted, since a fundamental interest of social neuroscience is not merely how subjects brains differ, but also how neuroimaging features translate into behaviour. Future analyses similar to those used in this experiment but applied to larger groups, may be better powered to detect group differences and pharmacotherapy effects in the strongly interconnected theory-of-mind network.

Positron emission tomography-based measures of brain metabolism added to the limited existing work on resting regional neural activity in SAD. In this study it was hypothesized that brain regions implicated as important in the disorder in MRI-based work, would demonstrate resting-state differences between SAD and control subjects and that moclobemide therapy would result in changes in resting regional metabolism in the SAD group. Contrary to these hypotheses, no group differences or post-therapy effects were detected: a finding most likely explained by the stringent statistical thresholds despite careful case-control matching employed in the experiment. This explanation is supported by the results of a secondary analysis, at a more liberal statistical threshold similar to that employed by other studies, which did detect group differences and post-therapy changes in several biologically relevant regions. While the implications based on the results of this secondary analysis are necessarily speculative, these findings do contribute to the existing knowledge of the disorder, albeit with a lesser weighting. Importantly, this experiment suggests that regional metabolic differences in SAD as well as post-therapy changes, are small, and/or that inter- and intra-subject variability of FDG PET scans are large enough to conceal these effects. Given the drive to perform experiments with more stringent control of false positive results, requiring stricter statistical thresholds, the current work becomes important in planning future experiments, which will need to utilize larger sample sizes. The sample sizes

of future studies on resting regional metabolism will also be informed by additional research quantifying measurement and biological variability between FDG PET scans.

Finally, in an experiment on reward processing, it was hypothesized that SAD participants would demonstrate differences to controls in the processing of monetary reward, and that changes in reward processing would be found in SAD participants post-therapy. Due to greater than anticipated exclusion of participant scans due to excessive motion, data collection for this experiment has been extended. A preliminary analysis of data collected to date found no evidence of disrupted monetary reward processing in the condition, or of a therapy effect on reward processing. While preliminary negative findings of this experiment may well reflect a lack of statistical power, they are consistent with the view that alterations of reward processes in SAD may be restricted to social reward. Given that there is mounting evidence of aberrant reward processing in SAD, the distinction between a general deficit in reward processing, and an isolated abnormality in the processing of social reward is important as it may inform future SAD research into ancillary neurotransmitter systems beyond the dopaminergic system, such as oxytocinergic and endocannabinoid systems, which may play a more specific role in social reward. If confirmed, the presence of reward processing disturbances in SAD, and the nature of the components involved, may also have prognostic implications in terms of the frequent comorbidity of SAD with mood and substance use disorders and may, potentially, guide future therapeutic strategies.

Summary of limitations

The experiments contained in this work had several limitations. Due to both financial constraints as well as limited SAD referrals, group sizes were relatively small. Stringent quality control of the scan data meant that several participants and their matched controls had to be excluded from the analyses, decreasing sample sizes still further. While the limitations of small group sizes in neuroimaging research are well-known, it can be argued that experiments such as these still contribute to existing knowledge. One of the main drawbacks of research using small groups is that sample heterogeneity results in a higher chance of positive findings being false. To mitigate against this in prospective work, case-control matching for age and gender was performed, an approach that other studies in SAD (many with similar sample sizes) have not utilized. Primary analyses were also confined to a priori

regions of interest, which further limited the risk of false positives (Cremers and Roelofs 2016).

Resource constraints also necessitated that therapy effects (in the SAD group) be investigated with an uncontrolled study design rather than a randomised control type design, and prevented the collection of repeat measures in the HC group. While this weakened the quality of evidence that the effects reported were therapy-specific (as opposed to, e.g. a placebo effect), such provisional results form the foundation of further study. Finally, it should be noted that the retrospective experiment, on resting functional connectivity on perfusion SPECT, was performed using different SAD and HC participant samples, with different therapy and measurement instruments, to those in the other experiments, which relied on prospectively acquired data on different subjects. This introduces a degree of heterogeneity which prevents the direct comparison of results across these experiments.

Conclusions and future directions

The goal of a comprehensive model that links the pathophysiology and behavioural features of SAD, from genotype to phenotype, is extremely ambitious. To date, piecemeal contributions from multiple studies, while valuable, have prevented definitive conclusions regarding all but the most rudimentary components of a unified model of the disorder. There is for example independent evidence in support of a genetic contribution to SAD (but few candidate genetic markers); developmental evidence that behaviourally-inhibited children have a high risk of developing SAD (but uncertainty regarding the mechanisms of this progression); evidence of hyperactivity in limbic and paralimbic fear circuitry in response to provocation (characterizing SAD by its negative valence features, but not by other research domains that might be important in its pathophysiology); and evidence of disturbances in resting-state networks (but uncertainty how these disturbances predict differences in regional activity during various tasks and how they correlate with behaviour).

To further refine models of SAD, substantial investment will be required. Initiatives in this regard will almost certainly heavily rely on the analysis of large collaborative databases. The advantages to these databanks are two-fold. Firstly, due to the large number of participants they contain, it is possible to conduct mega-analyses, which are geared for high power and

are able to better deal with participant heterogeneity. Secondly, these databases are frequently characterized by the variety of subject-specific measures they contain. This "deep phenotyping", combined with genetic profiling, allows researchers to build links between different components of hypothesized models, e.g. between genetic markers and behavioural data, or between resting neural networks and task-based neural activations. These advantages make the results obtained both more reliable and more generalizable to wider clinical populations. The benefits of "big data" approaches in psychiatry research raise the question of whether small studies still have a role to play. For several reasons, the investigators involved in this work believe they do. Firstly, the data acquired in small studies comprises a significant proportion of the large databases upon which mega-analyses, frequently with different research questions, are performed. It can be argued that a key component of small-scale experiments should be to acquire high-quality data that is then made available to the greater research community through contribution to shared databases. Indeed, several of the data obtained for this degree have been included in an analysis by the anxiety subgroup of the ENIGMA project (Thompson et al. 2017), in which data from multiple sites will be pooled to allow higher powered mega-analyses. The other key role of small experiments is exploratory: research involving a limited number of participants is typically more flexible than the protocols of large collaborative experiments allow, and permits investigators to pursue creative ideas, in novel directions. The results generated by such work frequently form the basis of hypotheses in larger directed, group efforts. In that respect, the findings reported in this work may already contribute to several future research directions. For example, it motivates for the inclusion of cerebellum in analyses that investigate regional and functional connectivity in the disorder; for the direct investigation of the role of the anterior cingulate cortex in modulating treatment response; and further studies to establish a possible link between graph metrics of the theory of mind network and observed biases in social attribution. Experiments in which investigation of social and monetary reward are included in the same imaging paradigm would also be beneficial in determining the specificity of reward processing deficits in the disorder. Additional future avenues for pilot research include work on novel molecular targets (serotonergic, endocannabinoid), which are particularly attractive given the potential therapeutic options these targets represent. Another important contribution that can be made by smaller studies is work directed at establishing the reliability of the measures utilized in psychiatric research, and quantifying the errors involved. This is especially true of neuroimaging methods, for which only limited data on inter- and intra-scan variability (whether biological or technical in origin) exists despite this being an important

determinant of the effect sizes detectable across groups and within the same subjects over time.

In parallel with a trend towards mega-analyses, has come a shift in research priorities in psychiatric conditions. Recognizing that current diagnostic systems may artificially categorize related psychopathologies as distinct entities, the NIMH Research Domain Criteria (RDoC) project for classifying mental illnesses has promoted a trans-diagnostic approach in which psychiatric disorders are investigated along various functional domains and constructs aimed at identifying the pathophysiological underpinnings of shared features. Ultimately, the goal of this new research direction is to establish a diagnostic system for mental disorders that is based on pathophysiological processes, rather than observable behaviours and clinical consensus. In the case of SAD, this paradigm entails a switch to research of anxiety disorders as a combined group (SAD, generalized anxiety disorder, posttraumatic stress disorder, obsessive compulsive disorder), rather than as distinct entities, and initially prioritizes investigation of the pathophysiological basis of shared features (such as the acute threat construct of negative valence systems; or reward learning construct of positive valence systems) over the diagnosis-unique elements (e.g. precipitation of anxiety in social situations in SAD).

Finally, when considering trends that are likely to shape future research efforts in SAD, it would be remiss not to mention technological advances that continue to refine neuroimaging research tools. With hybrid modalities such as PET/MR it is possible to acquire simultaneous data on blood flow, regional neurotransmitter concentrations, regional electrical activity (when acquired with simultaneous EEG recording), as well as physiological measures such as heart rate, which given the dynamic and variable nature of neural processes, would not be directly correlatable were they acquired serially. Recent advances in motion correction will make data acquired with PET and MRI even more reliable.

To conclude, the ultimate goals of SAD research are ambitious and our current knowledge is in many respects still rudimentary, but recent alignments of research objectives, coupled with technological and analytical advances, mean that there is continuous progress towards a more comprehensive understanding of the disorder. As a non-invasive means of dynamically visualizing the anatomy and function of the brain, neuroimaging is expected to continue to play an essential role in eventually achieving these aims.

References

Åhs F, Furmark T, Michelgård A, et al (2006) Hypothalamic blood flow correlates positively with stress-induced cortisol levels in subjects with social anxiety disorder. Psychosom Med 68:859–862 . doi: 10.1097/01.psy.0000242120.91030.d8

Åhs F, Gingnell M, Furmark T, Fredrikson M (2017) Within-session effect of repeated stress exposure on extinction circuitry function in social anxiety disorder. Psychiatry Res 261:85–90 . doi: 10.1016/j.pscychresns.2017.01.009

Åhs F, Sollers III JJ, Furmark T, et al (2009) High-frequency heart rate variability and cortico-striatal activity in men and women with social phobia. NeuroImage 47:815–820 . doi: 10.1016/j.neuroimage.2009.05.091

Akirav I, Maroun M (2007) The role of the medial prefrontal cortex-amygdala circuit in stress effects on the extinction of fear. Neural Plast 2007:30873

Albert PR, Vahid-Ansari F, Luckhart C (2014) Serotonin-prefrontal cortical circuitry in anxiety and depression phenotypes: pivotal role of pre- and post-synaptic 5-HT1A receptor expression. Front Behav Neurosci 8: . doi: 10.3389/fnbeh.2014.00199

Alden LE, Taylor CT (2004) Interpersonal processes in social phobia. Clin Psychol Rev 24:857–882 . doi: 10.1016/j.cpr.2004.07.006

American Psychiatric Association, DSM-5 Task Force (2013) Diagnostic and statistical manual of mental disorders: DSM-5. American Psychiatric Association, Arlington, VA

Amir N, Foa EB, Coles ME (1998) Negative interpretation bias in social phobia. Behav Res Ther 36:945–957

Andersson M (2015) Erratum to: Effective dose to adult patients from 338 radiopharmaceuticals estimated using ICRP biokinetic data, ICRP/ICRU computational reference phantoms and ICRP 2007 tissue weighting factors. EJNMMI Phys 2: . doi: 10.1186/s40658-015-0121-4

Apšvalka D, Gadie A, Clemence M, Mullins PG (2015) Event-related dynamics of glutamate and BOLD effects measured using functional magnetic resonance spectroscopy (fMRS) at 3T in a repetition suppression paradigm. Neuroimage 118:292–300

Arnold-Anteraper S, Triantafyllou C, Sawyer AT, et al (2014) Hyper-connectivity of subcortical resting-state networks in social anxiety disorder. Brain Connect 4: . doi: 10.1089/brain.2013.0180

Arthurs OJ, Boniface S (2002) How well do we understand the neural origins of the fMRI BOLD signal? Trends Neurosci 25:27–31

Banks SJ, Eddy KT, Angstadt M, et al (2007) Amygdala–frontal connectivity during emotion regulation. Soc Cogn Affect Neurosci 2:303–312 . doi: 10.1093/scan/nsm029

Bas-Hoogendam JM, Blackford JU, Brühl AB, et al (2016) Neurobiological candidate endophenotypes of social anxiety disorder. Neurosci Biobehav Rev 71:362–378 . doi: 10.1016/j.neubiorev.2016.08.040

Beck AT, Steer RA, Brown GK, Beck Depression Inventory—II M (1996) Manual for Beck Depression Inventory-II

Bélanger M, Allaman I, Magistretti PJ (2011) Brain Energy Metabolism: Focus on Astrocyte-Neuron Metabolic Cooperation. Cell Metab 14:724–738 . doi: 10.1016/j.cmet.2011.08.016

Bennett CM, Wolford GL, Miller MB (2009) The principled control of false positives in neuroimaging. Soc Cogn Affect Neurosci 4:417–422 . doi: 10.1093/scan/nsp053

Bernard JA, Seidler RD, Hassevoort KM, et al (2012) Resting state cortico-cerebellar functional connectivity networks: A comparison of anatomical and self-organizing map approaches. Front Neuroanat 6:31

Berthoz S, Armony JL, Blair RJR, Dolan RJ (2002) An fMRI study of intentional and unintentional (embarrassing) violations of social norms. Brain J Neurol 125:1696–1708

Blumenfeld H, McNally KA, Vanderhill SD, et al (2004) Positive and negative network correlations in temporal lobe epilepsy. Cereb Cortex 14:892–902

Bonnet U (2003) Moclobemide: Therapeutic Use and Clinical Studies. CNS Drug Rev 9:97–140 . doi: 10.1111/j.1527-3458.2003.tb00245.x

Borogovac A, Asllani I (2012) Arterial Spin Labeling (ASL) fMRI: Advantages, Theoretical Constrains and Experimental Challenges in Neurosciences. Int J Biomed Imaging 2012:e818456 . doi: 10.1155/2012/818456

Bruce SE, Yonkers KA, Otto MW, et al (2005) Influence of Psychiatric Comorbidity on Recovery and Recurrence in Generalized Anxiety Disorder, Social Phobia, and Panic Disorder: A 12-Year Prospective Study. Am J Psychiatry 162:1179 . doi: 10.1176/appi.ajp.162.6.1179

Brühl AB, Delsignore A, Komossa K, Weidt S (2014a) Neuroimaging in social anxiety disorder—A meta-analytic review resulting in a new neurofunctional model. Neurosci Biobehav Rev 47:260–280 . doi: 10.1016/j.neubiorev.2014.08.003

Brühl AB, Hänggi J, Baur V, et al (2014b) Increased cortical thickness in a frontoparietal network in social anxiety disorder. Hum Brain Mapp 35:2966–2977 . doi: 10.1002/hbm.22378

Brunet E, Sarfati Y, Hardy-Baylé MC, Decety J (2000) A PET investigation of the attribution of intentions with a nonverbal task. NeuroImage 11:157–166 . doi: 10.1006/nimg.1999.0525

Buckner RL, Krienen FM, Castellanos A, et al (2011) The organization of the human cerebellum estimated by intrinsic functional connectivity. J Neurophysiol 106:2322–2345 . doi: 10.1152/jn.00339.2011

Bullmore E, Sporns O (2009) Complex brain networks: graph theoretical analysis of structural and functional systems. Nat Rev Neurosci 10:186–198 . doi: 10.1038/nrn2575

Bzdok D, Schilbach L, Vogeley K, et al (2012) Parsing the neural correlates of moral cognition: ALE meta-analysis on morality, theory of mind, and empathy. Brain Struct Funct 217:783–796 . doi: 10.1007/s00429-012-0380-y

Caouette JD, Guyer AE (2014) Gaining insight into adolescent vulnerability for social anxiety from developmental cognitive neuroscience. Dev Cogn Neurosci 8:65–76 . doi: 10.1016/j.dcn.2013.10.003

Carey PD, Warwick J, Niehaus DJH, et al (2004) Single photon emission computed tomography (SPECT) of anxiety disorders before and after treatment with citalopram. BMC Psychiatry 4:30 . doi: 10.1186/1471-244X-4-30

Caulfield MD, Servatius RJ (2013) Focusing on the possible role of the cerebellum in anxiety disorders. In: New Insights into Anxiety Disorders. InTech, pp 41–70

Cavanna AE, Trimble MR (2006) The precuneus: a review of its functional anatomy and behavioural correlates. Brain 129:564–583 . doi: 10.1093/brain/awl004

Ceccarini J, Vrieze E, Koole M, et al (2012) Optimized In Vivo Detection of Dopamine Release Using 18F-Fallypride PET. J Nucl Med 53:1565–1572 . doi: 10.2967/jnumed.111.099416

Cervenka S, Hedman E, Ikoma Y, et al (2012) Changes in dopamine D2-receptor binding are associated to symptom reduction after psychotherapy in social anxiety disorder. Transl Psychiatry 2:e120 . doi: 10.1038/tp.2012.40

Christian BT, Lehrer DS, Shi B, et al (2006) Measuring dopamine neuromodulation in the thalamus: Using [F-18]fallypride PET to study dopamine release during a spatial attention task. NeuroImage 31:139–152 . doi: 10.1016/j.neuroimage.2005.11.052

Chua P, Krams M, Toni I, et al (1999) A functional anatomy of anticipatory anxiety. Neuroimage 9:563–571

Cremers HR, Roelofs K (2016) Social anxiety disorder: a critical overview of neurocognitive research. Wiley Interdiscip Rev Cogn Sci 7:218–232 . doi: 10.1002/wcs.1390

Cremers HR, Veer IM, Spinhoven P, et al (2015) Neural sensitivity to social reward and punishment anticipation in social anxiety disorder. Front Behav Neurosci 8: . doi: 10.3389/fnbeh.2014.00439

Crippa JAS, Derenusson GN, Ferrari TB, et al (2011) Neural basis of anxiolytic effects of cannabidiol (CBD) in generalized social anxiety disorder: a preliminary report. J Psychopharmacol Oxf Engl 25:121–130 . doi: 10.1177/0269881110379283

Cui Q, Vanman EJ, Long Z, et al (2017) Social anxiety disorder exhibit impaired networks involved in self and theory of mind processing. Soc Cogn Affect Neurosci. doi: 10.1093/scan/nsx050

Cuthbert BN, Insel TR (2013) Toward the future of psychiatric diagnosis: the seven pillars of RDoC. BMC Med 11:126 . doi: 10.1186/1741-7015-11-126

Danti S, Ricciardi E, Gentili C, et al (2010) Is social phobia a “mis-communication” disorder? Brain functional connectivity during face perception differs between patients with social phobia and healthy control subjects. Front Syst Neurosci 4: . doi: 10.3389/fnsys.2010.00152

Del-Ben CM, Deakin JFW, McKie S, et al (2005) The effect of citalopram pretreatment on neuronal responses to neuropsychological tasks in normal volunteers: an FMRI study. Neuropsychopharmacology 30:1724–1734 . doi: 10.1038/sj.npp.1300728

Delgado MR, Frank RH, Phelps EA (2005) Perceptions of moral character modulate the neural systems of reward during the trust game. Nat Neurosci 8:1611–1618 . doi: 10.1038/nn1575

Detre JA, Wang J (2002) Technical aspects and utility of fMRI using BOLD and ASL. Clin Neurophysiol 113:621–634

Devlin JT, Russell RP, Davis MH, et al (2000) Susceptibility-induced loss of signal: comparing PET and fMRI on a semantic task. Neuroimage 11:589–600

Di X, Biswal BB (2012) Metabolic brain covariant networks as revealed by FDG-PET with reference to resting-state fMRI networks. Brain Connect 2:275–283 . doi: 10.1089/brain.2012.0086

Ding J, Chen H, Qiu C, et al (2011) Disrupted functional connectivity in social anxiety disorder: a resting-state fMRI study. Magn Reson Imaging 29:701–711 . doi: 10.1016/j.mri.2011.02.013

Doruyter A, Dupont P, Stein D, et al (2017a) Nuclear neuroimaging in social anxiety disorder: a review (unpublished, presented in this thesis). (unpublished)

Doruyter A, Dupont P, Taljaard L, et al (2017b) Resting regional brain metabolism in social anxiety disorder and the effect of moclobemide therapy. Metab Brain Dis. doi: 10.1007/s11011-017-0145-7

Doruyter A, Groenewald N, Dupont P, et al (2017c) Resting-state fMRI and social cognition: an opportunity to connect. Hum Psychopharmacol Clin Exp (in press):

Doruyter A, Groenewold NA, Dupont P, et al (2017d) Resting-state fMRI and social cognition: An opportunity to connect. Hum Psychopharmacol Clin Exp e2627 . doi: 10.1002/hup.2627

Doruyter A, Lochner C, Jordaan GP, et al (2016) Resting functional connectivity in social anxiety disorder and the effect of pharmacotherapy. Psychiatry Res Neuroimaging 251:34–44 . doi: 10.1016/j.pscychresns.2016.04.009

du Plessis S, Vink M, Joska JA, et al (2015) HIV infection results in ventral–striatal reward system hypo-activation during cue processing: AIDS 29:1335–1343 . doi: 10.1097/QAD.0000000000000680

Ebner K, Muigg P, Singewald G, Singewald N (2008) Substance P in stress and anxiety: NK-1 receptor antagonism interacts with key brain areas of the stress circuitry. Ann N Y Acad Sci 1144:61–73 . doi: 10.1196/annals.1418.018

Eickhoff SB, Bzdok D, Laird AR, et al (2012) Activation likelihood estimation meta-analysis revisited. Neuroimage 59:2349–2361

Eickhoff SB, Laird AR, Grefkes C, et al (2009) Coordinate-based activation likelihood estimation meta-analysis of neuroimaging data: A random-effects approach based on empirical estimates of spatial uncertainty. Hum Brain Mapp 30:2907–2926

Etkin A, Egner T, Kalisch R (2011) Emotional processing in anterior cingulate and medial prefrontal cortex. Trends Cogn Sci 15:85–93 . doi: 10.1016/j.tics.2010.11.004

Etkin A, Wager TD (2007) Functional neuroimaging of anxiety: a meta-analysis of emotional processing in PTSD, social anxiety disorder, and specific phobia. Am J Psychiatry 164:1476–1488 . doi: 10.1176/appi.ajp.2007.07030504

Evans KC, Simon NM, Dougherty DD, et al (2009) A PET study of tiagabine treatment implicates ventral medial prefrontal cortex in generalized social anxiety disorder. Neuropsychopharmacol Off Publ Am Coll Neuropsychopharmacol 34:390–398 . doi: 10.1038/npp.2008.69

Fallgatter AJ (2009) Neuroimaging in psychiatry: from bench to bedside. Front Hum Neurosci 3: . doi: 10.3389/neuro.09.049.2009

Falquez R, Couto B, Ibanez A, et al (2014) Detaching from the negative by reappraisal: the role of right superior frontal gyrus (BA9/32). Front Behav Neurosci 8:165 . doi: 10.3389/fnbeh.2014.00165

Faria V, Ahs F, Appel L, et al (2014) Amygdala-frontal couplings characterizing SSRI and placebo response in social anxiety disorder. Int J Neuropsychopharmacol 17:1149–1157 . doi: 10.1017/S1461145714000352

Faria V, Appel L, Åhs F, et al (2012) Amygdala subregions tied to SSRI and placebo response in patients with social anxiety disorder. Neuropsychopharmacol Off Publ Am Coll Neuropsychopharmacol 37:2222–2232 . doi: 10.1038/npp.2012.72

First MB, Spitzer RL, Gibbon M, Williams JB (2002) Structured clinical interview for DSM-IV-TR axis I disorders, research version, patient edition. N Y Biom Res N Y State Psychiatr Inst

First MB, Spitzer RL, Gibbon M, Williams JBW (1996) Structured clinical interview for DSM-IV Axis I Disorders — clinician edition. Biometrics Research Department, New York State Research Institute, New York

Fowler JS, Logan J, Shumay E, et al (2015) Monoamine oxidase: radiotracer chemistry and human studies. J Label Compd Radiopharm 58:51–64 . doi: 10.1002/jlcr.3247

Fox AS, Kalin NH (2014) A translational neuroscience approach to understanding the development of social anxiety disorder and its pathophysiology. Am J Psychiatry

Franklin ME, Huppert J, Langner R, et al (2005) Interpretation Bias: A Comparison of Treated Social Phobics, Untreated Social Phobics, and Controls1. Cogn Ther Res 29:289–300 . doi: 10.1007/s10608-005-2412-8

Fredrikson M, Furmark T (2003) Amygdaloid regional cerebral blood flow and subjective fear during symptom provocation in anxiety disorders. Ann N Y Acad Sci 985:341–347

Freitas-Ferrari MC, Hallak EC, Trzesniak C, et al (2010) Neuroimaging in social anxiety disorder: A systematic review of the literature. Prog Neuropsychopharmacol Biol Psychiatry 34:565–580 . doi: 10.1016/j.pnpbp.2010.02.028

Frick A, Åhs F, Appel L, et al (2016) Reduced serotonin synthesis and regional cerebral blood flow after anxiolytic treatment of social anxiety disorder. Eur Neuropsychopharmacol J Eur Coll Neuropsychopharmacol 26:1775–1783 . doi: 10.1016/j.euroneuro.2016.09.004

Frick A, Åhs F, Engman J, et al (2015a) Serotonin Synthesis and Reuptake in Social Anxiety Disorder: A Positron Emission Tomography Study. JAMA Psychiatry 72:794–802 . doi: 10.1001/jamapsychiatry.2015.0125

Frick A, Ahs F, Linnman C, et al (2015b) Increased neurokinin-1 receptor availability in the amygdala in social anxiety disorder: a positron emission tomography study with [11C]GR205171. Transl Psychiatry 5:e597 . doi: 10.1038/tp.2015.92

Frick A, Howner K, Fischer H, et al (2013) Altered fusiform connectivity during processing of fearful faces in social anxiety disorder. Transl Psychiatry 3:e312 . doi: 10.1038/tp.2013.85

Frith C, Frith U (2006) The Neural Basis of Mentalizing. Neuron 50:531–534 . doi: 10.1016/j.neuron.2006.05.001

Frith CD (2007) The social brain? Philos Trans R Soc B Biol Sci 362:671–678 . doi: 10.1098/rstb.2006.2003

Fumita M, Innis RB (2002) In vivo molecular imaging: ligand development and research applications. In: Neuropsychopharmacology: The Fifth Generation of Progress : an Official Publication of the American College of Neuropsychopharmacology. Lippincott Williams & Wilkins, pp 411–425

Furmark T, Appel L, Henningsson S, et al (2008) A link between serotonin-related gene polymorphisms, amygdala activity, and placebo-induced relief from social anxiety. J Neurosci Off J Soc Neurosci 28:13066–13074 . doi: 10.1523/JNEUROSCI.2534-08.2008

Furmark T, Appel L, Michelgård A, et al (2005) Cerebral blood flow changes after treatment of social phobia with the neurokinin-1 antagonist GR205171, citalopram, or placebo. Biol Psychiatry 58:132–142 . doi: 10.1016/j.biopsych.2005.03.029

Furmark T, Henningsson S, Appel L, et al (2009) Genotype over-diagnosis in amygdala responsiveness: affective processing in social anxiety disorder. J Psychiatry Neurosci JPN 34:30–40

Furmark T, Marteinsdottir I, Frick A, et al (2016) Serotonin synthesis rate and the tryptophan hydroxylase-2: G-703T polymorphism in social anxiety disorder. J Psychopharmacol Oxf Engl 30:1028–1035 . doi: 10.1177/0269881116648317

Furmark T, Tillfors M, Garpenstrand H, et al (2004) Serotonin transporter polymorphism related to amygdala excitability and symptom severity in patients with social phobia. Neurosci Lett 362:189–192 . doi: 10.1016/j.neulet.2004.02.070

Furmark T, Tillfors M, Marteinsdottir I, et al (2002) Common changes in cerebral blood flow in patients with social phobia treated with citalopram or cognitive-behavioral therapy. Arch Gen Psychiatry 59:425–433

Gentili C, Ricciardi E, Gobbini MI, et al (2009) Beyond amygdala: Default Mode Network activity differs between patients with social phobia and healthy controls. Brain Res Bull 79:409–413 . doi: 10.1016/j.brainresbull.2009.02.002

Giménez M, Ortiz H, Soriano-Mas C, et al (2014) Functional effects of chronic paroxetine versus placebo on the fear, stress and anxiety brain circuit in Social Anxiety Disorder: Initial validation of an imaging protocol for drug discovery. Eur Neuropsychopharmacol 24:105–116 . doi: 10.1016/j.euroneuro.2013.09.004

Giménez M, Pujol J, Ortiz H, et al (2012) Altered brain functional connectivity in relation to perception of scrutiny in social anxiety disorder. Psychiatry Res 202:214–223 . doi: 10.1016/j.pscychresns.2011.10.008

Gottesman II, Gould TD (2003) The endophenotype concept in psychiatry: etymology and strategic intentions. Am J Psychiatry 160:636–645

Green MF, Penn DL, Bentall R, et al (2008) Social Cognition in Schizophrenia: An NIMH Workshop on Definitions, Assessment, and Research Opportunities. Schizophr Bull 34:1211–1220 . doi: 10.1093/schbul/sbm145

Greicius MD, Krasnow B, Reiss AL, Menon V (2003) Functional connectivity in the resting brain: A network analysis of the default mode hypothesis. Proc Natl Acad Sci 100:253–258 . doi: 10.1073/pnas.0135058100

Guy W (1976) Clinical Global Impression (CGI). ECDEU assessment manual for psychopharmacology, revised. US Department of Health, Education, and Welfare, Rockville, MD

Guyer AE, Choate VR, Detloff A, et al (2012) Striatal functional alteration during incentive anticipation in pediatric anxiety disorders. Am J Psychiatry 169:205–212

Haber SN, Knutson B (2009) The reward circuit: linking primate anatomy and human imaging. Neuropsychopharmacology 35:4–26

Hadley JA, Kraguljac NV, White DM, et al (2016) Change in brain network topology as a function of treatment response in schizophrenia: a longitudinal resting-state fMRI study using graph theory. NPJ Schizophr 2:16014 . doi: 10.1038/npjschz.2016.14

Hahn A, Stein P, Windischberger C, et al (2011) Reduced resting-state functional connectivity between amygdala and orbitofrontal cortex in social anxiety disorder. NeuroImage 56:881–889 . doi: 10.1016/j.neuroimage.2011.02.064

Hamilton JP, Furman DJ, Chang C, et al (2011) Default-Mode and Task-Positive Network Activity in Major Depressive Disorder: Implications for Adaptive and Maladaptive Rumination. Biol Psychiatry 70:327–333 . doi: 10.1016/j.biopsych.2011.02.003

Haneef Z, Levin HS, Chiang S (2015) Brain Graph Topology Changes Associated with Anti-Epileptic Drug Use. Brain Connect 5:284–291 . doi: 10.1089/brain.2014.0304

Hao L, Yang J, Wang Y, et al (2015) Neural correlates of causal attribution in negative events of depressed patients: Evidence from an fMRI study. Clin Neurophysiol 126:1331–1337 . doi: 10.1016/j.clinph.2014.10.146

Harari-Dahan O, Bernstein A (2014) A general approach-avoidance hypothesis of oxytocin: accounting for social and non-social effects of oxytocin. Neurosci Biobehav Rev 47:506–519

Haxby JV, Hoffman EA, Gobbini MI (2000) The distributed human neural system for face perception. Trends Cogn Sci 4:223–233 . doi: 10.1016/S1364-6613(00)01482-0

Heimberg RG, Klosko JS, Dodge CS, et al (1989) Anxiety disorders, depression, and attributional style: A further test of the specificity of depressive attributions. Cogn Ther Res 13:21–36 . doi: 10.1007/BF01178487

Heiss W-D, Herholz K (2006) Brain receptor imaging. J Nucl Med 47:302–312

Hertz L, Dienel GA (2002) Energy metabolism in the brain. Int Rev Neurobiol 51:1

Hezel DM, McNally RJ (2014) Theory of Mind Impairments in Social Anxiety Disorder. Behav Ther 45:530–540 . doi: 10.1016/j.beth.2014.02.010

Hommet C, Mondon K, Camus V, et al (2014) Neuroinflammation and β amyloid deposition in Alzheimer's disease: in vivo quantification with molecular imaging. Dement Geriatr Cogn Disord 37:1–18 . doi: 10.1159/000354363

Hoogendam JM, Kahn RS, Hillegers MHJ, et al (2013) Different developmental trajectories for anticipation and receipt of reward during adolescence. Dev Cogn Neurosci 6:113–124 . doi: 10.1016/j.dcn.2013.08.004

Howells FM, Hattingh CJ, Syal S, et al (2015) 1H-magnetic resonance spectroscopy in social anxiety disorder. Prog Neuropsychopharmacol Biol Psychiatry 58:97–104 . doi: 10.1016/j.pnpbp.2014.12.008

Ipser JC, Kariuki CM, Stein DJ (2008) Pharmacotherapy for social anxiety disorder: a systematic review. Expert Rev Neurother 8:235–57 . doi: http://dx.doi.org/10.1586/14737175.8.2.235

Johansson J, Öst L-G (1982) Perception of autonomic reactions and actual heart rate in phobic patients. J Psychopathol Behav Assess 4:133–143

Judenhofer MS, Wehrl HF, Newport DF, et al (2008) Simultaneous PET-MRI: a new approach for functional and morphological imaging. Nat Med 14:459–465 . doi: 10.1038/nm1700

Kameyama M, Murakami K, Jinzaki M (2016) Comparison of [15O] H2O Positron Emission Tomography and Functional Magnetic Resonance Imaging in Activation Studies. World J Nucl Med 15:3 . doi: 10.4103/1450-1147.172139

Kampman O, Viikki M, Järventausta K, Leinonen E (2014) Meta-analysis of anxiety disorders and temperament. Neuropsychobiology 69:175–186 . doi: 10.1159/000360738

Karhson DS, Hardan AY, Parker KJ (2016) Endocannabinoid signaling in social functioning: an RDoC perspective. Transl Psychiatry 6:e905 . doi: 10.1038/tp.2016.169

Kashdan TB (2007) Social anxiety spectrum and diminished positive experiences: Theoretical synthesis and meta-analysis. Clin Psychol Rev 27:348–365

Kassenbrock A, Vasdev N, Liang SH (2016) Selected PET Radioligands for Ion Channel Linked Neuroreceptor Imaging: Focus on GABA, NMDA and nACh Receptors. Curr Top Med Chem 16:1830

Katzelnick DJ, Kobak KA, DeLeire T, et al (2001) Impact of generalized social anxiety disorder in managed care. Am J Psychiatry 158:1999–2007 . doi: 10.1176/appi.ajp.158.12.1999

Kent JM, Coplan JD, Lombardo I, et al (2002) Occupancy of brain serotonin transporters during treatment with paroxetine in patients with social phobia: a positron emission tomography study with 11C McN 5652. Psychopharmacology (Berl) 164:341–348 . doi: 10.1007/s00213-002-1218-8

Kessler RC, Berglund P, Demler O, et al (2005) Lifetime prevalence and age-of-onset distributions of dsm-iv disorders in the national comorbidity survey replication. Arch Gen Psychiatry 62:593–602 . doi: 10.1001/archpsyc.62.6.593

Kestemont J, Ma N, Baetens K, et al (2015) Neural correlates of attributing causes to the self, another person and the situation. Soc Cogn Affect Neurosci 10:114–121 . doi: 10.1093/scan/nsu030

Kestemont J, Vandekerckhove M, Bulnes LC, et al (2016) Causal attribution in individuals with subclinical and clinical autism spectrum disorder: An fMRI study. Soc Neurosci 11:264–276 . doi: 10.1080/17470919.2015.1074104

Kestemont J, Vandekerckhove M, Ma N, et al (2012) Situation and person attributions under spontaneous and intentional instructions: an fMRI study

Kilts CD, Kelsey JE, Knight B, et al (2006) The neural correlates of social anxiety disorder and response to pharmacotherapy. Neuropsychopharmacol Off Publ Am Coll Neuropsychopharmacol 31:2243–2253 . doi: 10.1038/sj.npp.1301053

Kinderman P, Bentall RP (1996) A new measure of causal locus: the internal, personal and situational attributions questionnaire. Personal Individ Differ 20:261–264

Kinderman P, Dunbar R, Bentall RP (1998) Theory-of-mind deficits and causal attributions. Br J Psychol 89:191–204 . doi: 10.1111/j.2044-8295.1998.tb02680.x

Kirsch P (2015) Oxytocin in the socioemotional brain: implications for psychiatric disorders. Dialogues Clin Neurosci 17:463

Knutson B, Adams CM, Fong GW, Hommer D (2001) Anticipation of increasing monetary reward selectively recruits nucleus accumbens. J Neurosci 21:1–5

Knutson B, Heinz A (2015) Probing psychiatric symptoms with the monetary incentive delay task. Biol Psychiatry 77:418–420

Knutson B, Westdorp A, Kaiser E, Hommer D (2000) FMRI visualization of brain activity during a monetary incentive delay task. NeuroImage 12:20–27 . doi: 10.1006/nimg.2000.0593

Koob GF, Le Moal M (1997) Drug abuse: hedonic homeostatic dysregulation. Science 278:52–58

Laird AR, Fox PM, Eickhoff SB, et al (2011) Behavioral interpretations of intrinsic connectivity networks. J Cogn Neurosci 23:4022–4037 . doi: 10.1162/jocn_a_00077

Lancaster J., Tordesillas-Gutiérrez D, Martinez M, et al (2007) Bias between MNI and Talairach coordinates analyzed using the ICBM-152 brain template. Hum Brain Mapp 28:1194–1205 . doi: 10.1002/hbm.20345

Lancaster JL, Summerln JL, Rainey L, et al (1997) The Talairach Daemon, a database server for Talairach atlas labels. Neuroimage 5:S633

Lancaster JL, Woldorff MG, Parsons LM, et al (2000) Automated Talairach atlas labels for functional brain mapping. Hum Brain Mapp 10:120–131

Langer JK, Rodebaugh TL (2014) Comorbidity of Social Anxiety Disorder and Depression. doi: 10.1093/oxfordhb/9780199797004.013.030

Lanzenberger R, Wadsak W, Spindelegger C, et al (2010) Cortisol plasma levels in social anxiety disorder patients correlate with serotonin-1A receptor binding in limbic brain regions. Int J Neuropsychopharmacol 13:1129–1143 . doi: 10.1017/S1461145710000581

Lanzenberger RR, Mitterhauser M, Spindelegger C, et al (2007) Reduced serotonin-1A receptor binding in social anxiety disorder. Biol Psychiatry 61:1081–1089 . doi: 10.1016/j.biopsych.2006.05.022

Laukka P, Ahs F, Furmark T, Fredrikson M (2011) Neurofunctional correlates of expressed vocal affect in social phobia. Cogn Affect Behav Neurosci 11:413–425 . doi: 10.3758/s13415-011-0032-3

Lecrubier Y, Wittchen H-U, Faravelli C, et al (2000) A European perspective on social anxiety disorder. Eur Psychiatry 15:5–16

LeDoux J (1998) The emotional brain: The mysterious underpinnings of emotional life. Simon and Schuster, New York

LeDoux JE (2000) Emotion circuits in the brain. Annu Rev Neurosci 23:155

Lee DS, Kang H, Kim H, et al (2008) Metabolic connectivity by interregional correlation analysis using statistical parametric mapping (SPM) and FDG brain PET; methodological development and patterns of metabolic connectivity in adults. Eur J Nucl Med Mol Imaging 35:1681–1691

Li J, Liu J, Liang J, et al (2009) A distributed neural system for top-down face processing. Neurosci Lett 451:6–10 . doi: 10.1016/j.neulet.2008.12.039

Liao W, Chen H, Feng Y, et al (2010a) Selective aberrant functional connectivity of resting state networks in social anxiety disorder. NeuroImage 52:1549–1558 . doi: 10.1016/j.neuroimage.2010.05.010

Liao W, Qiu C, Gentili C, et al (2010b) Altered effective connectivity network of the amygdala in social anxiety disorder: a resting-state FMRI study. PloS One 5:e15238 . doi: 10.1371/journal.pone.0015238

Liao W, Xu Q, Mantini D, et al (2011) Altered gray matter morphometry and resting-state functional and structural connectivity in social anxiety disorder. Brain Res 1388:167–177 . doi: 10.1016/j.brainres.2011.03.018

Liebowitz MR (1987) Social phobia. Mod Probl Pharmacopsychiatry 22:141–73

Liebowitz MR, Gorman JM, Fyer AJ, Klein DF (1985) Social phobia: Review of a neglected anxiety disorder. Arch Gen Psychiatry 42:729–736

Linden DEJ (2006) How psychotherapy changes the brain-the contribution of functional neuroimaging. Mol Psychiatry 11:528

Linden DEJ (2012) The Challenges and Promise of Neuroimaging in Psychiatry. Neuron 73:8–22 . doi: 10.1016/j.neuron.2011.12.014

Liu F, Guo W, Fouche J-P, et al (2015a) Multivariate classification of social anxiety disorder using whole brain functional connectivity. Brain Struct Funct 220:101–115 . doi: 10.1007/s00429-013-0641-4

Liu F, Zhu C, Wang Y, et al (2015b) Disrupted cortical hubs in functional brain networks in social anxiety disorder. Clin Neurophysiol Off J Int Fed Clin Neurophysiol 126:1711–1716 . doi: 10.1016/j.clinph.2014.11.014

Liu X, Hairston J, Schrier M, Fan J (2011) Common and distinct networks underlying reward valence and processing stages: A meta-analysis of functional neuroimaging studies. Neurosci Biobehav Rev 35:1219–1236 . doi: 10.1016/j.neubiorev.2010.12.012

Liu Y (2011) Characterization of thymic lesions with F-18 FDG PET-CT: an emphasis on epithelial tumors. Nucl Med Commun 32:554–562 . doi: 10.1097/MNM.0b013e328345b984

Maldjian JA, Laurienti PJ, Burdette JH (2004) Precentral gyrus discrepancy in electronic versions of the Talairach atlas. Neuroimage 21:450–455

Maldjian JA, Laurienti PJ, Kraft RA, Burdette JH (2003) An automated method for neuroanatomic and cytoarchitectonic atlas-based interrogation of fMRI data sets. Neuroimage 19:1233–1239

Manning J, Reynolds G, Saygin ZM, et al (2015) Altered resting-state functional connectivity of the frontal-striatal reward system in social anxiety disorder. PloS One 10:e0125286 . doi: 10.1371/journal.pone.0125286

Manning JJB (2015) Individual differences in the frontal-striatal reward network: decision-making and psychiatric disease. Massachusetts Institute of Technology

Margulies DS, Kelly AMC, Uddin LQ, et al (2007) Mapping the functional connectivity of anterior cingulate cortex. NeuroImage 37:579–588 . doi: 10.1016/j.neuroimage.2007.05.019

Marquand AF, Rezek I, Buitelaar J, Beckmann CF (2016) Understanding Heterogeneity in Clinical Cohorts Using Normative Models: Beyond Case-Control Studies. Biol Psychiatry 80:552–561 . doi: 10.1016/j.biopsych.2015.12.023

Mars RB, Neubert F, Noonan MP, et al (2012) On the relationship between the "default mode network" and the "social brain." Front Hum Neurosci 6: . doi: 10.3389/fnhum.2012.00189

Mathew SJ, Coplan JD, Gorman JM (2001) Neurobiological Mechanisms of Social Anxiety Disorder. Am J Psychiatry 158:1558–1567 . doi: 10.1176/appi.ajp.158.10.1558

McCabe C, Mishor Z, Filippini N, et al (2011) SSRI administration reduces resting state functional connectivity in dorso-medial prefrontal cortex. Mol Psychiatry 16:592–594

McClure EB, Monk CS, Nelson EE, et al (2007) Abnormal attention modulation of fear circuit function in pediatric generalized anxiety disorder. Arch Gen Psychiatry 64:97–106 . doi: 10.1001/archpsyc.64.1.97

McKay J, Tkáč I (2016) Quantitative in vivo neurochemical profiling in humans: where are we now? Int J Epidemiol 45:1339–1350 . doi: 10.1093/ije/dyw235

McRobbie DW (2006) MRI from picture to proton. Cambridge University Press, Cambridge, UK; New York

Merikangas KR, Angst J (1995) Comorbidity and social phobia: evidence from clinical, epidemiologic, and genetic studies. Eur Arch Psychiatry Clin Neurosci 244:297–303 . doi: 10.1007/BF02190407

Miskovic V, Schmidt LA (2012) Social fearfulness in the human brain. Neurosci Biobehav Rev 36:459–478 . doi: 10.1016/j.neubiorev.2011.08.002

Moalosi TCG (2016) The value of different reconstruction algorithms for quantification of FDG PET brain imaging. Stellenbosch: Stellenbosch University

Montgomery SA, Asberg M (1979) A new depression scale designed to be sensitive to change. Br J Psychiatry 134:382–389

Moriyama TS, Felicio AC, Chagas MHN, et al (2011) Increased dopamine transporter density in Parkinson's disease patients with Social Anxiety Disorder. J Neurol Sci 310:53–57 . doi: 10.1016/j.jns.2011.06.056

Murray RJ, Schaer M, Debbané M (2012) Degrees of separation: A quantitative neuroimaging meta-analysis investigating self-specificity and shared neural activation between self- and other-reflection. Neurosci Biobehav Rev 36:1043–1059 . doi: 10.1016/j.neubiorev.2011.12.013

Nagata T, Suzuki F, Teo AR (2015) Generalized Social Anxiety Disorder: A still-neglected anxiety disorder three decades since Liebowitz's review. Psychiatry Clin Neurosci n/a-n/a . doi: 10.1111/pcn.12327

National Collaborating Centre for Mental Health (UK) (2013) Social Anxiety Disorder: Recognition, Assessment and Treatment. British Psychological Society, Leicester (UK)

Nelissen N, Dupont P, others (2012) Kinetic modelling in human brain imaging. In: Positron Emission Tomography-Current Clinical and Research Aspects. InTech

Ohayon MM, Schatzberg AF (2010) Social phobia and depression: prevalence and comorbidity. J Psychosom Res 68:235–243 . doi: 10.1016/j.jpsychores.2009.07.018

Oldfield RC (1971) The assessment and analysis of handedness: the Edinburgh inventory. Neuropsychologia 9:97–113

Olson IR, Plotzker A, Ezzyat Y (2007) The Enigmatic temporal pole: a review of findings on social and emotional processing. Brain 130:1718–1731 . doi: 10.1093/brain/awm052

Pannekoek JN, Veer IM, van Tol M, et al (2013) Resting-state functional connectivity abnormalities in limbic and salience networks in social anxiety disorder without comorbidity. Eur Neuropsychopharmacol 23:186–195 . doi: 10.1016/j.euroneuro.2012.04.018

Pantazatos SP, Talati A, Schneier FR, Hirsch J (2014) Reduced anterior temporal and hippocampal functional connectivity during face processing discriminates individuals with social anxiety disorder from healthy controls and panic disorder, and increases following treatment. Neuropsychopharmacology 39:425–434 . doi: 10.1038/npp.2013.211

Paterson LM, Kornum BR, Nutt DJ, et al (2013) 5-HT radioligands for human brain imaging with PET and SPECT. Med Res Rev 33:54–111

Phan KL, Coccaro EF, Angstadt M, et al (2013) Corticolimbic brain reactivity to social signals of threat before and after sertraline treatment in generalized social phobia. Biol Psychiatry 73:329–336 . doi: 10.1016/j.biopsych.2012.10.003

Phillips J, Hewedi DH, Eissa A, Moustafa AA (2015) The cerebellum and psychiatric disorders. Name Front Public Health 3:66

Plana I, Lavoie M-A, Battaglia M, Achim AM (2014) A meta-analysis and scoping review of social cognition performance in social phobia, posttraumatic stress disorder and other anxiety disorders. J Anxiety Disord 28:169–177 . doi: 10.1016/j.janxdis.2013.09.005

Plavén-Sigray P, Hedman E, Victorsson P, et al (2017) Extrastriatal dopamine D2-receptor availability in social anxiety disorder. Eur Neuropsychopharmacol J Eur Coll Neuropsychopharmacol. doi: 10.1016/j.euroneuro.2017.03.007

Prater KE, Hosanagar A, Klumpp H, et al (2013) Aberrant amygdala-frontal cortex connectivity during perception of fearful faces and at rest in generalized social anxiety disorder. Depress Anxiety 30:234–241 . doi: 10.1002/da.22014

Qiu C, Liao W, Ding J, et al (2011) Regional homogeneity changes in social anxiety disorder: a resting-state fMRI study. Psychiatry Res 194:47–53 . doi: 10.1016/j.pscychresns.2011.01.010

Ribeiro-da-Silva A, Hökfelt T (2000) Neuroanatomical localisation of Substance P in the CNS and sensory neurons. Neuropeptides 34:256–271 . doi: 10.1054/npep.2000.0834

Richard IH (2005) Anxiety disorders in Parkinson's disease. In: Advances in Neurology. Lippincott Williams & Wilkins, Philadelphia, pp 42–55

Richey JA, Ghane M, Valdespino A, et al (2017) Spatiotemporal dissociation of brain activity underlying threat and reward in social anxiety disorder. Soc Cogn Affect Neurosci 12:81–94 . doi: 10.1093/scan/nsw149

Richey JA, Rittenberg A, Hughes L, et al (2013) Common and distinct neural features of social and non-social reward processing in autism and social anxiety disorder. Soc Cogn Affect Neurosci 9:367–377 . doi: 10.1093/scan/nss146

Rilling J, Gutman D, Zeh T, et al (2002) A neural basis for social cooperation. Neuron 35:395–405

Rogers RD, Owen AM, Middleton HC, et al (1999) Choosing between small, likely rewards and large, unlikely rewards activates inferior and orbital prefrontal cortex. J Neurosci 19:9029–9038

Ross SA, Seibyl JP (2004) Research applications of selected 123I-labeled neuroreceptor SPECT imaging ligands. J Nucl Med Technol 32:209–214

Rubinov M, Sporns O (2010) Complex network measures of brain connectivity: Uses and interpretations. NeuroImage 52:1059–1069 . doi: 10.1016/j.neuroimage.2009.10.003

Rypma B, Fischer H, Rieckmann A, et al (2015) Dopamine D1 Binding Potential Predicts Fusiform BOLD Activity during Face-Recognition Performance. J Neurosci 35:14702–14707 . doi: 10.1523/JNEUROSCI.1298-15.2015

Schilbach L, Eickhoff SB, Rotarska-Jagiela A, et al (2008) Minds at rest? Social cognition as the default mode of cognizing and its putative relationship to the "default system" of the brain. Conscious Cogn 17:457–467

Schmahmann JD (2010) The role of the cerebellum in cognition and emotion: personal reflections since 1982 on the dysmetria of thought hypothesis, and its historical evolution from theory to therapy. Neuropsychol Rev 20:236–260

Schneier FR, Abi-Dargham A, Martinez D, et al (2009) Dopamine transporters, D2 receptors, and dopamine release in generalized social anxiety disorder. Depress Anxiety 26:411–418 . doi: 10.1002/da.20543

Schneier FR, Liebowitz MR, Abi-Dargham A, et al (2000) Low Dopamine D2 receptor binding potential in social phobia. Am J Psychiatry 157:457–9

Schneier FR, Martinez D, Abi-Dargham A, et al (2008) Striatal dopamine D2 receptor availability in OCD with and without comorbid social anxiety disorder: preliminary findings. Depress Anxiety 1091-4269 25:1–7 . doi: 10.1002/da.20268

Schneier FR, Pomplun M, Sy M, Hirsch J (2011) Neural response to eye contact and paroxetine treatment in generalized social anxiety disorder. Psychiatry Res 194:271–278 . doi: 10.1016/j.pscychresns.2011.08.006

Schulte-Rüther M, Markowitsch HJ, Fink GR, Piefke M (2007) Mirror neuron and theory of mind mechanisms involved in face-to-face interactions: a functional magnetic resonance imaging approach to empathy. J Cogn Neurosci 19:1354–1372

Schultz RT, Grelotti DJ, Klin A, et al (2003) The role of the fusiform face area in social cognition: implications for the pathobiology of autism. Philos Trans R Soc B Biol Sci 358:415–427

Schultz W (1997) Dopamine neurons and their role in reward mechanisms. Curr Opin Neurobiol 7:191–197

Sedeño L, Couto B, García-Cordero I, et al (2016) Brain Network Organization and Social Executive Performance in Frontotemporal Dementia. J Int Neuropsychol Soc JINS 22:250–262 . doi: 10.1017/S1355617715000703

Seidel E-M, Eickhoff SB, Kellermann T, et al (2010) Who is to blame? Neural correlates of causal attribution in social situations. Soc Neurosci 5:335–350 . doi: 10.1080/17470911003615997

Seidel E-M, Satterthwaite TD, Eickhoff SB, et al (2012) Neural correlates of depressive realism—An fMRI study on causal attribution in depression. J Affect Disord 138:268–276

Sheehan DV (1983) The anxiety disease. Scribner New York

Sheehan DV, Lecrubier Y, Sheenhan KH (1998) The Mini-International Neuropsychiatric Interview (MINI): the development and validation of a structured diagnostic psychiatric interview for DSM-IV and ICD-10. J Clin Psychiatry 59:22–33

Shenhav A, Botvinick MM, Cohen JD (2013) The expected value of control: An integrative theory of anterior cingulate cortex function. Neuron 79:217–240 . doi: 10.1016/j.neuron.2013.07.007

Shin D-J, Jung WH, He Y, et al (2014) The effects of pharmacological treatment on functional brain connectome in obsessive-compulsive disorder. Biol Psychiatry 75:606–614 . doi: 10.1016/j.biopsych.2013.09.002

Simpson SL, Lyday RG, Hayasaka S, et al (2013) A permutation testing framework to compare groups of brain networks. Front Comput Neurosci 7: . doi: 10.3389/fncom.2013.00171

Skuse DH, Gallagher L (2011) Genetic Influences on Social Cognition. Pediatr Res 69:85R–91R . doi: 10.1203/PDR.0b013e318212f562

Spielberger CD (1983) Manual for the State-Trait Anxiety Inventory STAI (Form Y)(" Self-Evaluation Questionnaire")

Spreckelmeyer KN, Krach S, Kohls G, et al (2009) Anticipation of monetary and social reward differently activates mesolimbic brain structures in men and women. Soc Cogn Affect Neurosci 4:158–165 . doi: 10.1093/scan/nsn051

Spreng RN, Mar RA, Kim AS (2009) The common neural basis of autobiographical memory, prospection, navigation, theory of mind, and the default mode: a quantitative meta-analysis. J Cogn Neurosci 21:489–510

Sripada CS, Angstadt M, Banks S, et al (2009) Functional neuroimaging of mentalizing during the trust game in social anxiety disorder. Neuroreport 20:984–989 . doi: 10.1097/WNR.0b013e32832d0a67

Stanley ML, Moussa MN, Paolini BM, et al (2013) Defining nodes in complex brain networks. Front Comput Neurosci 7: . doi: 10.3389/fncom.2013.00169

Stein DJ, Cameron A, Amrein R, Montgomery SA (2002) Moclobemide is effective and well tolerated in the long-term pharmacotherapy of social anxiety disorder with or without comorbid anxiety disorder. Int Clin Psychopharmacol 17:161–170

Stein DJ, Lim CCW, Roest AM, et al (2017) The cross-national epidemiology of social anxiety disorder: Data from the World Mental Health Survey Initiative. BMC Med 15:143 . doi: 10.1186/s12916-017-0889-2

Stein DJ, Ono Y, Tajima O, Muller JE (2004) The social anxiety disorder spectrum. J Clin Psychiatry 65 Suppl 14:27-33; quiz 34-36

Stein DJ, Ruscio AM, Lee S, et al (2010) Subtyping social anxiety disorder in developed and developing countries. Depress Anxiety 1091-4269 27:390–403 . doi: 10.1002/da.20639

Stein DJ, Seedat S, Herman A, et al (2008) Lifetime prevalence of psychiatric disorders in South Africa. Br J Psychiatry 192:112–117 . doi: 10.1192/bjp.bp.106.029280

Stein MB (1998) Neurobiological perspectives on social phobia: from affiliation to zoology. Biol Psychiatry 44:1277–1285 . doi: 10.1016/S0006-3223(98)00265-0

Stein MB, Leslie WD (1996) A brain single photon-emission computed tomography (SPECT) study of generalized social phobia. Biol Psychiatry 39:825–828 . doi: 10.1016/0006-3223(95)00570-6

Steinbrink J, Villringer A, Kempf F, et al (2006) Illuminating the BOLD signal: combined fMRI–fNIRS studies. Magn Reson Imaging 24:495–505 . doi: 10.1016/j.mri.2005.12.034

Steinglass JE, Lempert KM, Choo T-H, et al (2017) Temporal discounting across three psychiatric disorders: Anorexia nervosa, obsessive compulsive disorder, and social anxiety disorder. Depress Anxiety 34:463–470 . doi: 10.1002/da.22586

Stenger VA, Boada FE, Noll DC (2000) Three-Dimensional Tailored RF Pulses for the Reduction of Susceptibility Artifacts in T2* Weighted Functional MRI. Magn Reson Med 44:525–531 . doi: 10.1002/1522-2594(200010)44:4<525::AID-MRM5>3.0.CO;2-L

Stopa L, Clark DM (2000) Social phobia and interpretation of social events. Behav Res Ther 38:273–283 . doi: 10.1016/S0005-7967(99)00043-1

Takeuchi H, Taki Y, Nouchi R, et al (2014a) Association between resting-state functional connectivity and empathizing/systemizing. NeuroImage 99:312–322 . doi: 10.1016/j.neuroimage.2014.05.031

Takeuchi H, Taki Y, Sassa Y, et al (2014b) Regional Gray Matter Volume Is Associated with Empathizing and Systemizing in Young Adults. PLoS ONE 9:1–16 . doi: 10.1371/journal.pone.0084782

Tavor I, Jones OP, Mars RB, et al (2016) Task-free MRI predicts individual differences in brain activity during task performance. Science 352:216–220 . doi: 10.1126/science.aad8127

Thompson PM, Andreassen OA, Arias-Vasquez A, et al (2017) ENIGMA and the individual: Predicting factors that affect the brain in 35 countries worldwide. NeuroImage 145:389–408 . doi: 10.1016/j.neuroimage.2015.11.057

Tiihonen J, Kuikka J, Bergström K, et al (1997) Dopamine reuptake site densities in patients with social phobia. Am J Psychiatry 154:239–242 . doi: 10.1176/ajp.154.2.239

Tillfors M, Furmark T, Marteinsdottir I, et al (2001) Cerebral blood flow in subjects with social phobia during stressful speaking tasks: A PET study. Am J Psychiatry 158:1220–1226 . doi: 10.1176/appi.ajp.158.8.1220

Tillfors M, Furmark T, Marteinsdottir I, Fredrikson M (2002) Cerebral blood flow during anticipation of public speaking in social phobia: a PET study. Biol Psychiatry 52:1113–1119

Tong J, Meyer JH, Furukawa Y, et al (2013) Distribution of monoamine oxidase proteins in human brain: implications for brain imaging studies. J Cereb Blood Flow Metab Off J Int Soc Cereb Blood Flow Metab 33:863–871 . doi: 10.1038/jcbfm.2013.19

Tronel C, Largeau B, Santiago Ribeiro M, et al (2017) Molecular Targets for PET Imaging of Activated Microglia: The Current Situation and Future Expectations. Int J Mol Sci 18:802 . doi: 10.3390/ijms18040802

Turkeltaub PE, Eickhoff SB, Laird AR, et al (2012) Minimizing within-experiment and within-group effects in activation likelihood estimation meta-analyses. Hum Brain Mapp 33:1–13

Tzourio-Mazoyer N, Landeau B, Papathanassiou D, et al (2002) Automated anatomical labeling of activations in SPM using a macroscopic anatomical parcellation of the MNI MRI single-subject brain. Neuroimage 15:273–289

van Ameringen M, Mancini C, Szechtman H, et al (2004) A PET provocation study of generalized social phobia. Psychiatry Res 132:13–18 . doi: 10.1016/j.pscychresns.2004.07.005

van der Linden G, van Heerden B, Warwick J, et al (2000) Functional brain imaging and pharmacotherapy in social phobia: single photon emission computed tomography before and after treatment with the selective serotonin reuptake inhibitor citalopram. Prog Neuropsychopharmacol Biol Psychiatry 24:419–438

van der Wee NJ, van Veen JF, Stevens H, et al (2008a) Increased serotonin and dopamine transporter binding in psychotropic medication-naive patients with generalized social anxiety disorder shown by 123I-beta-(4-iodophenyl)-tropane SPECT. J Nucl Med Off Publ Soc Nucl Med 49:757–763 . doi: 10.2967/jnumed.107.045518

van der Wee NJ, van Veen JF, Stevens H, et al (2008b) Increased Serotonin and Dopamine Transporter Binding in Psychotropic Medication–Naıve Patients with Generalized Social Anxiety Disorder Shown by 123I-b-(4-Iodophenyl)-Tropane SPECT. J Nucl Med 49:757–763

van Overwalle F, D'aes T, Mariën P (2015) Social cognition and the cerebellum: A meta-analytic connectivity analysis: Social Cognition and Cerebellum Connectivity. Hum Brain Mapp 36:5137–5154 . doi: 10.1002/hbm.23002

van Wingen GA, Tendolkar I, Urner M, et al (2014) Short-term antidepressant administration reduces default mode and task-positive network connectivity in healthy individuals during rest. NeuroImage 88C:47–53 . doi: 10.1016/j.neuroimage.2013.11.022

Venneti S, Lopresti BJ, Wiley CA (2013) Molecular imaging of microglia/macrophages in the brain. Glia 61:10–23 . doi: 10.1002/glia.22357

Völlm B, Richardson P, McKie S, et al (2006) Serotonergic modulation of neuronal responses to behavioural inhibition and reinforcing stimuli: an fMRI study in healthy volunteers. Eur J Neurosci 23:552–560 . doi: 10.1111/j.1460-9568.2005.04571.x

Wang L, Xia M, Li K, et al (2015) The effects of antidepressant treatment on resting-state functional brain networks in patients with major depressive disorder. Hum Brain Mapp 36:768–778 . doi: 10.1002/hbm.22663

Wang X, Cao Q, Wang J, et al (2016) The effects of cognitive-behavioral therapy on intrinsic functional brain networks in adults with attention-deficit/hyperactivity disorder. Behav Res Ther 76:32–39 . doi: 10.1016/j.brat.2015.11.003

Wang Y, Ghumare E, Vandenberghe R, Dupont P (2017) Comparison of different generalizations of clustering coefficient and local efficiency for weighted undirected graphs. Neural Comput

Wang Y, Nelissen N, Adamczuk K, et al (2014) Reproducibility and robustness of graph measures of the associative-semantic network. PloS One 9:e115215

Warwick JM, Carey P, Jordaan GP, et al (2008) Resting brain perfusion in social anxiety disorder: a voxel-wise whole brain comparison with healthy control subjects. Prog Neuropsychopharmacol Biol Psychiatry 32:1251–1256

Warwick JM, Carey P, Van der Linden G, et al (2006) A comparison of the effects of citalopram and moclobemide on resting brain perfusion in social anxiety disorder. Metab Brain Dis 21:241–252 . doi: 10.1007/s11011-006-9009-2

Warwick JM, Carey PD, Cassimjee N, et al (2012) Dopamine transporter binding in social anxiety disorder: the effect of treatment with escitalopram. Metab Brain Dis 27:151–158 . doi: 10.1007/s11011-012-9280-3

Washburn D, Wilson G, Roes M, et al (2016) Theory of mind in social anxiety disorder, depression, and comorbid conditions. J Anxiety Disord 37:71–77 . doi: 10.1016/j.janxdis.2015.11.004

Wehrl HF, Hossain M, Lankes K, et al (2013) Simultaneous PET-MRI reveals brain function in activated and resting state on metabolic, hemodynamic and multiple temporal scales. Nat Med 19:1184–1189

Wei D, Allsop S, Tye K, Piomelli D (2017) Endocannabinoid Signaling in the Control of Social Behavior. Trends Neurosci 40:385–396 . doi: 10.1016/j.tins.2017.04.005

Weiner KS, Grill-Spector K (2012) The improbable simplicity of the fusiform face area. Trends Cogn Sci 16:251–254 . doi: 10.1016/j.tics.2012.03.003

Wenzel B, Mollitor J, Deuther-Conrad W, et al (2016) Development of a novel nonpeptidic 18F-nabeled radiotracer for in vivo imaging of oxytocin receptors with positron emission tomography. J Med Chem 59:1800–1817 . doi: 10.1021/acs.jmedchem.5b01080

Wildgruber D, Riecker A, Hertrich I, et al (2005) Identification of emotional intonation evaluated by fMRI. NeuroImage 24:1233–1241 . doi: 10.1016/j.neuroimage.2004.10.034

Wise RA, Rompré P-P (1989) Brain dopamine and reward. Annu Rev Psychol 40:191–225

Wittchen HU, Beloch E (1996) The impact of social phobia on quality of life. Int Clin Psychopharmacol 11 Suppl 3:15–23

Wittchen H-U, Fehm L (2003) Epidemiology and natural course of social fears and social phobia. Acta Psychiatr Scand 108:4–18 . doi: 10.1034/j.1600-0447.108.s417.1.x

Wu CC, Samanez-Larkin GR, Katovich K, Knutson B (2014) Affective traits link to reliable neural markers of incentive anticipation. NeuroImage 84:279–289

Xia M, Wang J, He Y (2013) BrainNet Viewer: a network visualization tool for human brain connectomics. PloS One 8:e68910

Yang R, Zhang H, Wu X, et al (2014) Hypothalamus-anchored resting brain network changes before and after sertraline treatment in major depression. BioMed Res Int 2014:915026 . doi: 10.1155/2014/915026

Yarkoni T, Poldrack RA, Nichols TE, et al (2011) Large-scale automated synthesis of human functional neuroimaging data. Nat Methods 8:665–670

Yuan M, Zhu H, Qiu C, et al (2016) Group cognitive behavioral therapy modulates the resting-state functional connectivity of amygdala-related network in patients with generalized social anxiety disorder. BMC Psychiatry 16:198 . doi: 10.1186/s12888-016-0904-8

Yun J-Y, Kim J-C, Ku J, et al (2017) The left middle temporal gyrus in the middle of an impaired social-affective communication network in social anxiety disorder. J Affect Disord 214:53–59 . doi: 10.1016/j.jad.2017.01.043

Zang Y, Jiang T, Lu Y, et al (2004) Regional homogeneity approach to fMRI data analysis. Neuroimage 22:394–400

Zang Y-F, He Y, Zhu C-Z, et al (2007) Altered baseline brain activity in children with ADHD revealed by resting-state functional MRI. Brain Dev 29:83–91

Zhang Y, Zhu C, Chen H, et al (2014) Frequency-dependent alterations in the amplitude of low-frequency fluctuations in social anxiety disorder. J Affect Disord 174:329–35

Zhu H, Qiu C, Meng Y, et al (2017) Altered Topological Properties of Brain Networks in Social Anxiety Disorder: A Resting-state Functional MRI Study. Sci Rep 7:43089 . doi: 10.1038/srep43089

Zink CF, Pagnoni G, Martin-Skurski ME, et al (2004) Human striatal responses to monetary reward depend on saliency. Neuron 42:509–517

Zou Q-H, Zhu C-Z, Yang Y, et al (2008) An improved approach to detection of amplitude of low-frequency fluctuation (ALFF) for resting-state fMRI: Fractional ALFF. J Neurosci Methods 172:137–141 . doi: 10.1016/j.jneumeth.2008.04.012

Appendix – Psychometric Measures

Properties of the various psychological instrument used in this thesis are briefly described below.

*Structured Clinical Interview for DSM-IV (SCID-I + selected parts of SCID-II) (*60 – 120 min)
A diagnostic exam used to determine DSM-IV Axis I disorders (major mental disorders) and Axis II disorders (personality disorders) (First et al. 2002).

The Edinburgh Handedness Inventory (5 minutes)
The Edinburgh Handedness Inventory is a 10- item list of items, which provides one with a measure of hand laterality (Oldfield 1971). Participants are required to indicate their preference in the use of hands in a number of activities. A laterality quotient is then calculated from the participant's response to the inventory, with scores ranging from 0 (extreme left handedness) to 48 (extreme right handedness).

Liebowitz Social Anxiety Scale (LSAS) (20-30 min)
A 24-item measure designed to assess both fear and avoidance of social (e.g., going to a party, meeting strangers) and performance situations (e.g., taking a test, giving a report to a group) occurring in the last week (Liebowitz 1987). Each of the items is rated from 0-3, with high scores representing more fear and/or avoidance.

Clinical Global Impressions Improvement scale (CGI-I) (1 min)
A 7 point scale that requires the clinician to assess how much the patient's illness has improved or worsened relative to a baseline state at the beginning of the intervention (Guy 1976). Rated as: 1, very much improved; 2, much improved; 3, minimally improved; 4, no change; 5, minimally worse; 6, much worse; or 7, very much worse.

The Sheehan Disability Scale (1-2 min)
Developed to assess functional impairment in three inter-related domains; work/school, social and family life (Sheehan 1983). Ratings are made on a 10 point visual analogue scale.

State Trait Anxiety Inventory State versions (STAI-S) (5 min)

Consists of a 20-item self-report measure that assesses state level of anxiety (Spielberger 1983). Form Y (an altered version of the original Form X) which has stronger psychometric properties in younger, less educated, or low-SES groups, was used. Respondents indicate how much each statement reflects how they feel right now (at this moment) on four-point Likert-type scales. Sample items from the state version include "I feel frightened" and "I feel pleasant."

Beck Depression Inventory II (BDI-II) (10 minutes)

One of the most widely used instruments for measuring the severity of depression (Beck et al. 1996). A 21-question multiple-choice self-report inventory.

The Internal, Personal, and Situational Attributions Questionnaire (IPSAQ) (20 min)

This measures attributional style (Kinderman and Bentall 1996). A 32-item questionnaire which can be self-administered or administered by a clinician. Clients are asked to read a series of hypothetical scenarios in which they have to imagine themselves having an interaction with another person. In these scenarios, clients must first decide what caused the scenario and record that response. Clients must then decide who/what caused the scenario (i.e. "Something about you?"; "Something about the other person or other people?"; or "Something about the situation (circumstances or chance)?"). The resulting data provide a measure of the client's causal locus of control."